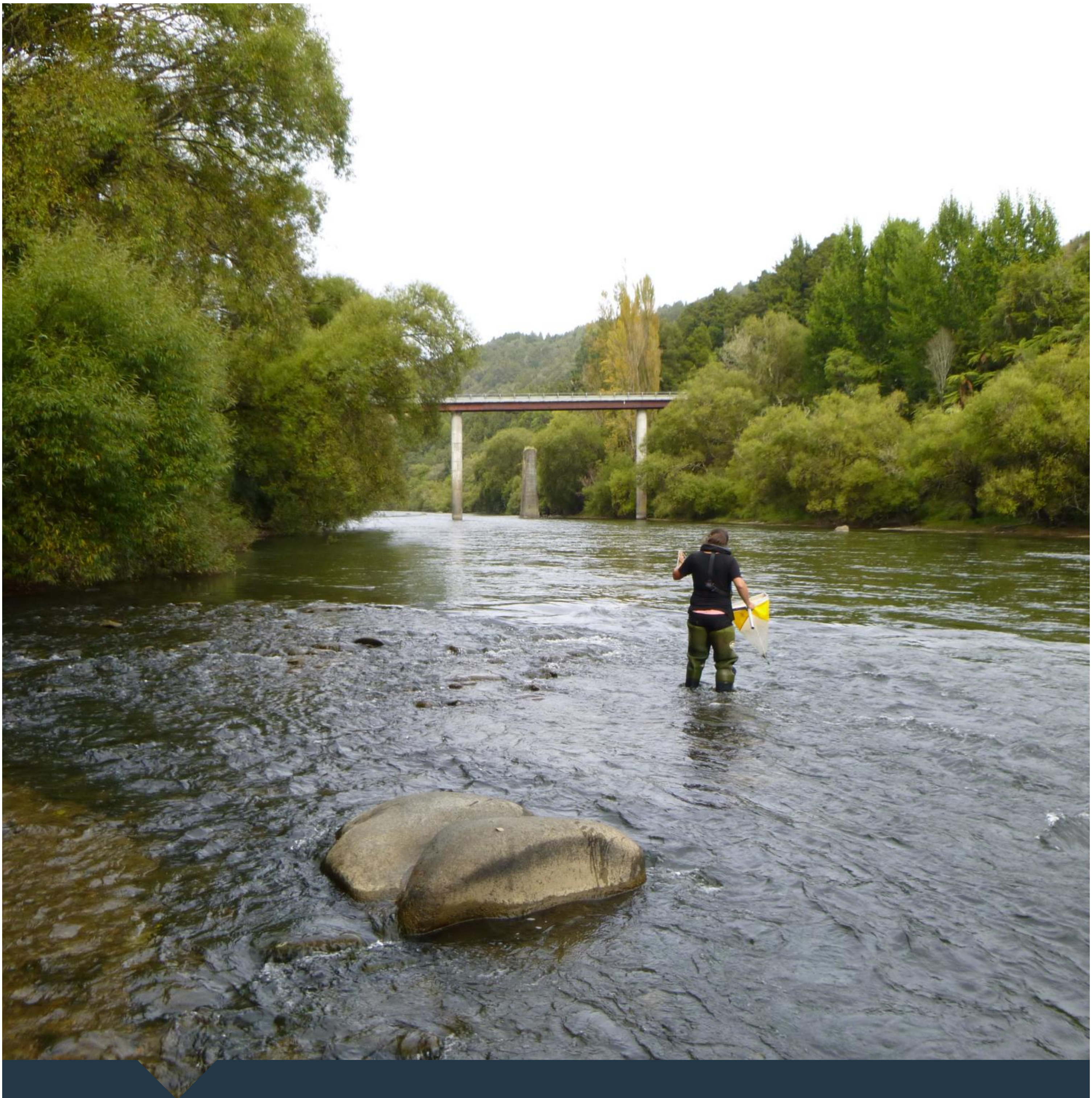

# Application of SedNetNZ using updated erosion mitigations with climate change scenarios in the Horizons region to support NPS-FM 2020 implementation

June 2023

horizons
REGIONAL COUNCIL

**Prepared for:**

Maree Patterson
Acting Science Manager

June 2023
Report No. 2023/EXT/1813
ISBN 9781991061324

**Prepared by:**

Simon Vale and Hugh Smith
Manaaki Whenua Landcare Research

CONTACT 24 hr freephone 0508 800 80 Help@horizons.govt.nz www.horizons.govt.nz

SERVICE CENTRES
Kairanga
Cnr Rongotea and
Kairanga-Bunnythorpe
Roads Palmerston North

Marton
19 Hammon Street

Taumarunui
34 Maata Street

REGIONAL HOUSES
Palmerston North
11-15 Victoria
Avenue

Whanganui
181 Guyton Street

DEPOTS
Taihape
243 Wairanu Road
Taihape

Woodville
116 Vogel Street

POSTAL ADDRESS
Horizons Regional Council, Private Bag 11025, Manawatū Mail Centre,
Palmerston North 4442

F 06-952 2929

Manaaki Whenua
Landcare Research

# Application of SedNetNZ using updated erosion mitigations with climate change scenarios in the Horizons region to support NPS-FM 2020 implementation

Prepared for: Horizons Regional Council

**June 2023**

# Application of SedNetNZ using updated erosion mitigations with climate change scenarios in the Horizons region to support NPS-FM 2020 implementation

*Contract Report: LC4295*

Simon Vale and Hugh Smith

*Manaaki Whenua – Landcare Research*

| *Reviewed by:* | *Approved for release by:* |
|---|---|
| Andrew Neverman<br>Scientist<br>Manaaki Whenua – Landcare Research | John Triantafilis<br>Portfolio Leader – Managing Land & Water<br>Manaaki Whenua – Landcare Research |

**Disclaimer**

*This report has been prepared by Landcare Research New Zealand Ltd for Horizons Regional Council. If used by other parties, no warranty or representation is given as to its accuracy and no liability is accepted for loss or damage arising directly or indirectly from reliance on the information in it.*

# Contents

# Summary

## Project and client

- Horizons Regional Council (HRC) previously contracted Manaaki Whenua – Landcare Research to model erosion and suspended sediment loads across the region for a range of erosion mitigation and climate change scenarios to support implementation of the National Policy Statement for Freshwater Management (NPS-FM) 2020 (Vale et al. 2022). The modelling focused on erosion mitigation measures implemented under the Sustainable Land Use Initiative (SLUI) and Whanganui Catchment Strategy (WCS) but did not explicitly represent other mitigation works, such as lowland riparian fencing and planting by HRC's Freshwater Team.
- SLUI commenced in 2006 and is New Zealand's largest hill-country erosion programme. To date, SLUI has completed whole farm plans for over 700 farms covering more than 500,000 ha of land, and has completed more than 35,200 ha of works, largely comprising afforestation, bush retirement, riparian retirement, space-planted trees, and gully tree planting.
- The HRC's Freshwater Team focuses on improving water quality and aquatic habitats, which mainly involves facilitating non-regulatory methods such as stream fencing and riparian planting. Landowners can apply for grants to implement these activities if they meet the eligibility criteria. Funding from the Manawatū Freshwater Improvement Fund and the regional Jobs for Nature fund has supported various projects, including stream fencing and plantings.
- The present report builds on the previous work by Vale et al. (2022) and involves modelling region-wide suspended sediment loads and the reductions in load required to achieve the NPS-FM 2020 attribute states for suspended fine sediment (visual clarity) under current land cover, as well as two future policy scenarios. The present modelling incorporates both SLUI/WCS and non-SLUI erosion mitigation works completed to date.

## Objectives

- To model region-wide mean annual suspended sediment loads under contemporary climate conditions for two policy scenarios.
  - *Policy Scenario 1 (PS1):* This scenario represents current policy, including the implementation of SLUI/WCS and non-SLUI/WCS works, and the existing policy settings. It accounts for the progress and maturity of works completed to date, as well as the projected rate of new farm plans and on-farm erosion mitigation implementation and maturity at 5-year intervals.
  - *Policy Scenario 2 (PS2):* This scenario represents future 'new policy'. It assumes the full implementation of Freshwater Farm Plans and appropriate works by specific dates, based on SLUI priority class, full implementation of stock exclusion regulations, and horticultural mitigations.
- To model the effect of future climate change projections on region-wide erosion and suspended sediment loads at mid- (2040) and late (2090) century for the two policy scenarios.

- To assess the load reductions required to meet NPS-FM 2020 attribute bands and the national bottom line (NBL) for suspended fine sediment (visual clarity) for the two policy scenarios, with and without the effects of climate change.

## Methods

- The SedNetNZ model was applied to the Horizons region to estimate mean annual suspended sediment loads across the River Environment Classification v2 (REC2) digital river network.
- The effect of future climate change on erosion and suspended sediment loads for the two policy scenarios was modelled following a similar approach to that described by Basher et al. (2020) and Neverman et al. (2023). This involved the use of rainfall and temperature grids from six regionally downscaled climate models (RCMs) and four representative concentration pathway (RCP) climate trajectories at mid- and late century to modify projected future erosion process rates under climate change.
- The proportional and absolute load reductions required to meet the NPS-FM 2020 attribute bands (A band and B band) and NBL were assessed for each of the scenarios. These were summarised by length and proportion by length of REC2 segments achieving each attribute state.

## Results

- Total erosion in the Horizons region is estimated at 8.8 Mt yr$^{-1}$, with a total net suspended sediment load of 8.3 Mt yr$^{-1}$ reaching the coast. The highest erosion rates (>2,500 t km$^{-2}$ yr$^{-1}$) are found in erosion-prone areas such as the Manawatū, Rangitīkei-Turakina, and Whangaehu Freshwater Management Units, as well as certain REC2 segments experiencing higher rates of bank erosion. By 2100 total erosion is projected to decrease to 4.6 Mt yr$^{-1}$ for PS1 and 3.6 Mt yr$^{-1}$ for PS2, resulting in region-wide reductions of 4.2 and 5.3 Mt yr$^{-1}$, or 48% and 60% for PS1 and PS2, respectively.
- The proportions (by length) of REC2 segments achieving the attribute bands (A band and B band) and the NBL were, respectively, 38%, 60%, and 75% in 2021. These proportions increase to 72%, 84%, and 90% for PS1 at 2100, and 74%, 85%, and 91% for PS2 at 2100. The achievement of these targets decreases for higher stream order segments. For example, in 2021, 38–43% of REC2 segments from stream orders ≤5 achieved the A band, while only 8% and 0% of segments from stream orders 6 and 7, respectively, achieved the A band.
- The regional pattern of suspended sediment load reductions and achieved attribute states is influenced by several factors: 1) SLUI erosion mitigation works primarily by targeting hill country areas, determining the selection order of new farm plans; 2) extensive implementation of riparian fencing and planting in lowland areas by 2025; and 3) variations in visual clarity thresholds based on the spatial pattern in the suspended sediment class used to define the thresholds.
- Projected total erosion for PS1 under different RCPs ranges from 8.4 to 12.5 Mt yr$^{-1}$ for mid-century and 4.9 to 10.1 Mt yr$^{-1}$ for late century, compared to loads without the effect of climate change. This represents a change of 7 to 46% and –4 to +79% for mid- and late century, respectively.

- Projected total erosion for PS2 under different RCPs ranges from 6.2 to 9.2 Mt yr$^{-1}$ for mid-century and 3.1 to 5.8 Mt yr$^{-1}$ for late century. This represents a change of 3 to 41% for mid-century and –16 to +58% for late century. Only the minimum and median RCP2.6 projections at late century show a decrease in sediment load (Figure S1).
- The proportion of REC2 segments (by length) achieving the NBL under future climate change ranges from 30% to 49% at mid-century and from 47% to 83% at late century for PS1. For PS2, the proportions are 43–78% at mid-century and 69–85% at late century, across all RCPs.

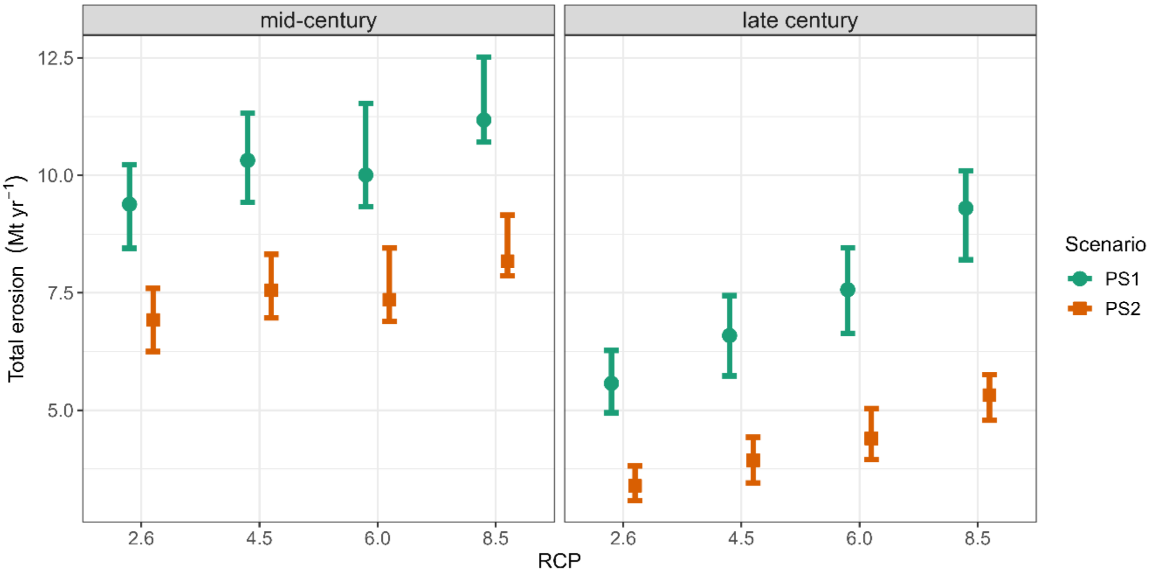

**Figure S1. Total erosion under projected climate change for the Horizons region at mid- and late century, by RCP for each erosion mitigation scenario (see Figure 16).**

## Model limitations

- The previous report by Vale et al. (2022) outlined specific limitations for each modelling component, including the representation of erosion processes, climate change projections, the reductions in sediment load required to meet visual clarity attribute bands, and the effectiveness of SLUI in reducing loads. These limitations, which can be found in Appendix E, should be considered when interpreting model outputs in the present report.
- The inclusion of erosion mitigation works completed by HRC's Freshwater Team (such as lowland riparian fencing) required modifications to the modelling approach. This introduced additional uncertainty due to several factors. For instance, the available spatial data for riparian fencing and planting only partially represents the existing fencing and planting in the region. Therefore, estimates for riparian fencing were augmented with information obtained from MWLR's Survey of Rural Decision Makers (SRDM), which may contain common survey response biases. Moreover, the SRDM stream definitions are not directly mappable to available river classifications. The main implication of this approach for estimating the current riparian fencing is that it may over- or underestimate the length of the remaining stream network available for

fencing, which affects the potential future reduction in sediment load achievable through additional riparian fencing.

## Conclusions and recommendations

- Model scenarios representing the implementation of future erosion mitigation policy show significant reductions in region-wide suspended sediment loads by late century, with PS1 achieving a 48% reduction and PS2 achieving a 60% reduction, without the effects of climate change. For PS2, most of this reduction in load (56%) is achieved by 2060.
- These sediment load reductions lead to similar proportions of REC2 segments meeting NPS-FM attribute bands between the two policy scenarios by late century, although PS2 achieves these improvements earlier.
- The projected climate change impact decreases the proportion of REC2 segments meeting the NBL for suspended fine sediment. PS1 and PS2 offset some of the climate-change-related increases in sediment loads.
- The sediment load reductions from PS1 and PS2 are greater than those achieved in previous scenario modelling by Vale et al. (2022), which results in a higher proportion of REC2 segments achieving NPS-FM attribute bands.
- Continued implementation of both hill country and lowland erosion mitigations will be required to reduce potentially significant impacts of climate change on suspended sediment loads by late century.
- Model predictions of sediment load reductions from erosion mitigations would benefit from region-specific data on erosion control effectiveness, implementation levels, and maturity of mitigation works at the farm and catchment scales. Also, utilising region-wide LiDAR data would improve the representation of erosion processes in SedNetNZ.

# 1 Introduction

Horizons Regional Council (HRC) previously contracted Manaaki Whenua – Landcare Research (MWLR) to model erosion and suspended sediment loads across the region for a range of erosion mitigation and climate change scenarios to support implementation of the National Policy Statement for Freshwater Management (NPS-FM) 2020 (Vale et al. 2022). Erosion mitigation focused on works completed under the Sustainable Land Use Initiative (SLUI) and Whanganui Catchment Strategy (WCS), but did not explicitly represent other mitigation works, such as the lowland riparian fencing and planting by HRC's Freshwater Team.

The previous work involved:

- modelling region-wide suspended sediment and sediment-associated phosphorus loads under current land cover and SLUI/WCS work to date
- assessing the load reductions required to achieve NPS-FM 2020 attribute states for suspended fine sediment (visual clarity)
- comparing reductions in modelled suspended sediment loads under future SLUI implementation scenarios relative to the current baseline with the load reductions required to achieve each NPS-FM 2020 attribute state
- modelling suspended sediment loads under future climate change for SLUI implementation scenarios and assessing the load reductions required to achieve each NPS-FM 2020 attribute state.

Following completion of the modelling (Vale et al. 2022), HRC approached MWLR to expand the work by incorporating additional data on non-SLUI erosion mitigation works, such as lowland fencing and planting by the HRC Freshwater Team, and to model future policy implementation scenarios. HRC asked MWLR to outline the scope of work required to:

- incorporate non-SLUI erosion mitigation works to date that were not previously included in the modelling (e.g. lowland fencing and planting by the Freshwater Team; horticultural erosion control measures)
- model future HRC policy implementation scenarios related to ongoing lowland fencing and planting initiatives, stock exclusion regulations (Resource Management (Stock Exclusion) Regulations 2020); and best-practice horticultural sediment management.

The new work would also assess the load reductions required to achieve NPS-FM 2020 attribute states for suspended fine sediment (visual clarity) under current and future policy scenarios; model suspended sediment loads under future climate change for policy scenarios; and assess the load reductions required to achieve each NPS-FM 2020 attribute state.

The present report is intended to be read in conjunction with the preceding report 'Application of SedNetNZ with SLUI erosion mitigation and climate change scenarios in the Horizons region to support NPS-FM 2020 implementation' by Vale et al. 2022. The previous report provides a comprehensive background and description of the SedNetNZ model, although, where appropriate, this information is also included in the appendices of the present report for ease of reference.

# 2 Background

## 2.1 SedNetNZ

A range of erosion processes occur in the Horizons region. Of notable importance are shallow landslides in response to intense rainfall events (Hancox 2004; Hancox & Wright 2005; Dymond et al. 2006; Basher 2013; Fuller et al. 2016), streambank erosion (Fuller & Heerdegen 2005; Fuller 2008), gully erosion in unconsolidated sands and silts (Miri 1999; Vale 2018; Vale, Smith, Matthews et al. 2021), and earthflows in the soft-rock hill country (Neverman et al. 2020; Dymond et al. 2006).

The SedNetNZ sediment budget model represents the diversity of erosion processes occurring in the Horizons region and more widely across New Zealand. This includes shallow landslide, earthflow, gully, surficial, and streambank erosion (Dymond et al. 2016; Smith, Spiekermann et al. 2019). Model outputs for these erosion processes are combined with losses due to floodplain deposition and lake sediment trapping to estimate mean annual suspended sediment loads at the REC2 subcatchment level.

Earlier versions of SedNetNZ have previously been applied in the Horizons region to assess the projected impact of SLUI (Dymond et al. 2014; Basher et al. 2018) and climate change on suspended sediment loads, but not for all erosion processes (Manderson et al. 2015; Basher et al. 2018, 2020). SedNetNZ has since undergone several significant updates, including improvements to the representation of bank erosion (Smith, Herzig et al. 2019; Smith et al. 2020), surficial erosion (Smith, Spiekermann et al. 2019; Neverman et al. 2021b), lake sediment trapping (Neverman et al. 2021b), and floodplain deposition (Vale, Smith, Neverman et al. 2021). These updates were included in the application of SedNetNZ to the Horizons region described by Vale et al. (2022).

## 2.2 Sustainable Land Use Initiative (SLUI)

The Sustainable Land Use Initiative (SLUI) began in 2006 and is New Zealand's largest hill-country erosion programme. It is funded from a mixture of the Ministry for Primary Industries (MPI)'s Hill Country Erosion Fund and HRC's rates and farmer contributions (Horizons Regional Council 2019b). SLUI has completed whole farm plans (WFPs) for over 700 farms covering more than 500,000 ha of land, and has completed more than 35,200 ha of works, largely comprising afforestation, bush retirement, riparian retirement, space-planted trees, and gully tree planting.

SLUI is informed by the Highly Erodible Land (HEL) model, which was previously developed by MWLR to spatially predict the amount of highly erodible land in the region. This analysis established that Manawatū-Whanganui has the largest area of HEL on private land in New Zealand, with approximately 263,000 ha of HEL under pasture in the region. To further target land management efforts, HRC developed a classification system within the region which separates land into 'top', 'high', 'low', and 'not' priority. Top priority land is estimated to contribute 40–55% of the sediment in the region's rivers and high priority land a further 25–30% of the sediment. This has made top and high priority land the main target for the programme to date (Horizons Regional Council 2019a).

WFPs are used as a tool to bring new land into the programme and for allocating grants. Approximately half of the top and high priority land in the region is within SLUI WFPs. The previously separate Whanganui Catchment Strategy (WCS), established before the SLUI, has been integrated into the programme. This included 39 WCS plans covering approximately 22,000 ha as at 30 June 2021 (Horizons Regional Council 2019a).

## 2.3 Non-SLUI mitigation works

The Freshwater Team at HRC undertakes a range of activities focused on improving water quality and aquatic habitats, which primarily involves supporting non-regulatory methods such as stream fencing and riparian planting. Landowners who meet certain criteria can apply for freshwater grants to carry out these activities.

The Manawatū Freshwater Improvement Fund, specific to the Manawatū catchment, has provided funding for 50 km of fencing and 40,000 plants in the financial years 2021/22 and 2022/23. The regional Jobs for Nature fund has allocated funding for 105 to 160 km of fencing and 100,000 to 140,000 plants from 2021/22 to 2023/24. Furthermore, the long-term plan beyond 2024/25 estimates an additional 80 km of fencing per year until approximately 2030.

To be eligible for funding, riparian fencing and waterway planting must meet various criteria, including factors such as location, slope, stream width, setback distance, planting density, species, and fence type. For instance, to comply with the stock exclusion regulations in the National Environmental Standards for Freshwater (NES-FW), fencing must be at least 3 m away from the edge of the stream bed. If the waterway is less than 1 m wide or not within a designated low-slope area, funding may still be available if a 2 m setback can be applied to provide suitable width of ungrazed riparian margin (Horizons Regional Council, unpublished document).

The Resource Management Act (Stock Exclusion) regulations (2020) require the exclusion of stock from lakes and wide rivers (>1 m wide), with a 3 m setback from the bed's edge and specific timelines. These regulations require the exclusion of dairy cattle, pigs, and all cattle and deer on land used for fodder or break feeding, and on irrigated pasture from all slopes, by 1 July 2023; exclusion of all dairy support cattle from all slopes by 1 July 2025; and exclusion of all beef cattle and deer from mapped low slopes (<10°) by 1 July 2025.

For areas in cultivation including horticulture, there are permitted activity setbacks of 5 m in the current regional plan. Thus, commercial vegetable-growing areas must maintain a 5 m setback to prevent cultivation within 5 m of the bed of a permanently flowing river, a non-permanently flowing stream with an active bed wider than 1 m, or a lake.

# 3 Objectives

The present report has three objectives.

- To model region-wide mean annual suspended sediment loads using SedNetNZ under contemporary climate conditions for the following policy scenarios.
    - *Policy Scenario 1 (PS1):* This represents current policy, including the implementation of SLUI/WCS and non-SLUI/WCS works and the existing policy settings. It includes the projected rate of new farm plans and on-farm erosion mitigation implementation across the region at 5-year intervals.
    - *Policy Scenario 2 (PS2):* This represents a future projection based on the full implementation of Freshwater Farm Plans (FWFPs) and relevant works according to SLUI priority class. It includes the full implementation of stock exclusion regulations and horticultural mitigations works across the region at 5-year intervals.
- To model the effect of future climate change projections on region-wide erosion and suspended sediment loads at mid- (2040) and late (2090) century for the two policy scenarios.
- To assess the load reductions required to meet NPS-FM 2020 attribute bands and the national bottom line for suspended fine sediment (visual clarity) for the two policy scenarios, with and without the effects of climate change.

# 4 Methods

In this section we describe the approach used to model the PS1 and PS2 scenarios in the Horizons region using SedNetNZ. The previous report by Vale et al. (2022) provided detailed descriptions of the SedNetNZ model, so our focus here is to describe changes in the modelling approach associated with the two policy scenarios.

The description of erosion process modelling from the previous report can be found in Appendix A. In addition, Appendix B describes the approach to estimating climate change impacts on erosion processes and sediment loads, including the climate models and representative concentration pathways (RCPs) used for future projections. Appendix C describes methods for estimating the sediment load reductions required to meet NPS-FM visual clarity attribute bands.

## 4.1 Policy scenarios

The region-wide simulations comprise the two policy scenarios summarised in Table 1. These scenarios represent the application of SLUI/WCS erosion mitigation, along with non-SLUI/WCS works, under current climate conditions for the year 2021 and at 5-year intervals from 2025 to 2100. The impact of projected climate change on suspended sediment loads was modelled for the two scenarios at mid- (2040) and late (2090) century. Six regional climate models (RCMs) were used to select the minimum, median, and maximum model projected change across four RCPs for each of the scenarios.

**Table 1. Summary of policy scenarios**

| Scenario | Description |
|---|---|
| Baseline 2021 update | The current policy scenario comprising recent land cover (LCDB v5) with SLUI/WCS and non-SLUI/WCS works and current policy settings. The baseline (2021) for both PS1 and PS2 represents SLUI and non-SLUI works implemented up to 1 July 2021, including the maturity level of implemented erosion control.<br>• SLUI works were modelled for the current extent of SLUI works for top, high, and low SLUI priority farms in keeping with the previous approach (Vale et al. 2022). SLUI 'not' priority farms were removed from this application, except where there were mass-movement-related (shallow landslide, earthflow, or gully) sediment loads.<br>• Non-SLUI works were modelled based on stream fencing and planting spatial data provided by the HRC Freshwater Team. This primarily occurs in lowland/SLUI 'not priority' farms.<br>• In the absence of data on the full extent of existing riparian fencing, the baseline stream fencing for lowland farms was approximated using district averages according to land use from the 2022 Survey of Rural Decision Makers (SRDM). These estimates were supplemented with the stream fencing and planting spatial data provided from HRC, and the highest value of either the SRDM or HRC fencing data was used for modelling at the REC2 stream segment level.<br>• Best-practice horticultural sediment management was represented by the presence of 5 m buffer strips around horticultural cultivation areas.<br>• Areas identified by HRC as 'sites of significance – aquatic' were assumed to be fully fenced with a 10 m setback. |
| Policy Scenario 1 (PS1) | The future projection for PS1 represents future implementation of SLUI and non-SLUI works, including the maturity level of erosion control works. The future projection comprised the following.<br>• SLUI works continue for SLUI/WCS at the current rate of SLUI/WCS farm plan implementation used in Vale et al. 2022 (i.e. new farms are mapped at the rate of 10,000 ha per year, and works implementation occurs at a rate of 1.14% once the farm is mapped). This only occurs for top, high, and low priority farms and 'not' SLUI priority farms, which have sediment loads generated from mass movement processes. This requires minor reselection of mapping dates due to the removal of 'not' priority farms from SLUI mapping.<br>• Non-SLUI works were modelled to reflect full implementation of stock exclusion regulations by 1 July 2025. This includes a further 80 km of fencing per year from 2025 to 2030 for land not included in the NES-FW to reflect ongoing fencing and planting rates from the HRC Freshwater Team. |
| Policy Scenario 2 (PS2) | The future projection for new policy (PS2) is based on the implementation of FWFPs, stock exclusion regulations, and horticultural mitigations by specific dates. This scenario was worked through in conjunction with HRC and based on the spatial application of erosion mitigations at the whole farm level. The scenario represents:<br>• FWFPs completed and certified by 2030 at 20% per year from 2025, randomised across the region.<br>• full implementation of appropriate works on top, high, and low HEL land classification within each farm by 2035, 2045 and 2065, respectively, across top, high, and low SLUI farm priority classes (appropriate works will be applied based on the proportion of past works for each SLUI farm priority class, and proportions of HEL land classes based on the proportions from currently mapped farms).<br>• non-SLUI works modelled to reflect full implementation of stock exclusion regulations by 1 July 2025, which includes a further 80 km of fencing per year from 2025 to 2030 for land not included in the NES-FW to reflect ongoing fencing and planting rates by the HRC Freshwater Team. |

Note: LCDB = Land Cover Database

## 4.2 Erosion mitigations

In the previous application of SedNetNZ in the Horizons region (Vale et al. 2022), SLUI sediment load reductions were applied across all SLUI farm priority classes based on WFPs. However, the inclusion of non-SLUI/WCS works and current policy considerations (such as stock exclusion regulations, riparian fencing and planting in lowland freshwater areas, and improved sediment management practices for horticulture) requires some adjustments to the approach.

The main modification involves distinguishing the SLUI ‘not’ priority farm classes from the top, high, and low priority classes. Non-SLUI mitigation works are primarily targeted at addressing bank and surficial erosion in the ‘not’ priority areas. However, a significant number of ‘not’ priority farms still contribute to sediment loads resulting from processes such as shallow landslides, earthflows, or gully erosion. In such cases, these farms are still considered for the implementation of SLUI mitigation works to address these erosion processes.

### 4.2.1 SLUI Whole Farm Plans

The estimation of sediment load reduction for each farm was based on the effectiveness, implementation, and maturity of various erosion mitigation measures implemented within SLUI WFPs. This approach was applied to both the existing mapped SLUI erosion mitigation measures and future mitigation measures for mapped and unmapped farms.

Sediment load reduction for a farm can be represented by:

$$Sediment\ reduction = \sum_{w=1}^{n}\left(\frac{E_w}{100} \times \frac{I_w}{100} \times \frac{M_w}{100}\right) \quad (1)$$

where $E$ is effectiveness (%), $I$ is the proportional extent of implementation (%), $M$ is maturity (%), $w$ is the type of erosion mitigation, and $n$ is the number of different types of erosion mitigation applied.

‘Effectiveness’ represents the capacity of the erosion mitigation applied to reduce sediment load once fully mature and is specific to each mitigation. Afforestation and bush retirement have an effectiveness value of 90% for mass movement erosion, based on published data, while riparian retirement is estimated at 80% (Dymond et al. 2010, 2016). Space-planted trees and gully tree planting have a value of 70% based on published data from Hawley and Dymond (1988) and Dymond et al. (2010). The effectiveness of afforestation and bush retirement at reducing surficial erosion (Table 2) was derived from the change in the cover factor ($C$) (see Appendix A, equation A1) based on the conversion of pasture to forest/scrub. Space-planted trees and gully tree planting do not typically achieve canopy closure, and therefore reductions from these mitigations were not applied to surficial erosion.

‘Maturity’ represents the proportion of time passed relative to the age at which a mitigation may be considered fully mature and thus fully effective. Maturity rates are outlined in Table 2 based on values used in previous work (e.g. Manderson et al. 2011; McIvor et al. 2011; Basher et al. 2018). Maturity was determined for currently mapped erosion control works based on the recorded year of implementation. In some situations, recent afforestation and retirement mitigation (<10 years old) mapped in SLUI are already captured in LCDB v5, which would be modelled as fully mature forest. Similarly, mature afforestation and bush retirement (>10 years old) should be captured as woody cover in LCDB v5, but this is not always the case.

To ensure the effects of erosion mitigation are not double-counted, mature afforestation and retirement works implemented earlier than 2012 (>10 years old) were added to LCDB v5 and classified as woody vegetation, while immature afforestation and retirement works implemented later than 2012 were added, classified as pasture, and then matured to the appropriate age. This ensures the sediment load reduction is consistently applied for both past and future mitigation, with the appropriate maturity level at each time interval. All other mitigations (such as space planting) were considered to be represented as pasture in LCDB v5 because they typically do not achieve canopy cover and are generally too small in area to be captured in LCDB.

**Table 2. Summary of maturity and effectiveness of the SLUI erosion mitigation, based on Basher et al. 2018**

| Erosion mitigation | Years to fully mature | Annual maturity rate | Effectiveness |
|---|---|---|---|
| Afforestation | 10 | 10% | 90% (mass movement)<br>50% (surficial) |
| Bush retirement | 10 | 10% | 90% (mass movement)<br>50% (surficial) |
| Riparian retirement | 2 | 50% | 80% |
| Space-planted trees | 15 | 6.66% | 70% |
| Gully tree planting | 15 | 6.66% | 70% |

'Implementation' in equation (1) represents the erosion works applied on a farm as a proportion of what may be considered full implementation of the WFP. Full implementation is difficult to estimate because there is no clearly defined mitigatable area or area of works for a given farm plan to be considered fully implemented. HRC provided an estimated average rate of on-farm works implementation of 1.14% per year (or 88 years to be fully implemented), which was used to model future rates of WFP implementation. This was based on the area of works completed on pasture for mapped high and top priority farms as a proportion of the total area of mapped pasture on high and top priority land over the last 10 years. This estimate required an assumption that all erosion control works were mapped in what was initially pasture, regardless of its classification in the latest LCDB v5 layer. This is important because mature afforestation and bush retirement mitigations will appear as woody cover in the latest LCDB layers and could misrepresent the true extent of implementation on a farm.

The proportion of each erosion mitigation type implemented within each farm was estimated based on the proportional area of each erosion mitigation. The proportional implementation of future works was estimated based on the past proportion of each erosion mitigation within each SLUI priority class (Table 3) and weighted based on the erosion process loads occurring within each intersecting farm-REC2 watershed. This can be expressed as:

$$I_w = I_{wfp} \times \left(W_p \times Erosion\ load_p\right) \tag{2}$$

where $I_w$ is the proportional implementation of the $w^{\text{th}}$ erosion mitigation type, $I_{wfp}$ is the proportional extent of WFP implementation, $W_p$ is the base proportion of each erosion mitigation for the associated SLUI priority class (Table 3), and $Erosion\ load_p$ is the combined load proportion for the erosion processes targeted by the $w^{\text{th}}$ erosion mitigation (Table 3).

This approach ensures that erosion control works are not applied to areas that do not experience the types of erosion the works are designed to mitigate. For example, if only bank erosion occurred in a given farm-REC2 watershed intersection, then the proportion of works would be weighted to include only riparian retirement. Implementation continues until 100% is reached for each WFP.

**Table 3. Past proportions of erosion mitigation applied to each priority class**

| Erosion mitigation | Proportion (%) | | | | | Erosion process mitigated |
|---|---|---|---|---|---|---|
| | All land classes | Land priority classes | | | | |
| | | Not | Low | High | Top | |
| Afforestation | 44.0 | 12.2 | 32.1 | 53.5 | 37.8 | Shallow landslide, earthflow, surficial |
| Retirement | 30.3 | 14.4 | 15.2 | 27.7 | 36.8 | Shallow landslide, earthflow, surficial |
| Riparian retirement | 9.9 | 34.8 | 17.5 | 7.5 | 9.9 | Bank erosion |
| Spaced planting | 14.3 | 37.2 | 33.1 | 9.9 | 13.8 | Shallow landslide, earthflow |
| Gully planting | 1.6 | 1.4 | 2.1 | 1.4 | 1.7 | Gully erosion |

### 4.2.2 Lowland riparian fencing

Estimating sediment load reductions due to lowland riparian fencing requires a different approach due to the nature of the data and ongoing implementation based on regulations. To address this, we applied a 30 m buffer to the REC2 digital stream network and used it to select relevant fences and plantings near the streams. This buffer accounts for variations in channel width and positional error in the data. We also considered land cover to exclude areas that are not suitable for fencing, such as natural cover areas within the DOC estate.

We estimate the fraction of REC2 stream link that has been fenced or planted ($FR_j$; equation 4) based on the intersection of the buffered fence and planting lines/polygons to approximate the proportional extent of fencing for a given REC2 segment.

However, the available spatial data on riparian fencing and planting only represents new initiatives and does not capture pre-existing fencing. To address this, we approximated the riparian fencing for the updated 2021 baseline using responses from the 2022 Survey of Rural Decision Makers (SRDM) according to district averages and land use (Table 4), following the approach of Neverman and Smith (2022). The SRDM uses terms such as 'free-flowing streams' and 'minor waterways/drains' to obtain information about riparian fencing extent from landowners. These terms are not clearly defined, so assumptions are required to appropriately apply the SRDM data to the REC2 segments.

We applied estimated fencing proportions for SRDM 'free-flowing streams' to ‘wide streams’ that meet the criteria for the Sustainable Dairying Water Accord and are third order or higher on both high- and low-slope land (as mapped by *Stock Exclusion Low Slope Land 2022* (Ministry for the Environment 2022b). For 'minor waterways, drains,' we used estimated proportions for ‘wide streams’ of first or second order on low-slope land. These estimates were supplemented by the HRC riparian fencing and planting data, and we used the higher estimate of the two data sources. The estimated extent of riparian fencing can be seen in Figure 1.

**Table 4. Summary of estimated fencing proportions from SRDM**

| District | Major (free-flowing streams) | | Minor (minor waterways/drains) | |
|---|---|---|---|---|
| | SnB[a] | DAI[a] | SnB[a] | DAI[a] |
| Horowhenua District | 0.50[b] | 0.87 | 0.30[b] | 0.56 |
| Manawatū District | 0.72 | 1.00 | 0.49 | 0.74 |
| Palmerston North City | 0.81 | 0.89[b] | 0.49 | 0.64[b] |
| Rangitikei District | 0.53 | 0.89[b] | 0.22 | 0.44 |
| Ruapehu District | 0.33 | 0.89[b] | 0.23 | 0.64[b] |
| Tararua District | 0.41 | 1.00 | 0.17 | 0.71 |
| Whanganui District | 0.41 | 0.89[b] | 0.30 | 0.64[b] |

[a] SnB refers to predominantly ‘sheep and beef’ and DAI refers to ‘dairy’ land use.

[b] Region averages were used where there were no survey data for the district.

Wide streams were classified based on the criteria defined in the Sustainable Dairying Water Accord (Dairy Environment Leadership Group 2013). Accord streams are freshwater waterways that are wider than 1 m, deeper than 30 cm, and have a permanent flow. The width of the streams was estimated using mean annual flow data for each REC2 segment (Booker & Hicks 2013; Semadeni-Davies & Elliott 2016; Whitehead & Booker 2020).

According to the Resource Management (Stock Exclusion) Regulations 2020, full implementation of riparian fencing is expected to be completed by 2025. To represent this in the modelling, we assumed that all wide streams intersecting with SnB and DAI land uses[1] within 'low slope land,' as well as all wide streams intersecting with DAI land use across all slopes, will be fenced by 2025 (as shown in Figure 1). Moreover, an additional 80 km per year of riparian fencing was randomly distributed across the region between 2025 and 2030 to represent ongoing work by the HRC Freshwater Team.

---

[1] Land use classification was based on the spatial layer provided by HRC.

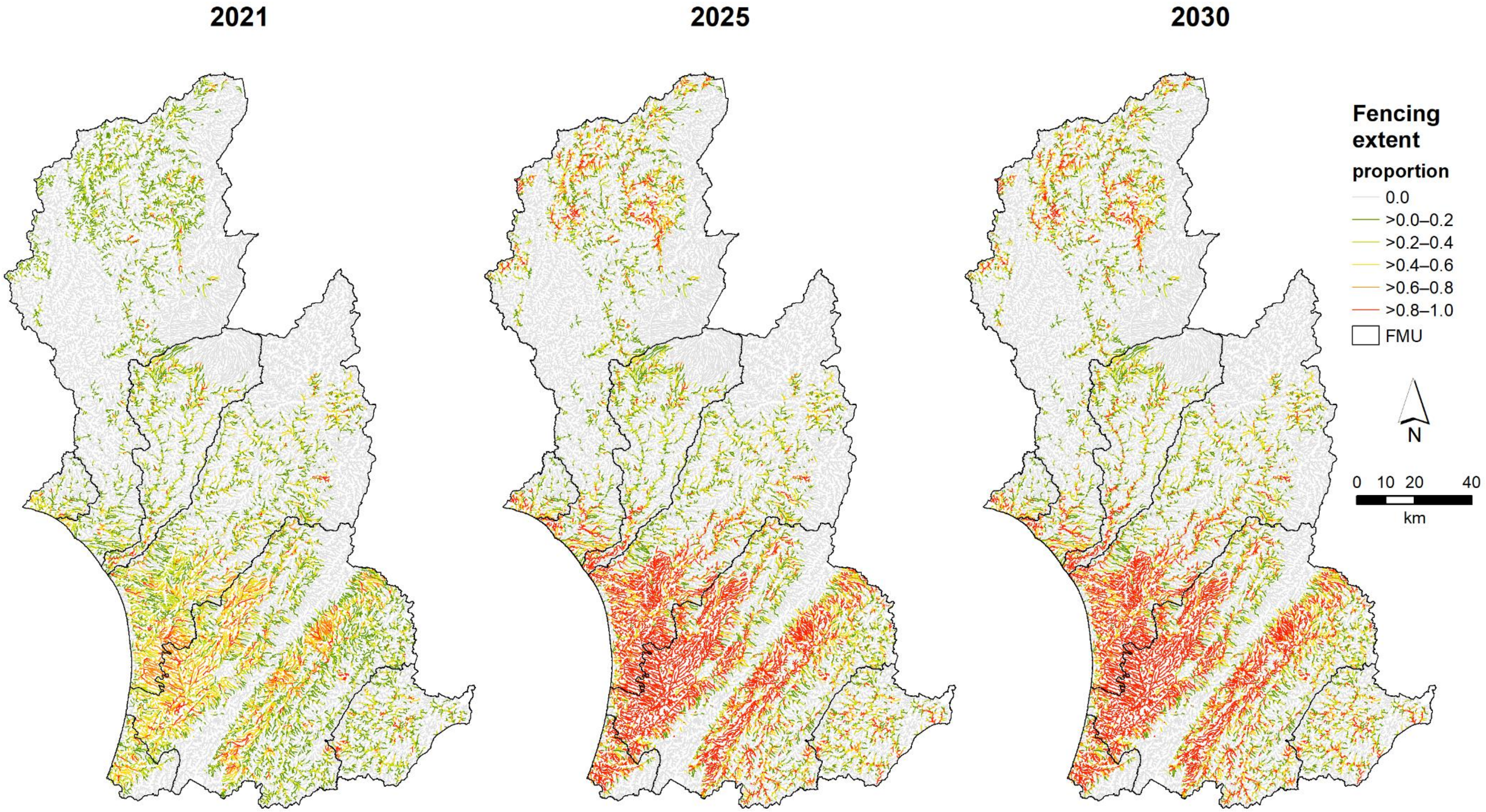

**Figure 1. Estimated extent of riparian fencing at the updated 2021 baseline, 2025, and 2030.**

### Reduction in hillslope sediment delivery to streams from surficial erosion

A sediment passing factor, the inverse of trapping efficiency, was calculated for the riparian buffer of the $j$th stream segment ($PF_{F_j}$) following Zhang et al. (2010):

$$PF_{F_j} = 1 - \frac{k(1-e^{-bw})}{100} \tag{3}$$

where $k$ and $b$ are fitted parameters equal to 90.9 and 0.446, respectively (Zhang et al. 2010), and $w$ is the buffer width. A mean buffer width for each REC2 segment was estimated based on the proportion of land class and the corresponding buffer width intersecting with the segment. A 3 m buffer width was used for wide streams intersecting with low-slope land; 2 m for wide streams intersecting with high-slope land; 5 m for streams intersecting with horticultural areas; and 10 m for streams intersecting with 'sites of aquatic significance', which were identified by HRC.

The reduction in suspended sediment load from surficial erosion due to fencing and stock exclusion in a reach ($S_{F_j}$) is a function of the proportion of the reach fenced ($FR_j$) and the buffer passing factor:

$$S_{F_j} = ES_j \times \left(1 - FR_j PF_{F_j}\right) \tag{4}$$

where $ES_j$ is the load from surficial erosion for the $j$th reach per REC2 watershed.

### Reduction in bank erosion

The reduced net suspended sediment load from bank erosion due to fencing and stock exclusion ($B_{F_j}$) is computed as:

$$B_{F_j} = B_j \times \left(1 - 0.8FR_j\right) \tag{5}$$

where $B_j$ is the net suspended sediment load from bank erosion without the effect of fences reducing erosion. A reduction of 80% in net suspended sediment load from bank erosion may be attributable to riparian fencing and stock exclusion (Dymond et al. 2016). This reflects the effect of reduced stock trampling and foraging on banks (Trimble 1994) as well as the potential for riparian woody vegetation to become better established in the absence of livestock over the longer term. The estimated 80% reduction assumes the buffer strip is no longer grazed and sufficient time has elapsed for banks to recover from previous trampling impacts, and for woody vegetation to become established and increase bank stability.

## 4.3 Selecting future SLUI farms for PS1

Under PS1 the selection of new WFPs occurred at a rate of 10,000 ha per year, which aligns with HRC's expected mapping rate for WFPs (Vale et al. 2022). Previously, the selection of new WFPs involved random sampling from unmapped farm boundaries, considering the proportions of top, high, low, and 'not' priority SLUI farms that had been mapped in the past. This prioritised top and high priority SLUI farms (Table 5). When a priority class had no remaining farms, the proportions of the remaining classes were adjusted, and random sampling continued until all unmapped farms were selected.

**Table 5. Past proportions of each SLUI farm priority**

| SLUI Priority | Past proportion of mapped farms (%) | Future area of new mapped farms per year (ha) |
|---|---|---|
| Not | 5 | 500 |
| Low | 20 | 2,000 |
| High | 40 | 4,000 |
| Top | 35 | 3,500 |
| **Total** | | **10,000** |

However, a minor adjustment was made to the new farm selection process in the present report. Farms in the 'not' priority class with no sediment load from mass movement processes were removed from the selection process for SLUI implementation. These farms were instead targeted for riparian fencing. This adjustment was made to maintain a similar selection order while still achieving the goal of mapping 10,000 ha of new farms each year. As a result, the implementation of new farm plans may start earlier for some farms compared to the modelling by Vale et al. (2022). Notably, a large proportion of top and high priority farms in the region have already been mapped.

Figure 2 provides the approximate proportions of each priority class selected each year. The total area of new farms mapped may exceed 10,000 ha if the final selected farm is large enough to reach the threshold.

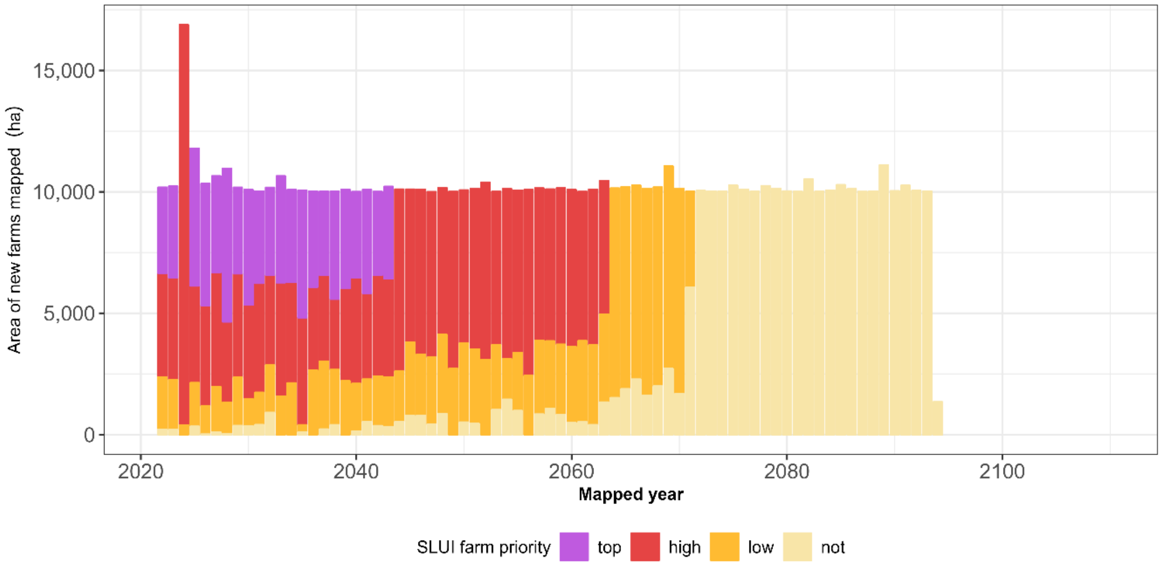

**Figure 2. Proportions of each priority class selected for new WFPs for PS1.**

## 4.4 Rate of implementation for PS2

Under PS2 it is assumed that all WFPs will be completed by 2030. The implementation of erosion mitigation works is based on the full implementation of appropriate works on top, high, and low land (HEL) classifications within specific timeframes. By 2035, works on top land will be fully implemented, followed by high land by 2045, and low land by 2065. These timeframes correspond to the SLUI farm priority classes of top, high, and low.

To estimate the proportion of each land classification within the unmapped farms, the average proportions of top, high, and low land currently mapped within the mapped WFPs are considered for each SLUI priority class.

To achieve the full implementation of appropriate works on top, high, and low land classifications by the specified timeframes, implementation rates of 10%, 5%, and 2.5%, respectively, are required. These rates, combined with the proportions of each land classification within the farms, determine the overall rate of implementation for each farm. The implementation rates are applied starting from 2025. The approach to determine maturation and effectiveness of the mitigation works remains the same as described in section 4.2.1.

# 5 Results

## 5.1 Suspended sediment loads

Mean annual suspended sediment loads are provided in two forms: 'total erosion', which represents the total suspended sediment load (t $yr^{-1}$) produced from all erosion processes in each REC2 watershed; and 'total net load', which represents the net suspended sediment load routed through the stream network to the coast accounting for lake trapping and floodplain deposition. These modelled loads do not include the impacts of climate change, which are described in section 5.3.

### Total erosion

Total erosion loads for each scenario are presented in Table 6 and Figure 3. The tables summarise erosion loads by FMU from 2021 to 2100 and provide load reductions achieved relative to the updated 2021 baseline loads for each policy scenario. The proportion of total load by erosion process for 2021 baseline is provided in Table 7. Mean annual suspended sediment yields (t $km^{-2}$ $yr^{-1}$) are provided for 2021 in Figure 4 and for 2100 for both policy scenarios in Figure 5.

Region-wide total erosion was estimated as 8.8 Mt $yr^{-1}$ for 2021. The highest sediment yields (>2,500 t $km^{-2}$ $yr^{-1}$) occur in a band of gully and shallow landslide-prone land mostly restricted to hill country in the Manawatū, Rangitīkei-Turakina, and Whangaehu FMUs. High sediment yields are also observed in a number of REC2 watersheds that produce high bank erosion loads (Figure 4). The proportion of each erosion process contributing to total erosion load varies across FMUs, which reflects the erosion terrains within each FMU (Table 6). Sediment load from shallow landslide erosion represented the dominant contribution (67%) across the region. However, contribution varied from 33% to 77% across the FMUs. Sediment load from bank erosion represented a 5% contribution across the region, however contributed varied from <1% to 32% across the FMUs.

By 2100 the estimated total erosion reduces to 4.6 Mt $yr^{-1}$ for PS1 and 3.6 Mt $yr^{-1}$ for PS2. This represents a region-wide reduction of 4.2 Mt $yr^{-1}$ (48%) for PS1 and 5.3 Mt $yr^{-1}$ (60%) for PS2 compared to the 2021 baseline loads.

Proportional reductions at 2100 vary across FMUs, ranging from 20% to 60% for PS1 and 21% to 70% for PS2. The smallest reductions are observed in the Waiopehu FMU, while the largest reductions occur in the Puketoi ki Tai and Whangaehu FMUs. Absolute load reductions by 2100 range from 0.01 to 1.2 Mt $yr^{-1}$ for PS1 and 0.01 to 1.4 Mt $yr^{-1}$ for PS2, with the Manawatū and Whanganui FMUs experiencing the largest reductions.

The rate of reduction in each FMU for PS1 depends on factors such as the proportion of SLUI farm priority classes, the order of new farms selected for implementation, the implementation rate, and the requirement for riparian fencing completion by 2025 (Figure 1). The impact of riparian fencing and planting is evident in the Waiopehu FMU, where a significant reduction is observed between 2021 and 2025 due to the relative extent of lowland riparian fencing and planting compared to other FMUs.

### Total net load

Total net suspended sediment loads for each scenario are presented in Table 8 and Figure 6. The tables summarise net sediment loads for selected rivers and total net load delivered to the coast from 2021 to 2100, and also provide load reductions achieved relative to the updated 2021 baseline loads for each policy scenario. Mean annual net suspended sediment loads for 2021 are visualised in Figure 7.

Region-wide total net suspended sediment load delivered to the coast for 2021 was 8.3 Mt $yr^{-1}$. The largest net sediment loads occurred in the Whanganui (2.7 Mt $yr^{-1}$) and Manawatū (2.3 Mt $yr^{-1}$) Rivers. By 2100 the total net sediment load delivered to the coast reduces to 4.3 Mt $yr^{-1}$ for PS1 and 3.3 Mt $yr^{-1}$ for PS2. This represents a region-wide net sediment load reduction of 4.0 Mt $yr^{-1}$ (48%) for PS1 and 5.0 Mt $yr^{-1}$ (60%) for PS2 compared to the 2021 baseline loads.

Proportional net suspended sediment load reductions at 2100 vary across FMUs, ranging from 18% to 60% for PS1 and 18% to 74% for PS2. The Ōhau River experiences the smallest reductions, while the Ākitio River (for PS1) and the Turakina River (for PS2) have the largest proportional reductions. Absolute net load reductions for selected rivers by 2100 range from 0.01 to 1.1 Mt $yr^{-1}$ for PS1 and 0.01 to 1.4 Mt $yr^{-1}$ for PS2. The Ōhau River has the smallest absolute load reduction, while the Manawatū and Whanganui Rivers have the largest reductions.

Overall, the projections indicate significant reductions in net suspended sediment loads delivered to the coast by 2100 under both PS1 and PS2 scenarios.

**Table 6. Total erosion load and difference from 2021 baseline for each scenario**

| | | Total erosion (Mt yr$^{-1}$) | | | | | Difference from 2021 baseline | | | | | | | |
|---|---|---|---|---|---|---|---|---|---|---|---|---|---|---|
| **Scenario** | **FMU** | **2021** | **2040** | **2060** | **2080** | **2100** | **2040** | | **2060** | | **2080** | | **2100** | |
| | | | | | | | **Mt yr$^{-1}$** | **%** | **Mt yr$^{-1}$** | **%** | **Mt yr$^{-1}$** | **%** | **Mt yr$^{-1}$** | **%** |
| PS1 | Kai Iwi | 0.11 | 0.10 | 0.09 | 0.08 | 0.07 | -0.01 | -8% | -0.02 | -15% | -0.03 | -25% | -0.04 | -34% |
| | Manawatū | 2.44 | 2.14 | 1.88 | 1.58 | 1.27 | -0.30 | -12% | -0.56 | -23% | -0.85 | -35% | -1.17 | -48% |
| | Puketoi ki Tai | 0.50 | 0.42 | 0.35 | 0.28 | 0.21 | -0.08 | -16% | -0.15 | -30% | -0.23 | -45% | -0.30 | -59% |
| | Rangitīkei-Turakina | 1.94 | 1.72 | 1.47 | 1.19 | 0.90 | -0.22 | -11% | -0.46 | -24% | -0.75 | -39% | -1.04 | -54% |
| | Waiopehu | 0.06 | 0.05 | 0.05 | 0.05 | 0.05 | -0.01 | -13% | -0.01 | -14% | -0.01 | -16% | -0.01 | -20% |
| | Whangaehu | 0.97 | 0.84 | 0.69 | 0.53 | 0.39 | -0.13 | -14% | -0.28 | -29% | -0.44 | -45% | -0.58 | -60% |
| | Whanganui | 2.79 | 2.57 | 2.33 | 2.03 | 1.72 | -0.22 | -8% | -0.46 | -16% | -0.76 | -27% | -1.07 | -38% |
| | **Total** | **8.80** | **7.84** | **6.87** | **5.74** | **4.60** | **-0.96** | **-11%** | **-1.93** | **-22%** | **-3.06** | **-35%** | **-4.20** | **-48%** |
| PS2 | Kai Iwi | 0.11 | 0.09 | 0.07 | 0.06 | 0.06 | -0.03 | -23% | -0.05 | -41% | -0.05 | -46% | -0.05 | -46% |
| | Manawatū | 2.44 | 1.69 | 1.10 | 1.02 | 1.02 | -0.74 | -30% | -1.34 | -55% | -1.42 | -58% | -1.42 | -58% |
| | Puketoi ki Tai | 0.50 | 0.31 | 0.17 | 0.15 | 0.15 | -0.19 | -38% | -0.34 | -66% | -0.35 | -70% | -0.35 | -70% |
| | Rangitīkei-Turakina | 1.94 | 1.27 | 0.71 | 0.64 | 0.64 | -0.66 | -34% | -1.23 | -63% | -1.29 | -67% | -1.29 | -67% |
| | Waiopehu | 0.06 | 0.05 | 0.05 | 0.04 | 0.04 | -0.01 | -16% | -0.01 | -20% | -0.01 | -21% | -0.01 | -21% |
| | Whangaehu | 0.97 | 0.60 | 0.31 | 0.29 | 0.29 | -0.37 | -38% | -0.66 | -68% | -0.68 | -70% | -0.68 | -70% |
| | Whanganui | 2.79 | 2.05 | 1.47 | 1.36 | 1.35 | -0.73 | -26% | -1.32 | -47% | -1.43 | -51% | -1.44 | -52% |
| | **Total** | **8.80** | **6.06** | **3.87** | **3.57** | **3.55** | **-2.74** | **-31%** | **-4.93** | **-56%** | **-5.23** | **-59%** | **-5.25** | **-60%** |

**Table 7 Proportion of erosion load contribution by each erosion process at 2021 baseline**

| | Proportion erosion process contribution at 2021 baseline (%) | | | | |
|---|---|---|---|---|---|
| **FMU** | **Shallow landslide erosion** | **Earthflow erosion** | **Gully erosion** | **Surficial erosion** | **Bank erosion** |
| Kai Iwi | 77 | 0 | 18 | 5 | <1 |
| Manawatū | 55 | 2 | 24 | 11 | 8 |
| Puketoi ki Tai | 72 | 18 | 0 | 8 | 3 |
| Rangitīkei-Turakina | 66 | 1 | 22 | 7 | 4 |
| Waiopehu | 33 | 0 | 0 | 35 | 32 |
| Whangaehu | 76 | <1 | 13 | 6 | 6 |
| Whanganui | 76 | 3 | 4 | 14 | 3 |
| **Region-wide** | **67** | **3** | **15** | **10** | **5** |

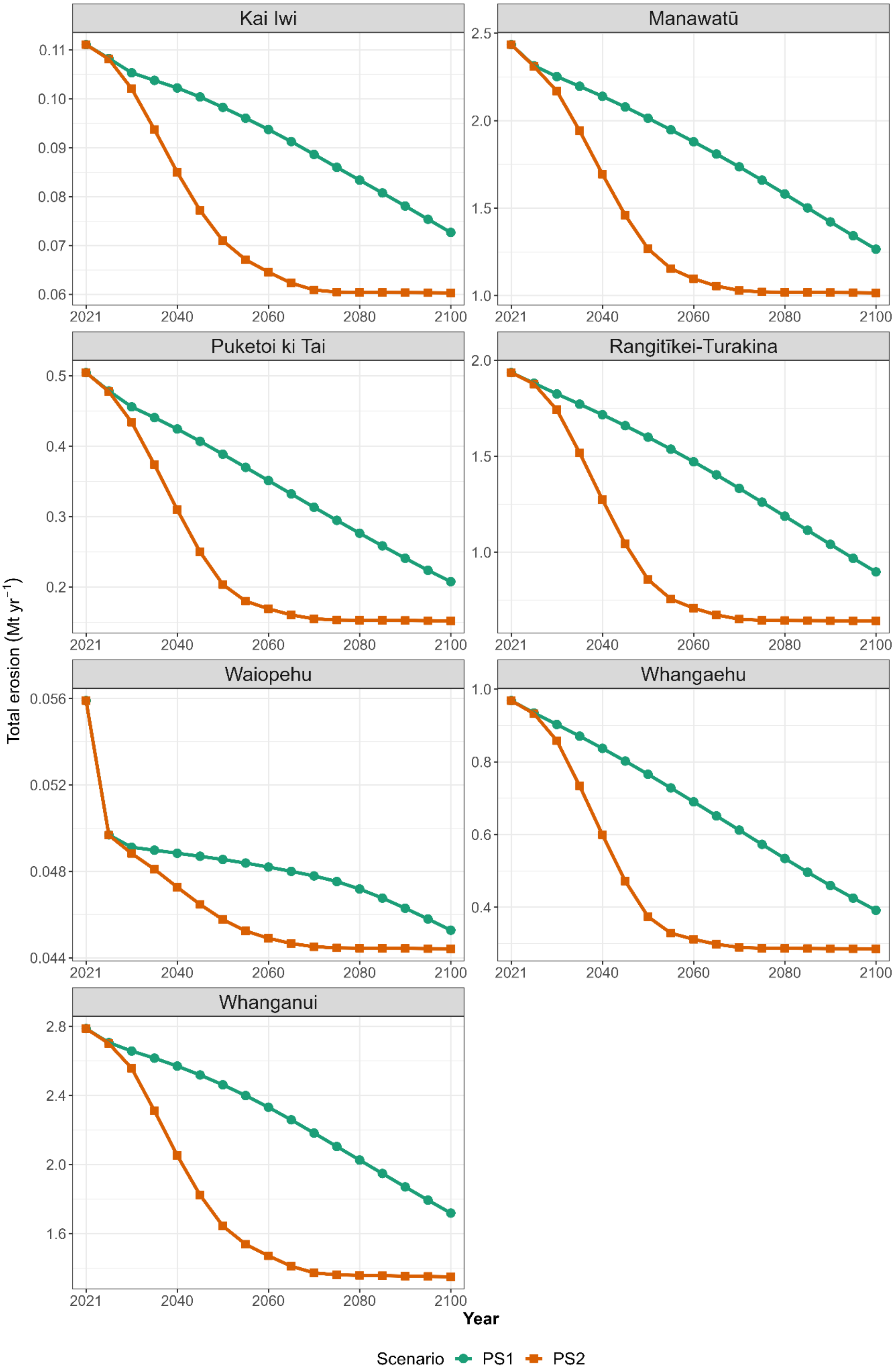

**Figure 3. Total erosion loads (Mt yr$^{-1}$) summarised by FMU for PS1 and PS2 at 5-year intervals.**

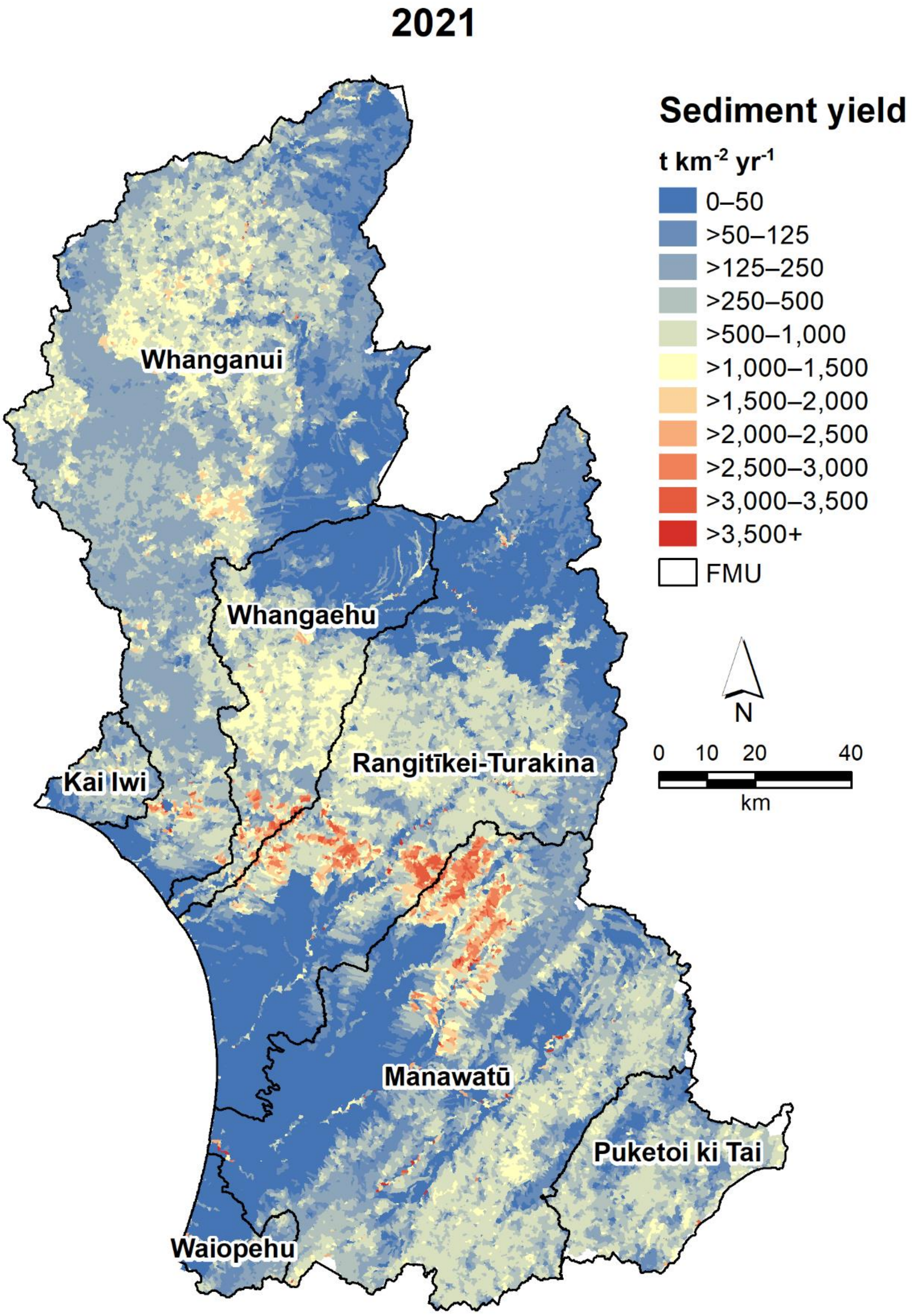

**Figure 4. Mean annual suspended sediment yield (t km$^{-2}$ yr$^{-1}$) at the updated 2021 baseline.**

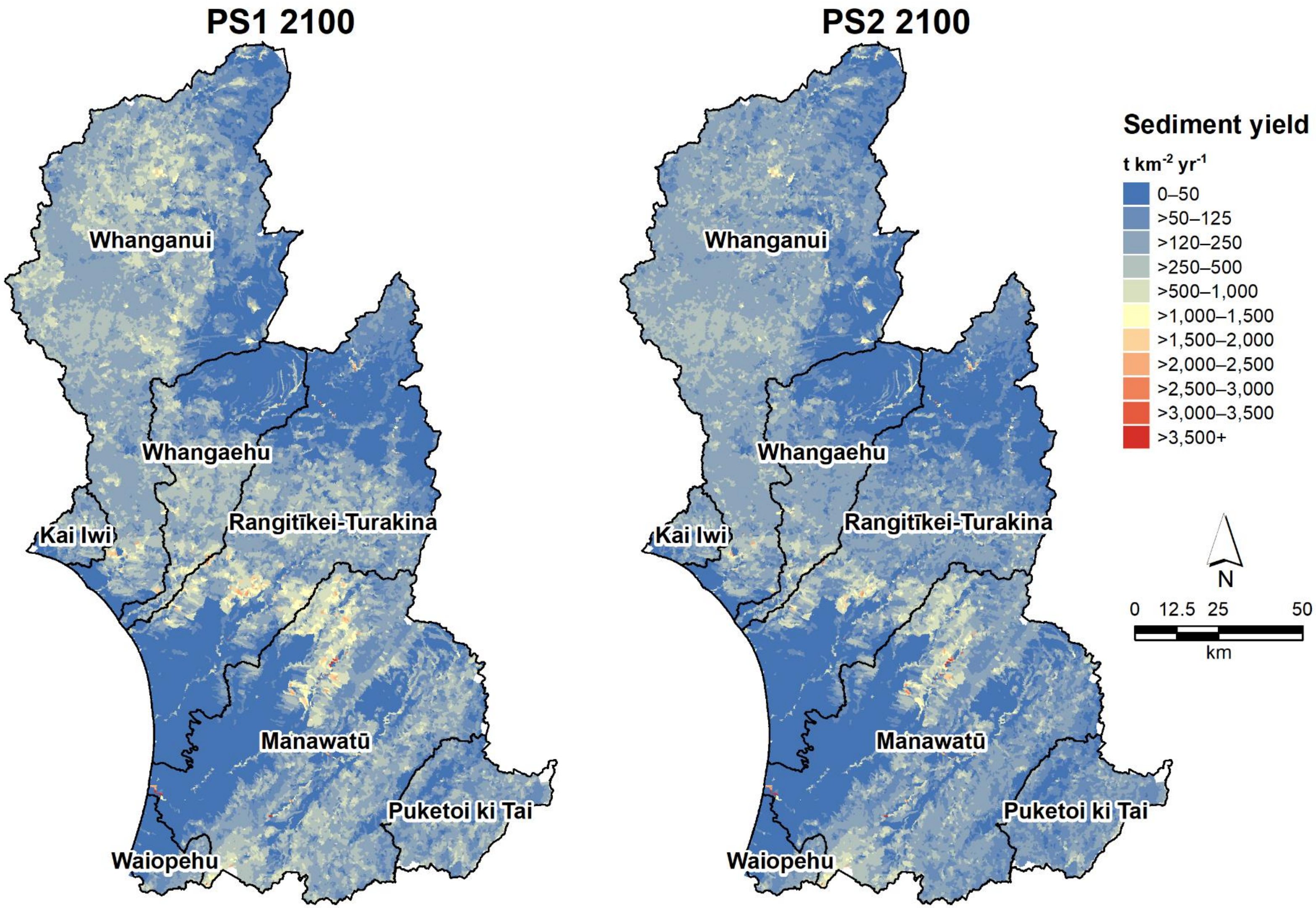

**Figure 5. Mean annual suspended sediment yield (t km$^{-2}$ yr$^{-1}$) for PS1 and PS2 at 2100.**

**Table 8. Total net load and difference from 2021 of selected rivers for PS1 and PS2**

| Scenario | River | Total net load ($Mt\ yr^{-1}$) | | | | | Difference from 2021 | | | | | | | |
|---|---|---|---|---|---|---|---|---|---|---|---|---|---|---|
| | | 2021 | 2040 | 2060 | 2080 | 2100 | 2040 | | 2060 | | 2080 | | 2100 | |
| | | | | | | | $Mt\ yr^{-1}$ | % | $Mt\ yr^{-1}$ | % | $Mt\ yr^{-1}$ | % | $Mt\ yr^{-1}$ | % |
| PS1 | Kai iwi | 0.06 | 0.06 | 0.05 | 0.05 | 0.04 | -0.01 | -8% | -0.01 | -16% | -0.02 | -25% | -0.02 | -35% |
| | Whanganui | 2.65 | 2.44 | 2.21 | 1.92 | 1.63 | -0.21 | -8% | -0.43 | -16% | -0.72 | -27% | -1.02 | -38% |
| | Whangaehu | 0.92 | 0.80 | 0.66 | 0.51 | 0.37 | -0.13 | -14% | -0.27 | -29% | -0.41 | -45% | -0.55 | -59% |
| | Turakina | 0.65 | 0.58 | 0.48 | 0.37 | 0.26 | -0.07 | -11% | -0.17 | -26% | -0.28 | -43% | -0.39 | -59% |
| | Rangitīkei | 1.17 | 1.03 | 0.90 | 0.74 | 0.57 | -0.14 | -12% | -0.27 | -23% | -0.43 | -37% | -0.60 | -51% |
| | Manawatū | 2.30 | 2.01 | 1.77 | 1.48 | 1.18 | -0.29 | -12% | -0.53 | -23% | -0.82 | -35% | -1.12 | -49% |
| | Ākitio | 0.22 | 0.18 | 0.15 | 0.12 | 0.09 | -0.04 | -18% | -0.07 | -32% | -0.10 | -47% | -0.13 | -60% |
| | Ōhau | 0.04 | 0.03 | 0.03 | 0.03 | 0.03 | -0.01 | -13% | -0.01 | -13% | -0.01 | -15% | -0.01 | -18% |
| | **Total*** | **8.33** | **7.41** | **6.48** | **5.41** | **4.33** | **-0.92** | **-11%** | **-1.84** | **-22%** | **-2.92** | **-35%** | **-4.00** | **-48%** |
| PS2 | Kai iwi | 0.06 | 0.05 | 0.04 | 0.04 | 0.04 | -0.02 | -24% | -0.03 | -41% | -0.03 | -44% | -0.03 | -44% |
| | Whanganui | 2.65 | 1.95 | 1.40 | 1.29 | 1.28 | -0.70 | -26% | -1.25 | -47% | -1.36 | -51% | -1.37 | -52% |
| | Whangaehu | 0.92 | 0.57 | 0.30 | 0.27 | 0.27 | -0.35 | -38% | -0.63 | -68% | -0.65 | -70% | -0.65 | -70% |
| | Turakina | 0.65 | 0.41 | 0.19 | 0.17 | 0.17 | -0.24 | -37% | -0.46 | -70% | -0.48 | -74% | -0.48 | -74% |
| | Rangitīkei | 1.17 | 0.78 | 0.46 | 0.42 | 0.42 | -0.39 | -33% | -0.71 | -60% | -0.75 | -64% | -0.75 | -64% |
| | Manawatū | 2.30 | 1.59 | 1.02 | 0.95 | 0.95 | -0.71 | -31% | -1.28 | -55% | -1.35 | -59% | -1.35 | -59% |
| | Ākitio | 0.22 | 0.13 | 0.07 | 0.07 | 0.07 | -0.08 | -39% | -0.14 | -66% | -0.15 | -69% | -0.15 | -69% |
| | Ōhau | 0.04 | 0.03 | 0.03 | 0.03 | 0.03 | -0.01 | -15% | -0.01 | -18% | -0.01 | -18% | -0.01 | -18% |
| | **Total*** | **8.33** | **5.72** | **3.64** | **3.35** | **3.34** | **-2.61** | **-31%** | **-4.69** | **-56%** | **-4.98** | **-60%** | **-4.99** | **-60%** |

[*] 'Total' refers to the total net load delivered to the coast for the whole region.

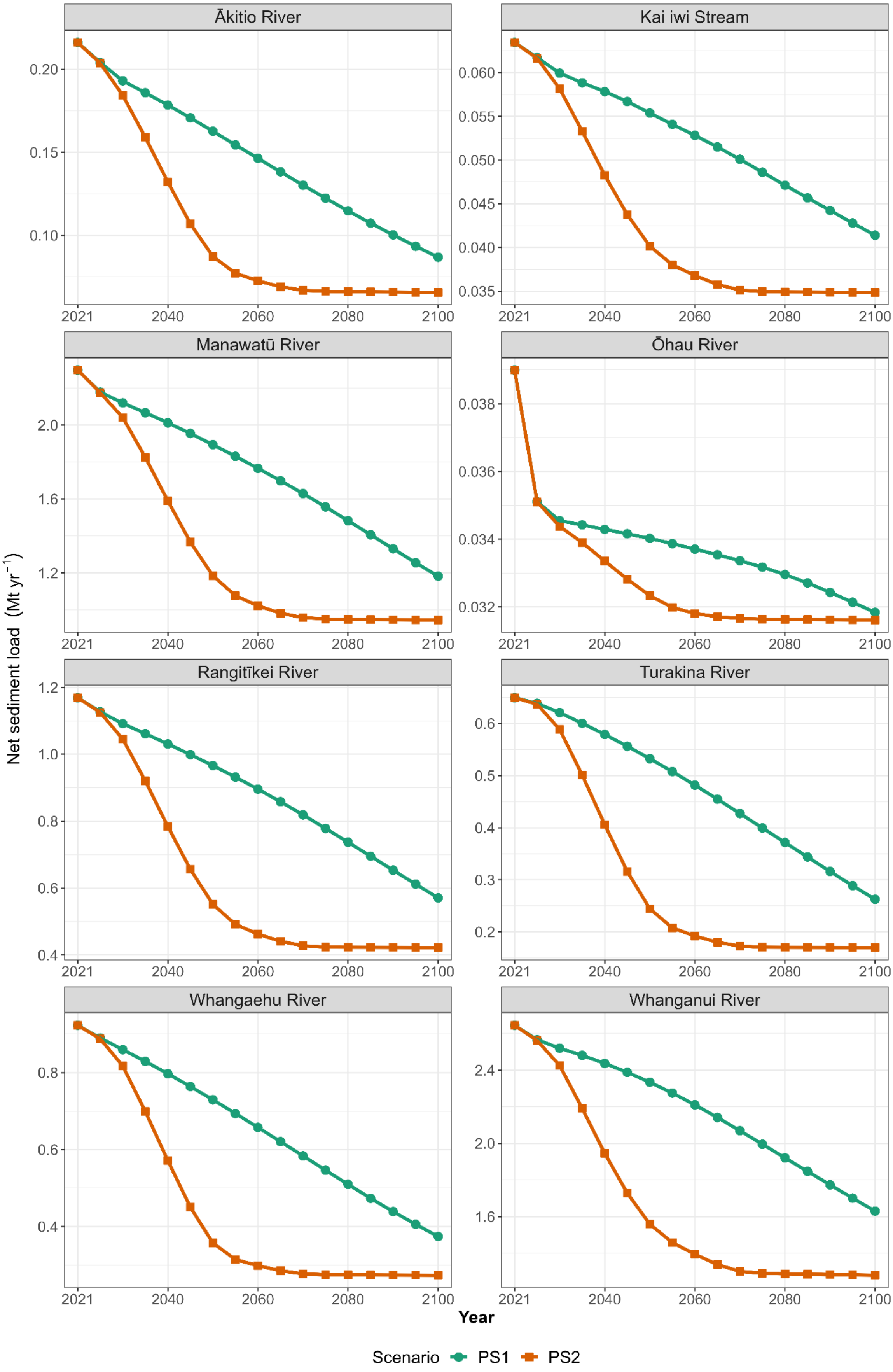

**Figure 6. Total net suspended sediment load (Mt yr$^{-1}$) for selected river catchments for PS1 and PS2 at 5-year intervals.**

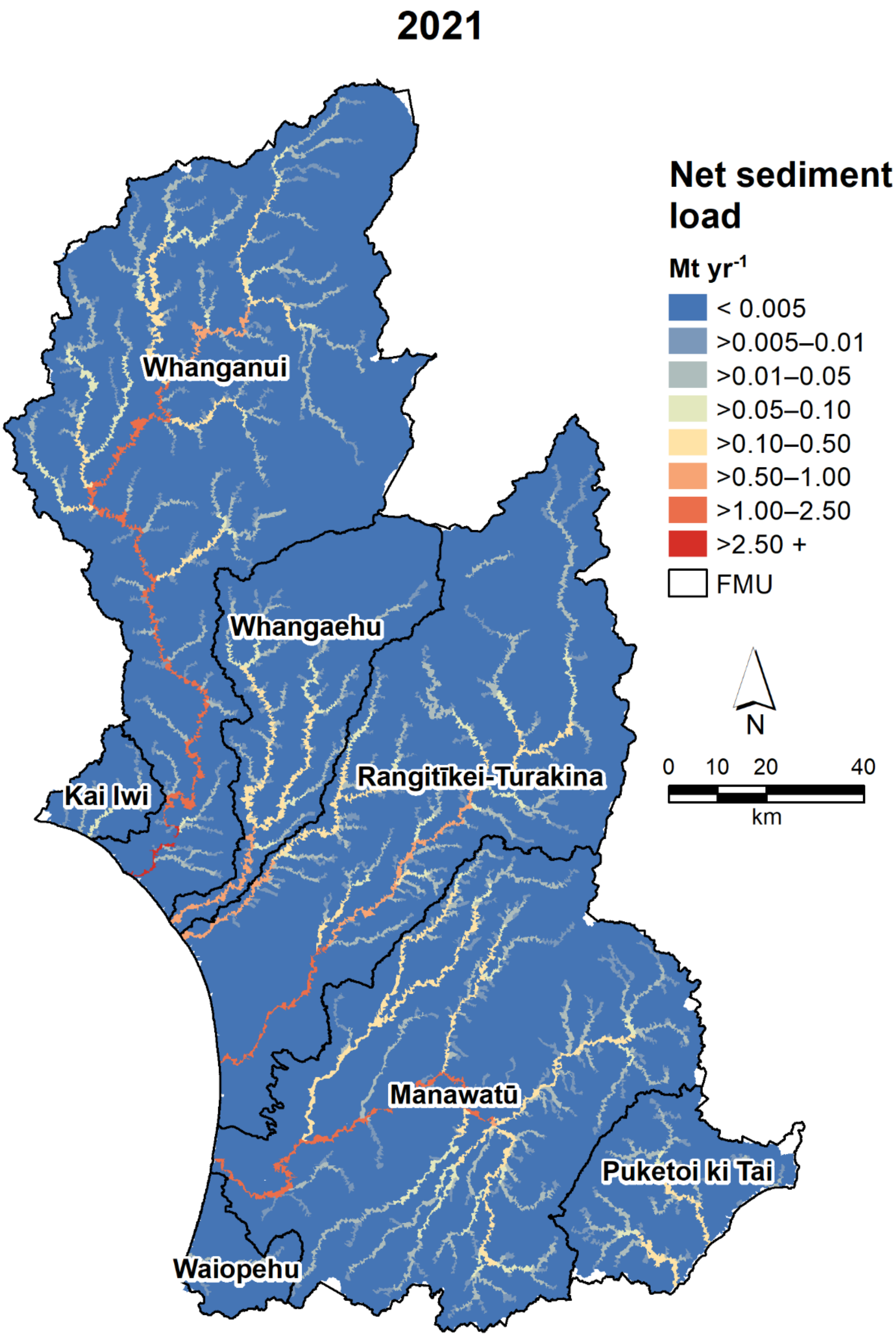

**Figure 7. Mean annual net suspended sediment load (Mt yr$^{-1}$) at the updated 2021 baseline.**

## 5.2 Sediment load reductions required to meet NPS-FM visual clarity attribute bands

The required reductions in suspended sediment load to meet the NPS-FM 2020 attribute bands were modelled as proportional and absolute reductions for each REC2 segment. The results are summarised in Table 9 for PS1 and in Table 10 for PS2, and visualised in Figures 8–11 for proportional reductions and Figures 12–15 for absolute load reductions. Appendix F provides additional summaries of the length and proportions of REC2 segments achieving NPS-FM 2020 attribute bands according to stream order for each FMU.

The region-wide proportions of REC2 segments achieving A band, B band, and national bottom line (NBL) in 2021 were 38%, 60%, and 75%, respectively. By 2100 these proportions increase to 72%, 84%, and 90% for PS1, and 74%, 85%, and 91% for PS2. For higher-order REC2 segments, the proportion achieving each attribute band is low compared to lower-order segments. For example, in 2021, 38–43% of REC2 segments from stream orders ≤5 achieved the A band, but only 8% and 0% of segments from stream orders 6 and 7, respectively. Similarly, 70–78% of REC2 segments from stream orders ≤5 achieved the NBL, but only 46% and 13% of segments from stream orders 6 and 7, respectively. This is probably because higher-order streams require larger absolute load reductions that depend on reductions occurring throughout the upstream catchment area.

Large proportional reductions required at 2021 occur throughout the region; however, the highest reductions are particularly evident in the lowland coastal areas of Manawatū and Rangitīkei-Turakina, and are also observed along a number of higher-order REC2 segments (Figure 8). The proportion of REC2 segments achieving the NBL increases over time for PS1 and PS2, but this occurs earlier for PS2 than for PS1 due to the earlier implementation of SLUI erosion mitigation in upstream catchment areas. There are still some lowland REC2 segments that require proportional reductions to achieve the NBL by 2100, although these represent low absolute loads (Figure 13).

The regional pattern of sediment load reductions and achieved attribute states can be attributed to three main factors:

- the focus of SLUI erosion mitigation works on hill country areas, which determines the selection order of new farm plans
- extensive implementation of riparian fencing and planting in lowland areas by 2025
- the spatial variation in visual clarity thresholds, which are based on the spatial distribution of suspended sediment classes used to define threshold values.

Sediment load reductions in the hill country were modelled based on the implementation of specific works within the SLUI programme. These works primarily target farms with highly erodible hill country. Within SLUI, priority is given to top and high priority farms, which are typically found in hill country areas. When identifying new farms for WFPs, these top and high priority farms are prioritised for selection. Most lowland farms are classified as 'not' priority and are considered the lowest priority in SLUI. As a result, the largest reductions in sediment load for lowland 'not' priority farms are expected to occur once stream fencing and planting initiatives are completed by 2025. Further reductions in sediment load for 'not' priority farms where some mass movement erosion occurs will mostly take place beyond 2025.

Riparian fencing implementation focuses on lowland streams. The current extent of fencing is determined based on available spatial data on riparian fencing and planting. Estimates from the SRDM are also used, according to district and land use. The baseline visual clarity is linked to the updated 2021 baseline sediment load estimate, which is influenced by the estimated extent of current fencing. As a result, the potential sediment load reductions that can be achieved are constrained by the length of the remaining stream network available for fencing. While SRDM provides some ability to estimate the extent of fencing, particularly at a district and land-use level, this approach does introduce some unknown uncertainty, especially at the level of individual REC2 segment watersheds.

The attribute band visual clarity thresholds for a given REC2 segment are determined by the assigned suspended sediment class. There are four suspended sediment classes, and although they consider factors such as climate, topography, and geology via the River Environment Classification to assign the class (Ministry for the Environment 2020), this can result in abrupt changes in visual clarity thresholds and required load reductions between adjacent REC2 segments (Appendix C).

**Table 9. Length and proportion of REC2 segments achieving each visual clarity attribute band, summarised by stream order for PS1**

| PS1 | Stream order | Total length km | REC2 segments achieving for selected years | | | | | | | | | |
|---|---|---|---|---|---|---|---|---|---|---|---|---|
| | | | 2021 | | 2040 | | 2060 | | 2080 | | 2100 | |
| | | | km | % | km | % | km | % | km | % | km | % |
| A band | 1 | 18,148 | 7,221 | 40% | 8,733 | 48% | 10,313 | 57% | 11,827 | 65% | 12,890 | 71% |
| | 2 | 9,101 | 3,565 | 39% | 4,299 | 47% | 5,036 | 55% | 5,861 | 64% | 6,527 | 72% |
| | 3 | 4,521 | 1,779 | 39% | 2,084 | 46% | 2,455 | 54% | 2,936 | 65% | 3,290 | 73% |
| | 4 | 2,381 | 905 | 38% | 1,101 | 46% | 1,349 | 57% | 1,599 | 67% | 1,845 | 78% |
| | 5 | 1,388 | 593 | 43% | 642 | 46% | 693 | 50% | 903 | 65% | 1,052 | 76% |
| | 6 | 676 | 52 | 8% | 88 | 13% | 158 | 23% | 318 | 47% | 519 | 77% |
| | 7 | 505 | - | 0% | - | 0% | 5 | 1% | 117 | 23% | 189 | 37% |
| | **Total** | **36,720** | **14,115** | **38%** | **16,947** | **46%** | **20,009** | **54%** | **23,560** | **64%** | **26,312** | **72%** |
| B band | 1 | 18,148 | 11,386 | 63% | 12,653 | 70% | 13,726 | 76% | 14,555 | 80% | 15,180 | 84% |
| | 2 | 9,101 | 5,619 | 62% | 6,225 | 68% | 6,797 | 75% | 7,262 | 80% | 7,611 | 84% |
| | 3 | 4,521 | 2,762 | 61% | 3,045 | 67% | 3,333 | 74% | 3,631 | 80% | 3,828 | 85% |
| | 4 | 2,381 | 1,399 | 59% | 1,532 | 64% | 1,718 | 72% | 1,917 | 81% | 2,078 | 87% |
| | 5 | 1,388 | 793 | 57% | 889 | 64% | 1,020 | 73% | 1,127 | 81% | 1,224 | 88% |
| | 6 | 676 | 130 | 19% | 223 | 33% | 333 | 49% | 508 | 75% | 598 | 88% |
| | 7 | 505 | 4 | 1% | 39 | 8% | 119 | 23% | 178 | 35% | 241 | 48% |
| | **Total** | **36,720** | **22,094** | **60%** | **24,607** | **67%** | **27,047** | **74%** | **29,179** | **79%** | **30,760** | **84%** |
| NBL | 1 | 18,148 | 14,116 | 78% | 15,061 | 83% | 15,505 | 85% | 15,914 | 88% | 16,239 | 89% |
| | 2 | 9,101 | 6,909 | 76% | 7,434 | 82% | 7,703 | 85% | 7,943 | 87% | 8,124 | 89% |
| | 3 | 4,521 | 3,412 | 75% | 3,671 | 81% | 3,835 | 85% | 3,953 | 87% | 4,063 | 90% |
| | 4 | 2,381 | 1,751 | 74% | 1,917 | 81% | 2,021 | 85% | 2,137 | 90% | 2,210 | 93% |
| | 5 | 1,388 | 978 | 70% | 1,075 | 77% | 1,133 | 82% | 1,219 | 88% | 1,297 | 93% |
| | 6 | 676 | 308 | 46% | 398 | 59% | 485 | 72% | 595 | 88% | 634 | 94% |
| | 7 | 505 | 66 | 13% | 141 | 28% | 189 | 37% | 241 | 48% | 337 | 67% |
| | **Total** | **36,720** | **27,540** | **75%** | **29,699** | **81%** | **30,871** | **84%** | **32,002** | **87%** | **32,904** | **90%** |

**Table 10. Length and proportion of REC2 segments achieving each visual clarity attribute band, summarised by stream order for PS2**

| PS2 | Stream order | Total length km | REC2 segments achieving for selected years | | | | | | | | | |
|---|---|---|---|---|---|---|---|---|---|---|---|---|
| | | | 2021 | | 2040 | | 2060 | | 2080 | | 2100 | |
| | | | km | % | km | % | km | % | km | % | km | % |
| A band | 1 | 18,148 | 7,221 | 40% | 11,383 | 63% | 12,932 | 71% | 13,082 | 72% | 13,149 | 72% |
| | 2 | 9,101 | 3,565 | 39% | 5,658 | 62% | 6,539 | 72% | 6,627 | 73% | 6,656 | 73% |
| | 3 | 4,521 | 1,779 | 39% | 2,798 | 62% | 3,338 | 74% | 3,385 | 75% | 3,395 | 75% |
| | 4 | 2,381 | 905 | 38% | 1,541 | 65% | 1,949 | 82% | 1,959 | 82% | 1,961 | 82% |
| | 5 | 1,388 | 593 | 43% | 872 | 63% | 1,129 | 81% | 1,138 | 82% | 1,142 | 82% |
| | 6 | 676 | 52 | 8% | 246 | 36% | 557 | 82% | 619 | 92% | 619 | 92% |
| | 7 | 505 | - | 0% | 62 | 12% | 260 | 52% | 286 | 57% | 286 | 57% |
| | **Total** | **36,720** | **14,115** | **38%** | **22,561** | **61%** | **26,704** | **73%** | **27,096** | **74%** | **27,208** | **74%** |
| B band | 1 | 18,148 | 11,386 | 63% | 14,399 | 79% | 15,185 | 84% | 15,250 | 84% | 15,298 | 84% |
| | 2 | 9,101 | 5,619 | 62% | 7,173 | 79% | 7,613 | 84% | 7,669 | 84% | 7,689 | 84% |
| | 3 | 4,521 | 2,762 | 61% | 3,577 | 79% | 3,850 | 85% | 3,873 | 86% | 3,882 | 86% |
| | 4 | 2,381 | 1,399 | 59% | 1,895 | 80% | 2,113 | 89% | 2,125 | 89% | 2,127 | 89% |
| | 5 | 1,388 | 793 | 57% | 1,086 | 78% | 1,248 | 90% | 1,254 | 90% | 1,254 | 90% |
| | 6 | 676 | 130 | 19% | 446 | 66% | 670 | 99% | 670 | 99% | 670 | 99% |
| | 7 | 505 | 4 | 1% | 164 | 33% | 297 | 59% | 427 | 84% | 427 | 85% |
| | **Total** | **36,720** | **22,094** | **60%** | **28,740** | **78%** | **30,976** | **84%** | **31,268** | **85%** | **31,346** | **85%** |
| NBL | 1 | 18,148 | 14,116 | 78% | 15,846 | 87% | 16,249 | 90% | 16,300 | 90% | 16,336 | 90% |
| | 2 | 9,101 | 6,909 | 76% | 7,903 | 87% | 8,132 | 89% | 8,168 | 90% | 8,180 | 90% |
| | 3 | 4,521 | 3,412 | 75% | 3,930 | 87% | 4,079 | 90% | 4,091 | 90% | 4,093 | 91% |
| | 4 | 2,381 | 1,751 | 74% | 2,086 | 88% | 2,225 | 93% | 2,233 | 94% | 2,233 | 94% |
| | 5 | 1,388 | 978 | 70% | 1,169 | 84% | 1,296 | 93% | 1,299 | 94% | 1,299 | 94% |
| | 6 | 676 | 308 | 46% | 577 | 85% | 671 | 99% | 671 | 99% | 671 | 99% |
| | 7 | 505 | 66 | 13% | 238 | 47% | 430 | 85% | 443 | 88% | 443 | 88% |
| | **Total** | **36,720** | **27,540** | **75%** | **31,748** | **86%** | **33,082** | **90%** | **33,205** | **90%** | **33,254** | **91%** |

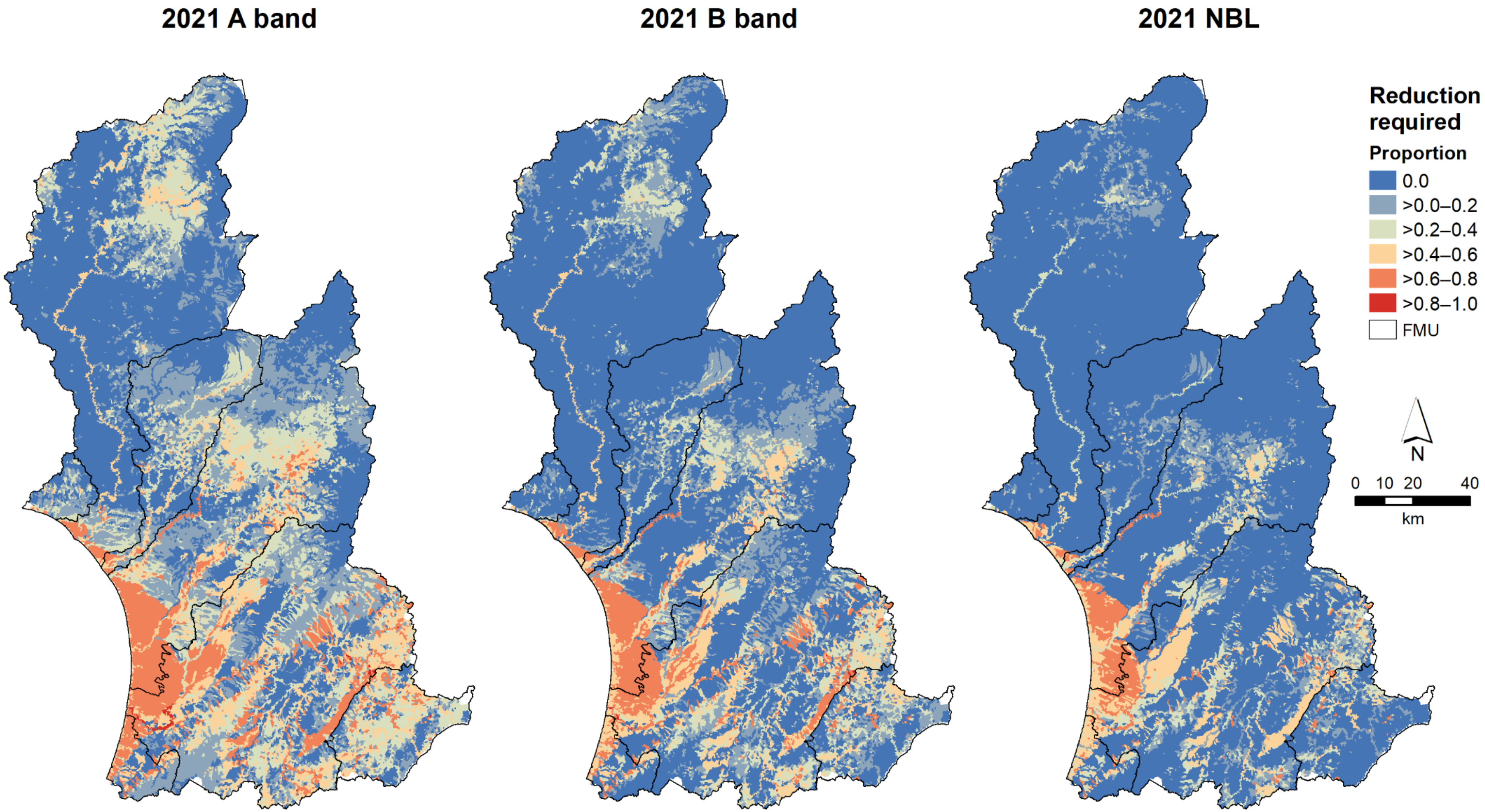

**Figure 8. Proportional reduction in net load required to achieve NPS-FM visual clarity attribute bands and NBL at the updated 2021 baseline.**

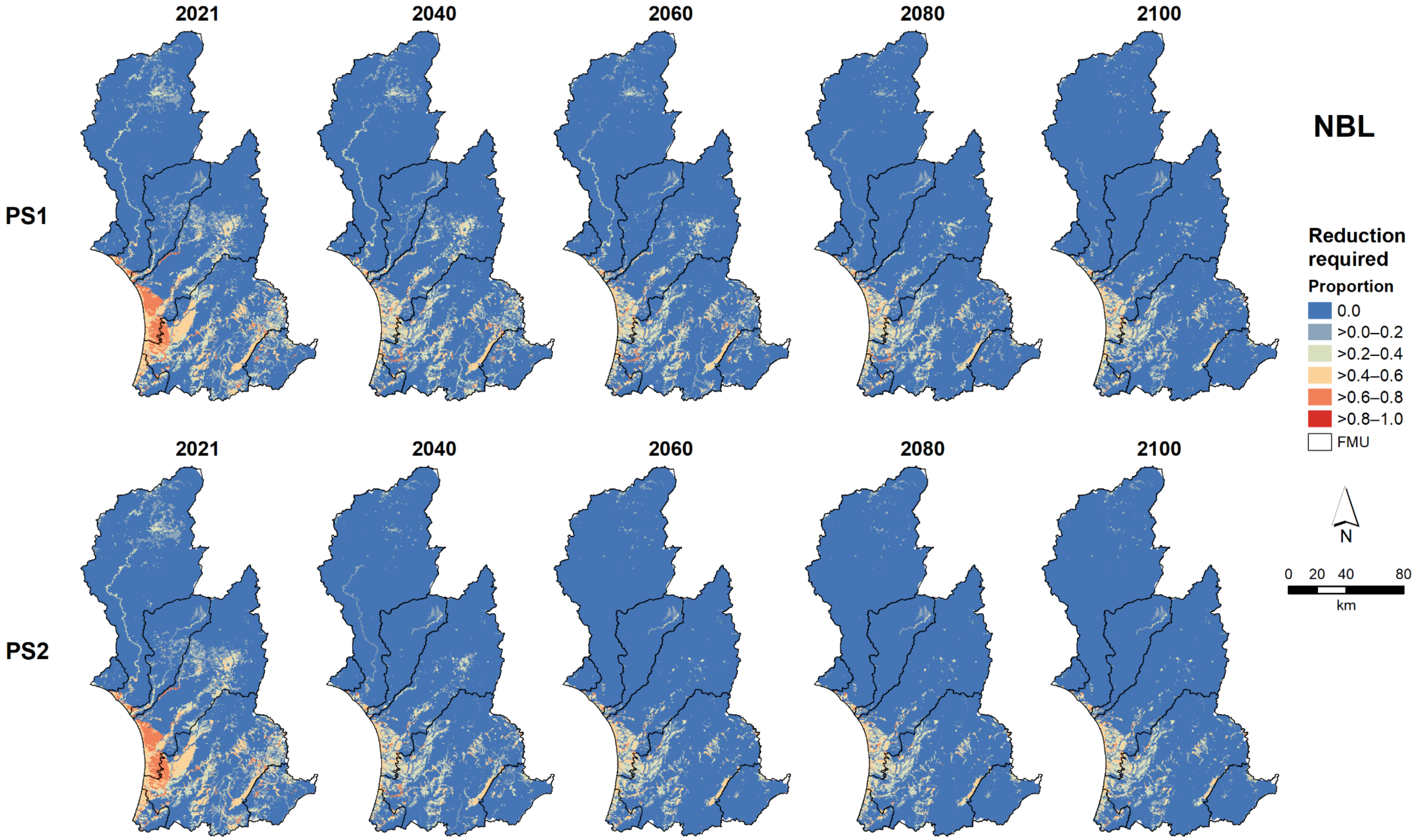

**Figure 9. Proportional reduction in net load required to achieve NPS-FM visual clarity NBL from 2021 to 2100 for PS1 and PS2.**

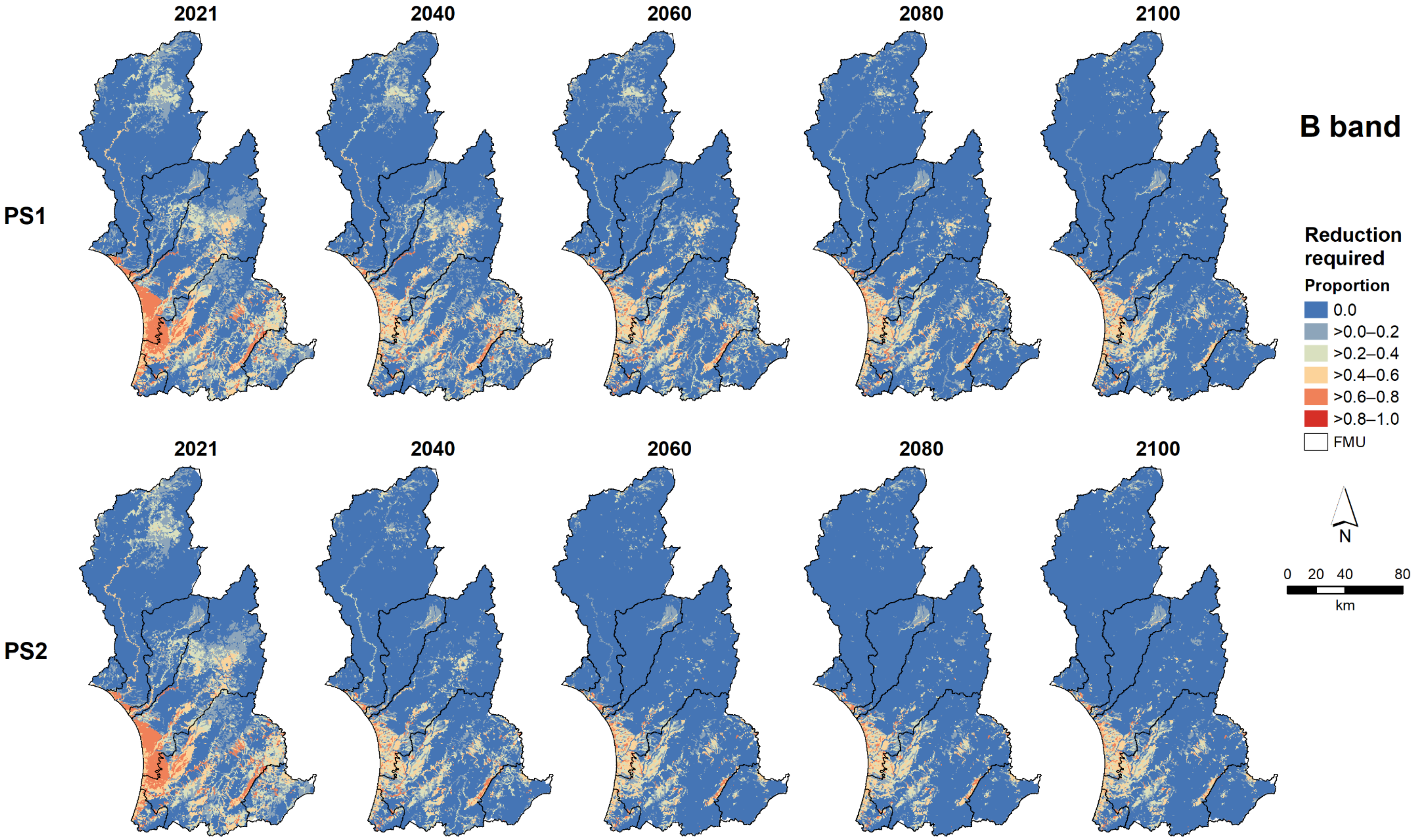

**Figure 10. Proportional reduction in net load required to achieve NPS-FM visual clarity B band from 2021 to 2100 for PS1 and PS2.**

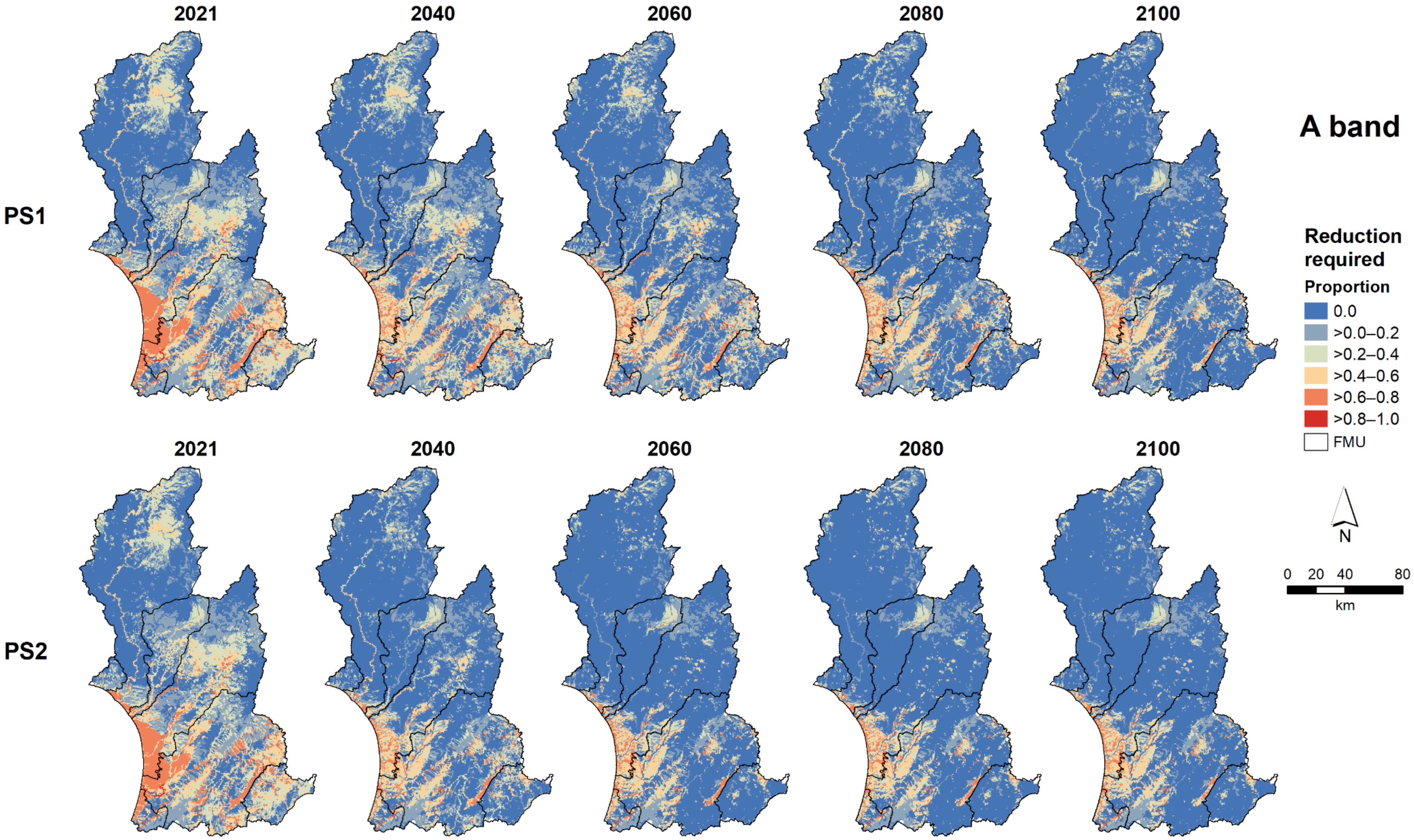

**Figure 11. Proportional reduction in net load required to achieve NPS-FM visual clarity A band from 2021 to 2100 for PS1 and PS2.**

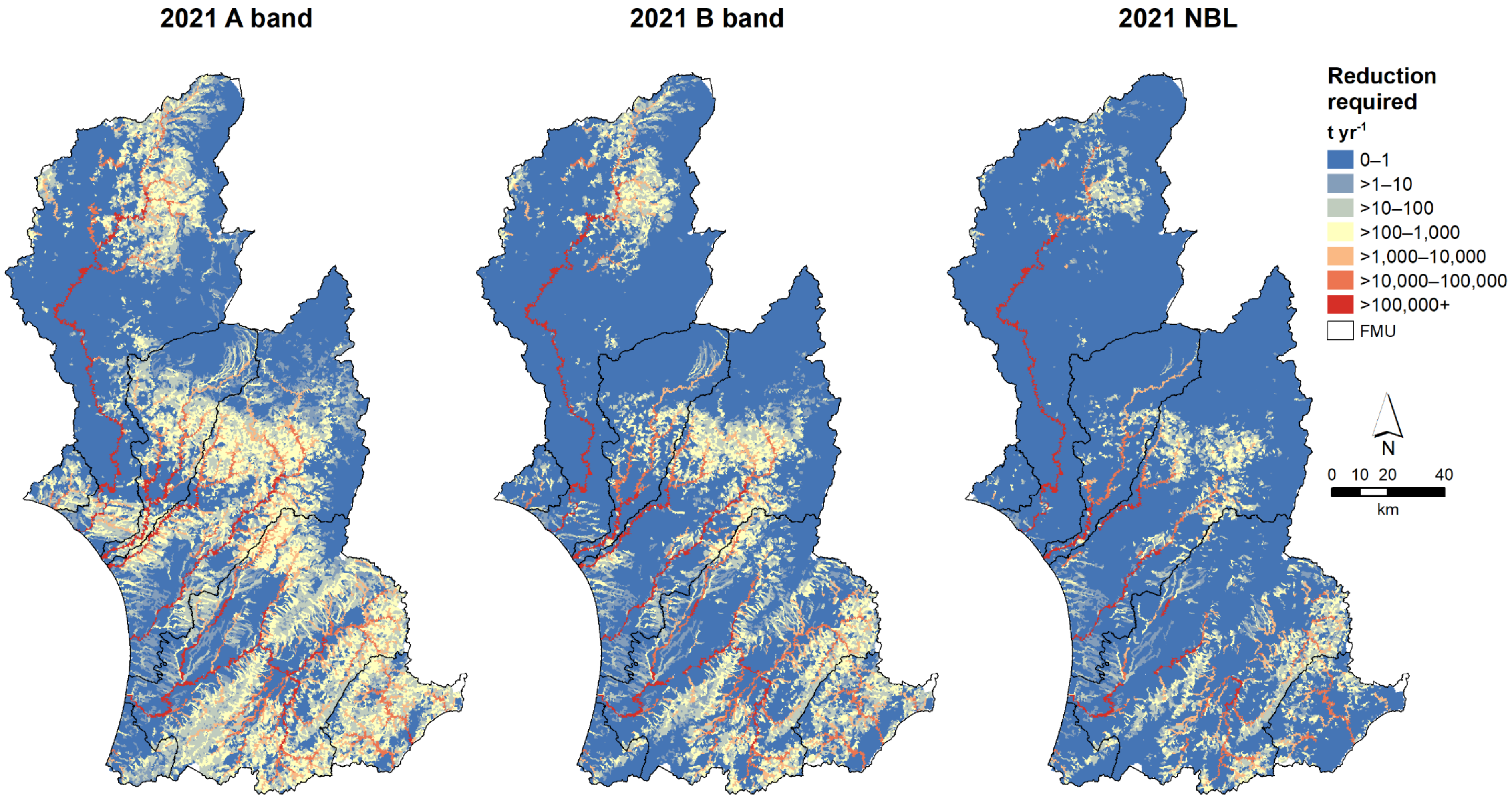

**Figure 12. Absolute net load reduction required to achieve NPS-FM visual clarity attribute bands and NBL at the updated 2021 baseline.**

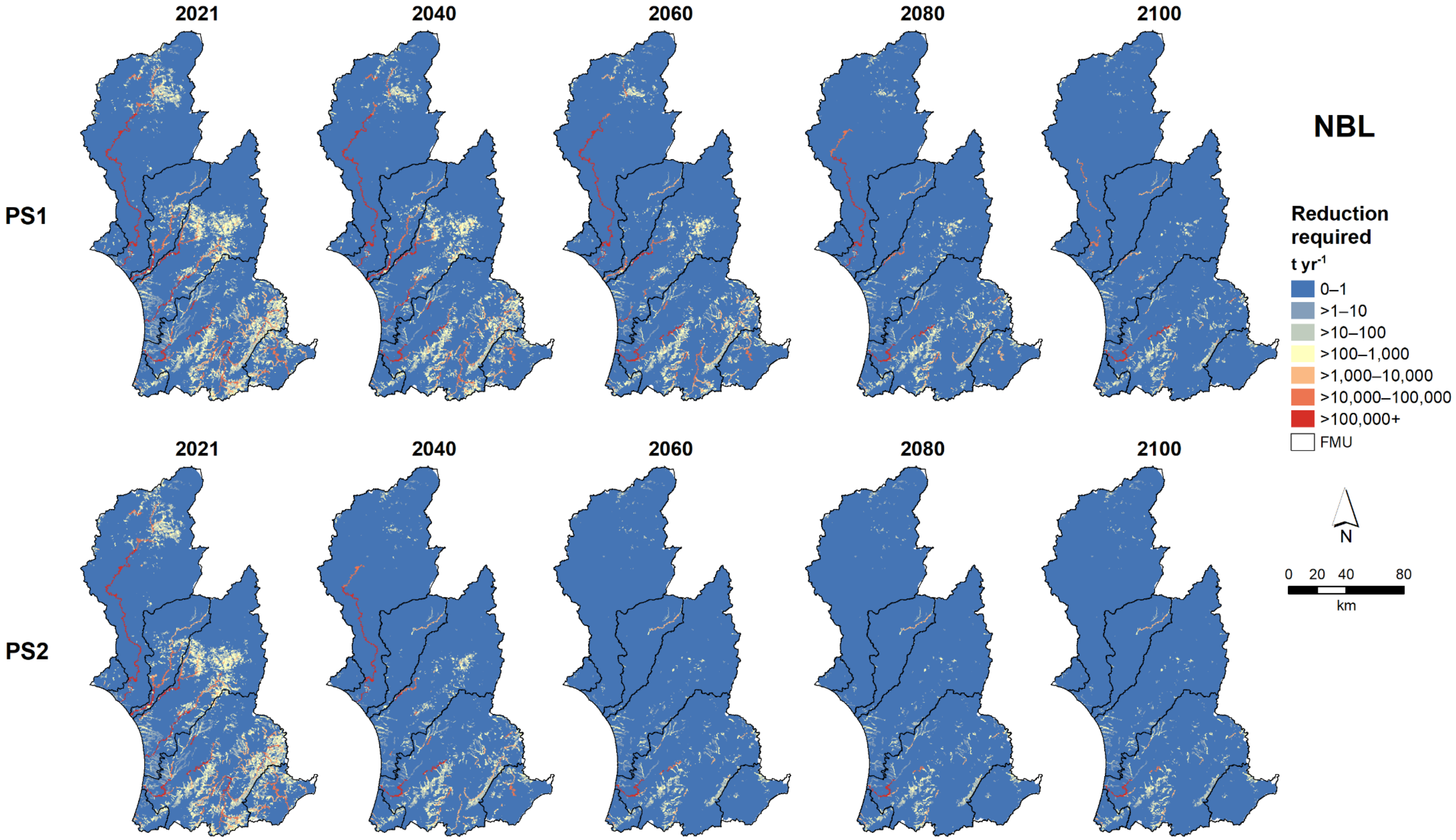

Figure 13. Absolute net load reduction required to achieve NPS-FM visual clarity NBL from 2021 to 2100 for PS1 and PS2.

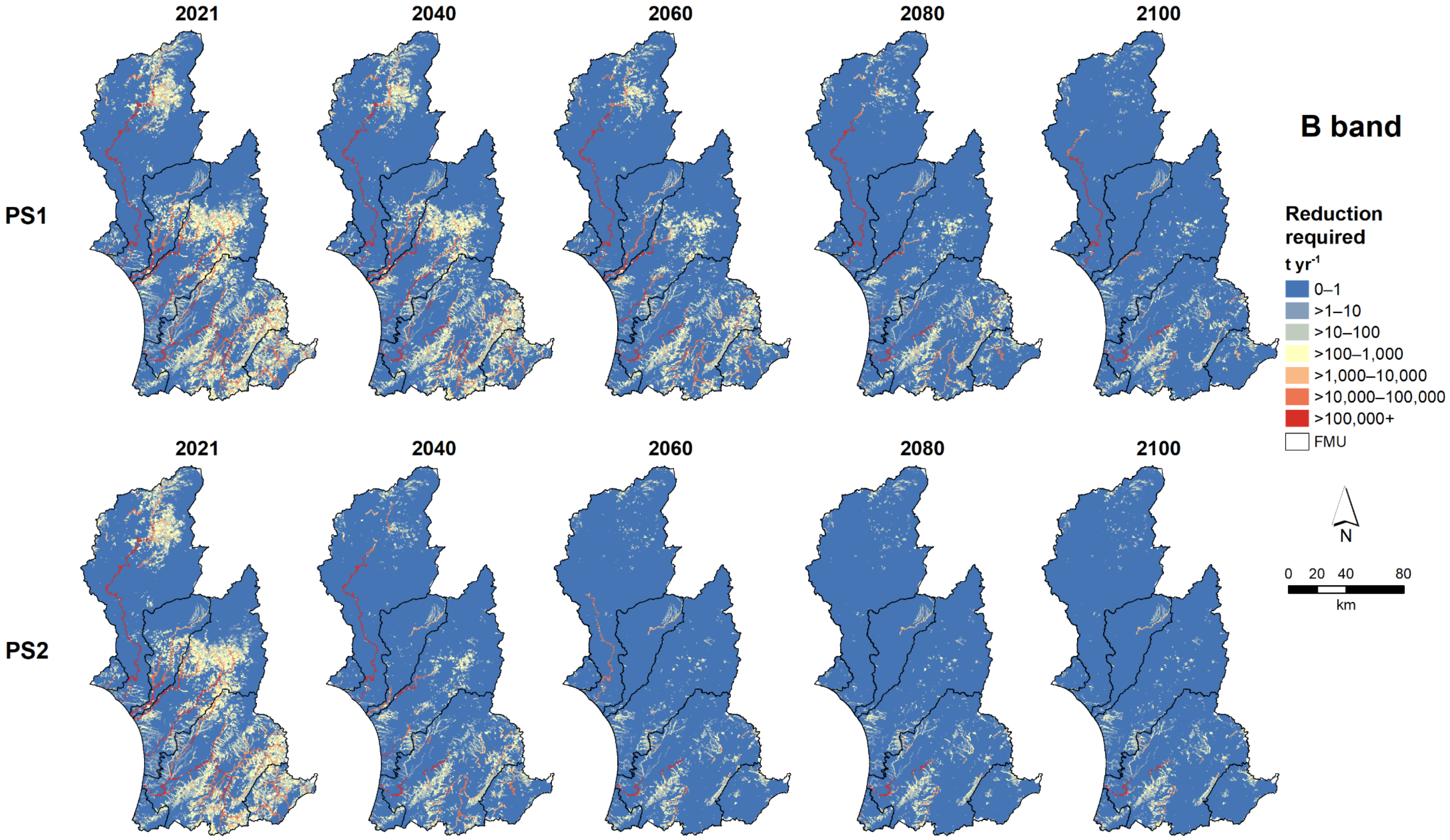

**Figure 14. Absolute net load reduction required to achieve NPS-FM visual clarity B band from 2021 to 2100 for PS1 and PS2.**

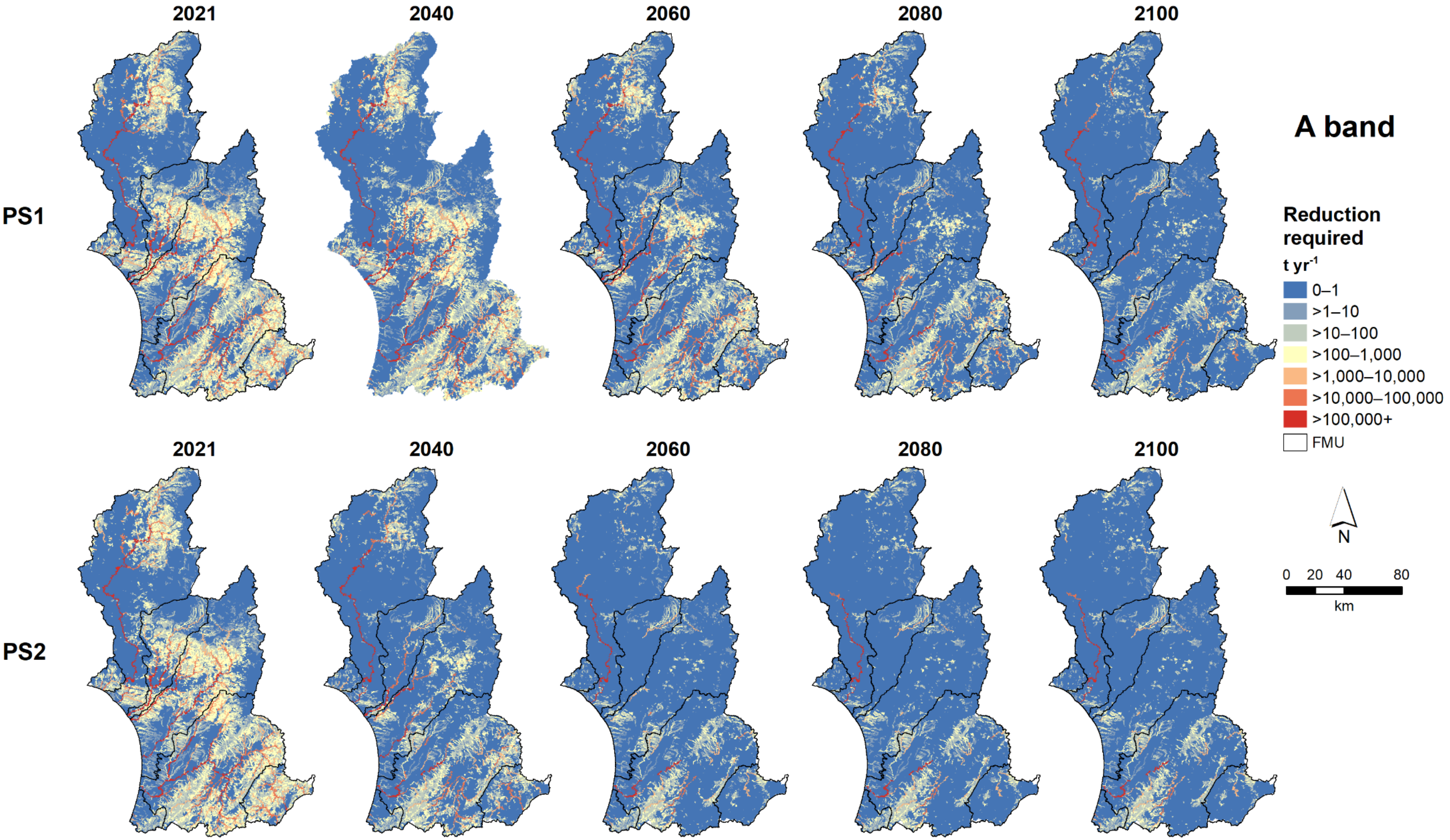

**Figure 15. Absolute net load reduction required to achieve NPS-FM visual clarity A band from 2021 to 2100 for PS1 and PS2.**

## 5.3 Impact of climate change

### 5.3.1 Suspended sediment loads

Suspended sediment loads under projected climate change were modelled for PS1 and PS2. The results are reported as the minimum, median and maximum based on the six regional climate models (RCMs) for each RCP at mid- (2040) and late (2090) century.

Region-wide total erosion loads under climate change are summarised in Table 11 and visualised in Figure 16. Projected mean annual suspended sediment yields are shown for the minimum RCP2.6 and maximum RCP8.5 at mid- and late century in Figure 17 and Figure 18. Total erosion loads for individual FMUs are provided in Tables 12–15 and shown in Figure 19.

The modelled climate change projections result in a wide range of predicted changes to sediment loads. This reflects the variability between each of the climate models and the diverging climate trajectories represented by each RCP. RCP2.6 represents a greenhouse gas mitigation pathway resulting in the lowest sediment load increases, with late century being lower than mid-century. RCP4.5 and RCP6.0 are stabilisation pathways, and RCP8.5 represents a worst-case scenario with very high greenhouse gas concentrations that result in large, predicted increases in sediment load. Therefore, total erosion is expected to increase from RCP 2.6 to RCP 8.5 at mid- and late century, with more pronounced differences between each RCP observed at late century due to the range in greenhouse gas trajectories represented across the RCPs (Figure 16).

For PS1 the total erosion across all RCPs is estimated to be between 8.4 and 12.5 Mt $yr^{-1}$ for mid-century, and between 4.9 and 10.1 Mt $yr^{-1}$ for late century. This represents a difference of 7% to 46% for mid-century and –4% to +79% for late century, compared to loads modelled without the impacts of climate change.

For PS2, the total erosion across all RCPs is estimated to range from 6.2 to 9.2 Mt $yr^{-1}$ for mid-century, and from 3.1 to 5.8 Mt $yr^{-1}$ for late century. This corresponds to a change of 3% to 41% for mid-century and –16% to +58% for late century. Only the minimum and median projections of RCP2.6 at late century shows a decrease in sediment load.

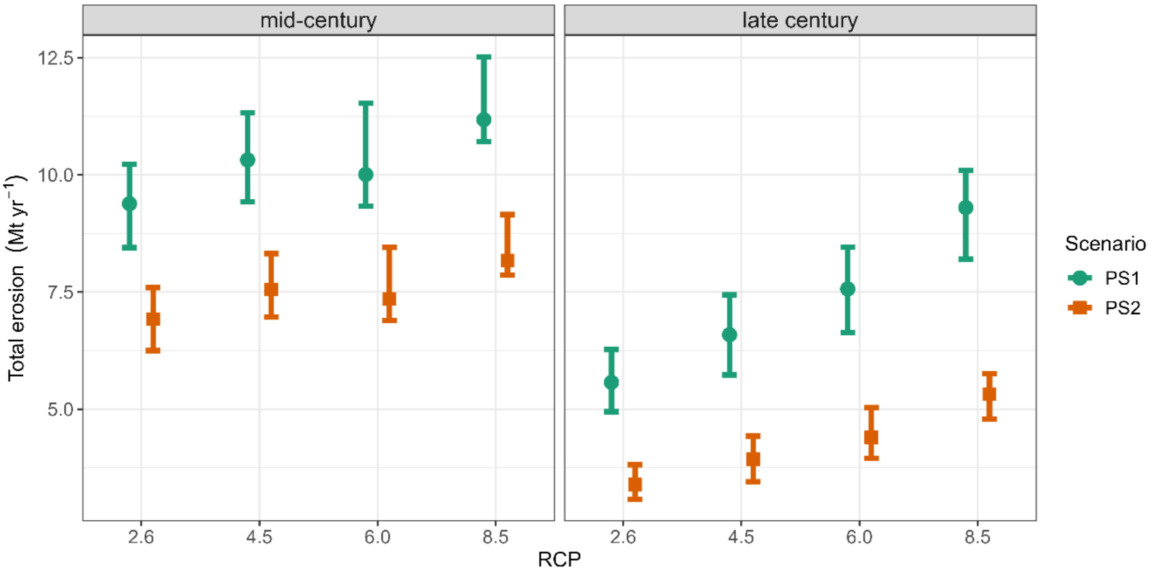

**Figure 16. Total erosion loads under projected climate change for the Horizons region at mid- and late century, by RCP for each erosion mitigation scenario.**

The projected changes in total erosion due to climate change vary across the region, resulting in different proportional changes for each FMU. The Waiopehu, Kai Iwi, and Whanganui FMUs show the largest reductions or smallest increases in erosion at both mid- and late century. In contrast, the Manawatū and Rangitīkei-Turakina FMUs experience the largest increases in erosion (Tables 12–15). There is a west–east pattern, whereby FMUs dominated by western coastal catchments exhibit smaller increases or even decreases in sediment load compared to the rest of the region. This pattern is also evident in the spatial yield maps (Figures 17 & 18), with minimal changes observed in lowland areas near the coast compared to inland hill country. The Waiopehu FMU shows a significant range of values compared to other FMUs, indicating greater variability between climate model projections in that specific area (Figure 19).

**Table 11. Total erosion by mid- and late century for each climate change scenario, represented by minimum, median, and maximum results for each RCP summarised for the whole region**

| Period | Scenario | Baseline load (Mt yr$^{-1}$) 2040 or 2090 | Statistic | Total erosion (Mt yr$^{-1}$) | | | | Difference from mid- and late century baseline loads without climate change (Mt yr$^{-1}$, %) | | | | | | | |
|---|---|---|---|---|---|---|---|---|---|---|---|---|---|---|---|
| | | | | RCP2.6 | RCP4.5 | RCP6.0 | RCP8.5 | RCP2.6 | | RCP4.5 | | RCP6.0 | | RCP8.5 | |
| Mid-century | PS1 | 7.84 | min | 8.4 | 9.4 | 9.3 | 10.7 | 0.6 | 7% | 1.6 | 19% | 1.5 | 18% | 2.9 | 34% |
| | | | med | 9.4 | 10.3 | 10.0 | 11.2 | 1.5 | 16% | 2.5 | 26% | 2.2 | 23% | 3.3 | 36% |
| | | | max | 10.2 | 11.3 | 11.5 | 12.5 | 2.4 | 23% | 3.5 | 34% | 3.7 | 36% | 4.7 | 46% |
| | PS2 | 6.06 | min | 6.2 | 7.0 | 6.9 | 7.9 | 0.2 | 3% | 0.9 | 14% | 0.8 | 13% | 1.8 | 29% |
| | | | med | 6.9 | 7.6 | 7.4 | 8.2 | 0.9 | 12% | 1.5 | 22% | 1.3 | 19% | 2.1 | 30% |
| | | | max | 7.6 | 8.3 | 8.5 | 9.2 | 1.5 | 20% | 2.3 | 30% | 2.4 | 31% | 3.1 | 41% |
| Late century | PS1 | 5.16 | min | 4.9 | 5.7 | 6.6 | 8.2 | -0.2 | -4% | 0.6 | 12% | 1.5 | 30% | 3.0 | 62% |
| | | | med | 5.6 | 6.6 | 7.6 | 9.3 | 0.4 | 7% | 1.4 | 26% | 2.4 | 43% | 4.1 | 74% |
| | | | max | 6.3 | 7.4 | 8.5 | 10.1 | 1.1 | 18% | 2.3 | 36% | 3.3 | 53% | 4.9 | 79% |
| | PS2 | 3.56 | min | 3.1 | 3.5 | 4.0 | 4.8 | -0.5 | -16% | -0.1 | -3% | 0.4 | 13% | 1.2 | 40% |
| | | | med | 3.4 | 3.9 | 4.4 | 5.3 | -0.2 | -5% | 0.4 | 11% | 0.8 | 25% | 1.8 | 52% |
| | | | max | 3.8 | 4.4 | 5.0 | 5.8 | 0.3 | 7% | 0.9 | 23% | 1.5 | 39% | 2.2 | 58% |

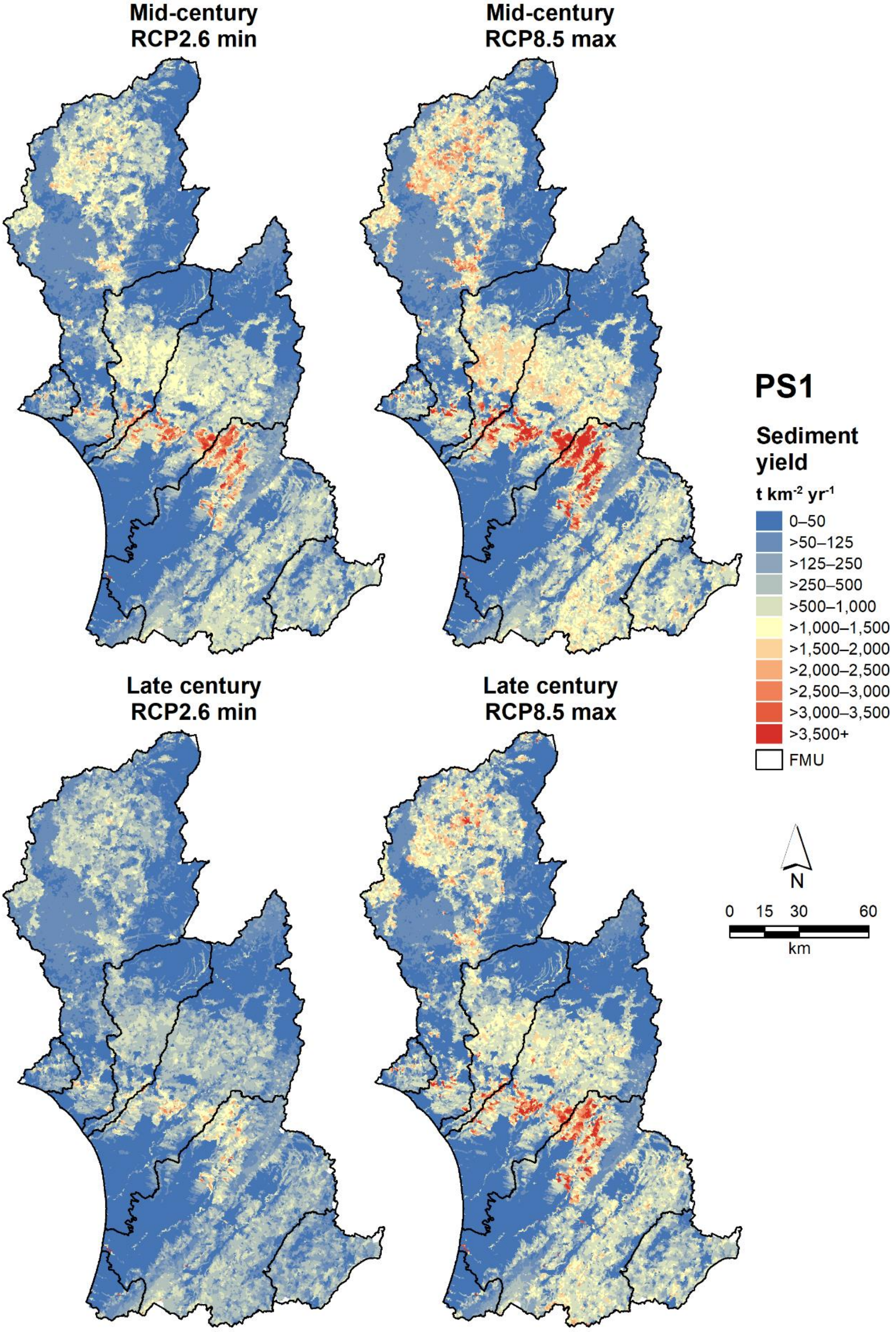

**Figure 17. Mean annual suspended sediment yield under projected climate change at mid- and late century, represented by RCP2.6 minimum and RCP8.5 maximum, for PS1.**

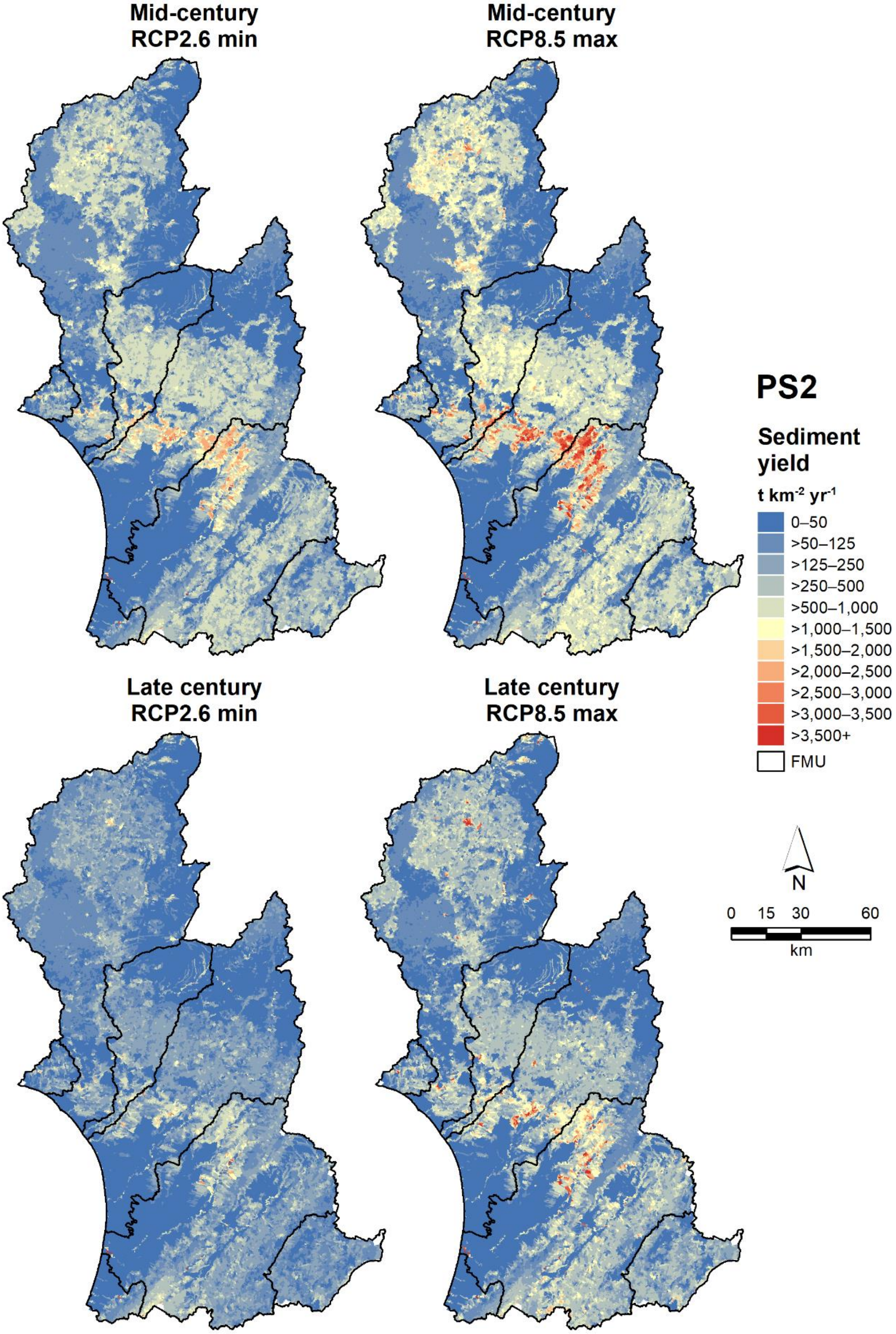

**Figure 18. Mean annual suspended sediment yield under projected climate change at mid- and late century, represented by RCP2.6 minimum and RCP8.5 maximum, for PS2.**

**Table 12. Total erosion loads at mid-century represented by minimum, median, and maximum results for each RCP, summarised by FMU for PS1**

| PS1 | FMU | Baseline load (Mt yr$^{-1}$) 2040 | Statistic | Total erosion (Mt yr$^{-1}$) | | | | Difference from mid-century baseline load without climate change (Mt yr$^{-1}$, %) | | | | | | | |
|---|---|---|---|---|---|---|---|---|---|---|---|---|---|---|---|
| | | | | RCP2.6 | RCP4.5 | RCP6.0 | RCP8.5 | RCP2.6 | | RCP4.5 | | RCP6.0 | | RCP8.5 | |
| Mid-century | Kai Iwi | 0.10 | min | 0.10 | 0.10 | 0.10 | 0.11 | -0.01 | -7% | 0.00 | 2% | 0.00 | -1% | 0.01 | 13% |
| | | | med | 0.10 | 0.11 | 0.11 | 0.12 | 0.00 | 1% | 0.01 | 11% | 0.01 | 7% | 0.02 | 17% |
| | | | max | 0.11 | 0.12 | 0.13 | 0.13 | 0.01 | 10% | 0.02 | 19% | 0.03 | 22% | 0.03 | 28% |
| | Manawatū | 2.14 | min | 2.47 | 2.76 | 2.73 | 3.15 | 0.33 | 13% | 0.62 | 25% | 0.59 | 24% | 1.01 | 41% |
| | | | med | 2.78 | 3.05 | 2.96 | 3.32 | 0.64 | 23% | 0.91 | 33% | 0.82 | 30% | 1.18 | 42% |
| | | | max | 3.09 | 3.42 | 3.48 | 3.76 | 0.95 | 31% | 1.28 | 41% | 1.34 | 43% | 1.62 | 52% |
| | Puketoi ki Tai | 0.42 | min | 0.47 | 0.53 | 0.52 | 0.59 | 0.05 | 10% | 0.10 | 22% | 0.09 | 20% | 0.17 | 35% |
| | | | med | 0.53 | 0.57 | 0.56 | 0.62 | 0.10 | 19% | 0.15 | 28% | 0.13 | 25% | 0.19 | 37% |
| | | | max | 0.57 | 0.63 | 0.64 | 0.69 | 0.14 | 25% | 0.20 | 36% | 0.22 | 38% | 0.27 | 48% |
| | Rangitīkei-Turakina | 1.72 | min | 1.98 | 2.18 | 2.18 | 2.49 | 0.26 | 13% | 0.46 | 23% | 0.46 | 23% | 0.78 | 39% |
| | | | med | 2.20 | 2.42 | 2.34 | 2.63 | 0.48 | 22% | 0.70 | 32% | 0.62 | 28% | 0.92 | 42% |
| | | | max | 2.35 | 2.61 | 2.66 | 2.90 | 0.63 | 27% | 0.90 | 38% | 0.94 | 40% | 1.18 | 50% |
| | Waiopehu[a] | 0.05 | min | 0.05 | 0.05 | 0.05 | 0.05 | 0.00 | -7% | 0.00 | 2% | 0.00 | -2% | 0.00 | 7% |
| | | | med | 0.05 | 0.05 | 0.05 | 0.05 | 0.00 | 2% | 0.00 | 0% | 0.00 | 2% | 0.00 | 4% |
| | | | max | 0.06 | 0.06 | 0.05 | 0.06 | 0.01 | 16% | 0.01 | 10% | 0.00 | 7% | 0.01 | 12% |
| | Whangaehu | 0.84 | min | 0.94 | 1.04 | 1.03 | 1.18 | 0.10 | 11% | 0.20 | 22% | 0.19 | 21% | 0.34 | 37% |
| | | | med | 1.05 | 1.15 | 1.11 | 1.24 | 0.21 | 20% | 0.31 | 30% | 0.27 | 26% | 0.41 | 39% |
| | | | max | 1.13 | 1.25 | 1.26 | 1.38 | 0.29 | 26% | 0.41 | 37% | 0.43 | 38% | 0.54 | 48% |
| | Whanganui | 2.57 | min | 2.46 | 2.77 | 2.73 | 3.13 | -0.11 | -5% | 0.20 | 8% | 0.16 | 6% | 0.56 | 23% |
| | | | med | 2.68 | 2.97 | 2.88 | 3.20 | 0.11 | 4% | 0.40 | 15% | 0.31 | 12% | 0.63 | 24% |
| | | | max | 2.93 | 3.24 | 3.31 | 3.60 | 0.36 | 12% | 0.67 | 23% | 0.74 | 25% | 1.03 | 35% |

[a] The selected RCMs do not consistently equate to the equivalent min/median/max values for Waiopehu due to relative differences in total erosion between RCMs at catchment/FMU versus regional scales. For consistency, we present sediment load results for the selected RCMs across all sub-catchments, which allows comparison between sub-catchments for the same RCM.

**Table 13. Total erosion loads at late century represented by minimum, median, and maximum results for each RCP, summarised by FMU for PS1**

| PS1 | FMU | Baseline load (Mt yr$^{-1}$) 2090 | Statistic | Total erosion (Mt yr$^{-1}$) | | | | Difference from late-century baseline load without climate change (Mt yr$^{-1}$, %) | | | | | | | |
|---|---|---|---|---|---|---|---|---|---|---|---|---|---|---|---|
| | | | | RCP2.6 | RCP4.5 | RCP6.0 | RCP8.5 | RCP2.6 | | RCP4.5 | | RCP6.0 | | RCP8.5 | |
| Late century | Kai Iwi | 0.08 | min | 0.06 | 0.07 | 0.08 | 0.10 | -0.01 | -22% | 0.00 | -6% | 0.01 | 8% | 0.02 | 34% |
| | | | med | 0.07 | 0.08 | 0.09 | 0.11 | -0.01 | -8% | 0.00 | 6% | 0.02 | 22% | 0.04 | 49% |
| | | | max | 0.08 | 0.09 | 0.10 | 0.12 | 0.00 | 1% | 0.02 | 19% | 0.03 | 33% | 0.04 | 56% |
| | Manawatū | 1.42 | min | 1.52 | 1.77 | 2.04 | 2.53 | 0.10 | 6% | 0.34 | 23% | 0.62 | 41% | 1.10 | 73% |
| | | | med | 1.74 | 2.03 | 2.37 | 2.89 | 0.32 | 18% | 0.61 | 35% | 0.95 | 55% | 1.47 | 85% |
| | | | max | 1.94 | 2.34 | 2.67 | 3.15 | 0.52 | 27% | 0.92 | 47% | 1.25 | 64% | 1.73 | 89% |
| | Puketoi ki Tai | 0.24 | min | 0.25 | 0.28 | 0.33 | 0.40 | 0.01 | 3% | 0.04 | 17% | 0.09 | 35% | 0.16 | 64% |
| | | | med | 0.27 | 0.32 | 0.37 | 0.46 | 0.03 | 12% | 0.08 | 30% | 0.13 | 48% | 0.21 | 78% |
| | | | max | 0.31 | 0.37 | 0.41 | 0.49 | 0.07 | 21% | 0.13 | 41% | 0.17 | 54% | 0.25 | 82% |
| | Rangitīkei-Turakina | 1.04 | min | 1.08 | 1.26 | 1.48 | 1.82 | 0.04 | 4% | 0.22 | 20% | 0.43 | 40% | 0.78 | 72% |
| | | | med | 1.23 | 1.47 | 1.69 | 2.08 | 0.19 | 15% | 0.43 | 35% | 0.65 | 53% | 1.04 | 85% |
| | | | max | 1.38 | 1.65 | 1.85 | 2.28 | 0.34 | 25% | 0.61 | 44% | 0.81 | 59% | 1.24 | 90% |
| | Waiopehu | 0.05 | min | 0.04 | 0.04 | 0.05 | 0.05 | 0.00 | -7% | 0.00 | -9% | 0.00 | 0% | 0.01 | 12% |
| | | | med | 0.04 | 0.05 | 0.05 | 0.05 | 0.00 | -5% | 0.00 | 2% | 0.01 | 11% | 0.01 | 16% |
| | | | max | 0.05 | 0.05 | 0.06 | 0.06 | 0.00 | 8% | 0.01 | 16% | 0.01 | 26% | 0.01 | 18% |
| | Whangaehu | 0.46 | min | 0.46 | 0.53 | 0.61 | 0.76 | 0.00 | 0% | 0.07 | 15% | 0.15 | 33% | 0.30 | 65% |
| | | | med | 0.52 | 0.62 | 0.71 | 0.87 | 0.06 | 12% | 0.16 | 30% | 0.25 | 48% | 0.41 | 78% |
| | | | max | 0.59 | 0.70 | 0.79 | 0.95 | 0.13 | 22% | 0.24 | 41% | 0.33 | 57% | 0.49 | 84% |
| | Whanganui | 1.87 | min | 1.53 | 1.77 | 2.05 | 2.54 | -0.34 | -22% | -0.10 | -7% | 0.18 | 12% | 0.67 | 44% |
| | | | med | 1.69 | 2.03 | 2.28 | 2.84 | -0.18 | -11% | 0.15 | 9% | 0.41 | 24% | 0.96 | 57% |
| | | | max | 1.93 | 2.24 | 2.57 | 3.05 | 0.06 | 3% | 0.37 | 19% | 0.70 | 36% | 1.18 | 61% |

**Table 14. Total erosion loads at mid-century represented by minimum, median, and maximum results for each RCP, summarised by FMU for PS2**

| PS2 | FMU | Baseline load (Mt yr$^{-1}$) 2040 | Statistics | Total erosion (Mt yr$^{-1}$) | | | | Difference from mid-century baseline load without climate change (Mt yr$^{-1}$, %) | | | | | | | |
|---|---|---|---|---|---|---|---|---|---|---|---|---|---|---|---|
| | | | | RCP2.6 | RCP4.5 | RCP6.0 | RCP8.5 | RCP2.6 | | RCP4.5 | | RCP6.0 | | RCP8.5 | |
| Mid-century | Kai Iwi | 0.09 | min | 0.08 | 0.08 | 0.08 | 0.09 | -0.01 | -13% | 0.00 | -4% | -0.01 | -7% | 0.00 | 7% |
| | | | med | 0.08 | 0.09 | 0.09 | 0.09 | 0.00 | -5% | 0.00 | 5% | 0.00 | 0% | 0.01 | 10% |
| | | | max | 0.09 | 0.10 | 0.10 | 0.11 | 0.00 | 4% | 0.01 | 13% | 0.02 | 17% | 0.02 | 22% |
| | Manawatū | 1.69 | min | 1.92 | 2.14 | 2.12 | 2.43 | 0.23 | 12% | 0.45 | 23% | 0.42 | 22% | 0.73 | 38% |
| | | | med | 2.16 | 2.35 | 2.29 | 2.55 | 0.46 | 21% | 0.65 | 30% | 0.59 | 27% | 0.85 | 40% |
| | | | max | 2.41 | 2.64 | 2.68 | 2.88 | 0.71 | 30% | 0.94 | 39% | 0.98 | 41% | 1.19 | 49% |
| | Puketoi ki Tai | 0.31 | min | 0.33 | 0.37 | 0.37 | 0.42 | 0.02 | 7% | 0.06 | 19% | 0.06 | 17% | 0.11 | 32% |
| | | | med | 0.37 | 0.40 | 0.39 | 0.43 | 0.06 | 16% | 0.09 | 24% | 0.08 | 22% | 0.12 | 33% |
| | | | max | 0.40 | 0.44 | 0.45 | 0.49 | 0.09 | 23% | 0.13 | 33% | 0.14 | 35% | 0.18 | 44% |
| | Rangitīkei-Turakina | 1.27 | min | 1.43 | 1.57 | 1.58 | 1.79 | 0.15 | 11% | 0.30 | 21% | 0.30 | 21% | 0.52 | 36% |
| | | | med | 1.59 | 1.74 | 1.68 | 1.89 | 0.32 | 20% | 0.46 | 29% | 0.41 | 26% | 0.61 | 39% |
| | | | max | 1.70 | 1.88 | 1.91 | 2.08 | 0.43 | 25% | 0.61 | 36% | 0.64 | 37% | 0.80 | 47% |
| | Waiopehu[a] | 0.05 | min | 0.04 | 0.05 | 0.05 | 0.05 | 0.00 | -7% | 0.00 | 2% | 0.00 | -2% | 0.00 | 7% |
| | | | med | 0.05 | 0.05 | 0.05 | 0.05 | 0.00 | 2% | 0.00 | -2% | 0.00 | 2% | 0.00 | 2% |
| | | | max | 0.06 | 0.05 | 0.05 | 0.05 | 0.01 | 16% | 0.01 | 11% | 0.00 | 7% | 0.01 | 11% |
| | Whangaehu | 0.60 | min | 0.65 | 0.72 | 0.71 | 0.81 | 0.05 | 7% | 0.12 | 18% | 0.11 | 18% | 0.21 | 33% |
| | | | med | 0.73 | 0.79 | 0.77 | 0.86 | 0.13 | 17% | 0.19 | 26% | 0.17 | 23% | 0.26 | 35% |
| | | | max | 0.79 | 0.86 | 0.87 | 0.95 | 0.19 | 24% | 0.26 | 34% | 0.27 | 35% | 0.35 | 44% |
| | Whanganui | 2.05 | min | 1.80 | 2.03 | 1.99 | 2.27 | -0.25 | -14% | -0.03 | -1% | -0.06 | -3% | 0.22 | 12% |
| | | | med | 1.95 | 2.15 | 2.09 | 2.31 | -0.10 | -5% | 0.09 | 5% | 0.04 | 2% | 0.25 | 13% |
| | | | max | 2.16 | 2.35 | 2.40 | 2.60 | 0.10 | 5% | 0.30 | 14% | 0.34 | 16% | 0.55 | 25% |

[a] The selected RCMs do not consistently equate to the equivalent min/median/max values for Waiopehu due to relative differences in total erosion between RCMs at catchment/FMU versus regional scales. For consistency, we present sediment load results for the selected RCMs across all sub-catchments, which allows comparison between sub-catchments for the same RCM.

**Table 15. Total erosion loads at late century represented by minimum, median, and maximum results for each RCP, summarised by FMU for PS2**

| PS2 | FMU | Baseline load (Mt yr$^{-1}$) 2090 | Statistics | Total erosion (Mt yr$^{-1}$) | | | | Difference from late-century baseline load without climate change (Mt yr$^{-1}$, %) | | | | | | | |
|---|---|---|---|---|---|---|---|---|---|---|---|---|---|---|---|
| | | | | RCP2.6 | RCP4.5 | RCP6.0 | RCP8.5 | RCP2.6 | | RCP4.5 | | RCP6.0 | | RCP8.5 | |
| Late century | Kai Iwi | 0.06 | min | 0.05 | 0.05 | 0.06 | 0.07 | -0.02 | -33% | -0.01 | -20% | 0.00 | -7% | 0.01 | 20% |
| | | | med | 0.05 | 0.06 | 0.06 | 0.08 | -0.01 | -20% | 0.00 | -8% | 0.00 | 8% | 0.02 | 34% |
| | | | max | 0.06 | 0.06 | 0.07 | 0.08 | -0.01 | -9% | 0.00 | 7% | 0.01 | 22% | 0.02 | 42% |
| | Manawatū | 1.02 | min | 1.05 | 1.18 | 1.35 | 1.64 | 0.03 | 3% | 0.16 | 16% | 0.34 | 32% | 0.63 | 60% |
| | | | med | 1.17 | 1.35 | 1.55 | 1.86 | 0.16 | 13% | 0.33 | 28% | 0.53 | 45% | 0.84 | 72% |
| | | | max | 1.31 | 1.56 | 1.77 | 2.02 | 0.30 | 23% | 0.54 | 41% | 0.76 | 58% | 1.00 | 76% |
| | Puketoi ki Tai | 0.15 | min | 0.15 | 0.16 | 0.19 | 0.22 | -0.01 | -4% | 0.01 | 6% | 0.03 | 23% | 0.07 | 49% |
| | | | med | 0.16 | 0.18 | 0.20 | 0.25 | 0.00 | 2% | 0.03 | 19% | 0.05 | 34% | 0.10 | 62% |
| | | | max | 0.18 | 0.21 | 0.23 | 0.27 | 0.02 | 14% | 0.06 | 31% | 0.08 | 43% | 0.12 | 66% |
| | Rangitīkei-Turakina | 0.64 | min | 0.62 | 0.71 | 0.82 | 0.99 | -0.02 | -3% | 0.06 | 10% | 0.17 | 28% | 0.35 | 55% |
| | | | med | 0.70 | 0.82 | 0.92 | 1.12 | 0.05 | 8% | 0.17 | 25% | 0.27 | 39% | 0.47 | 68% |
| | | | max | 0.78 | 0.92 | 1.03 | 1.22 | 0.14 | 17% | 0.27 | 35% | 0.38 | 49% | 0.57 | 73% |
| | Waiopehu | 0.04 | min | 0.04 | 0.04 | 0.04 | 0.05 | 0.00 | -7% | 0.00 | -10% | 0.00 | -2% | 0.00 | 10% |
| | | | med | 0.04 | 0.05 | 0.05 | 0.05 | 0.00 | -5% | 0.00 | 2% | 0.00 | 10% | 0.01 | 12% |
| | | | max | 0.05 | 0.05 | 0.06 | 0.05 | 0.00 | 6% | 0.01 | 15% | 0.01 | 26% | 0.01 | 15% |
| | Whangaehu | 0.29 | min | 0.26 | 0.29 | 0.33 | 0.41 | -0.03 | -10% | 0.01 | 2% | 0.05 | 18% | 0.12 | 47% |
| | | | med | 0.29 | 0.34 | 0.38 | 0.46 | 0.01 | 3% | 0.05 | 18% | 0.10 | 33% | 0.18 | 60% |
| | | | max | 0.33 | 0.39 | 0.44 | 0.51 | 0.05 | 14% | 0.11 | 32% | 0.16 | 47% | 0.22 | 67% |
| | Whanganui | 1.36 | min | 0.92 | 1.02 | 1.16 | 1.40 | -0.44 | -48% | -0.33 | -36% | -0.19 | -21% | 0.05 | 5% |
| | | | med | 0.98 | 1.15 | 1.23 | 1.51 | -0.38 | -38% | -0.21 | -21% | -0.12 | -12% | 0.15 | 16% |
| | | | max | 1.11 | 1.24 | 1.44 | 1.62 | -0.24 | -22% | -0.11 | -10% | 0.08 | 7% | 0.26 | 23% |

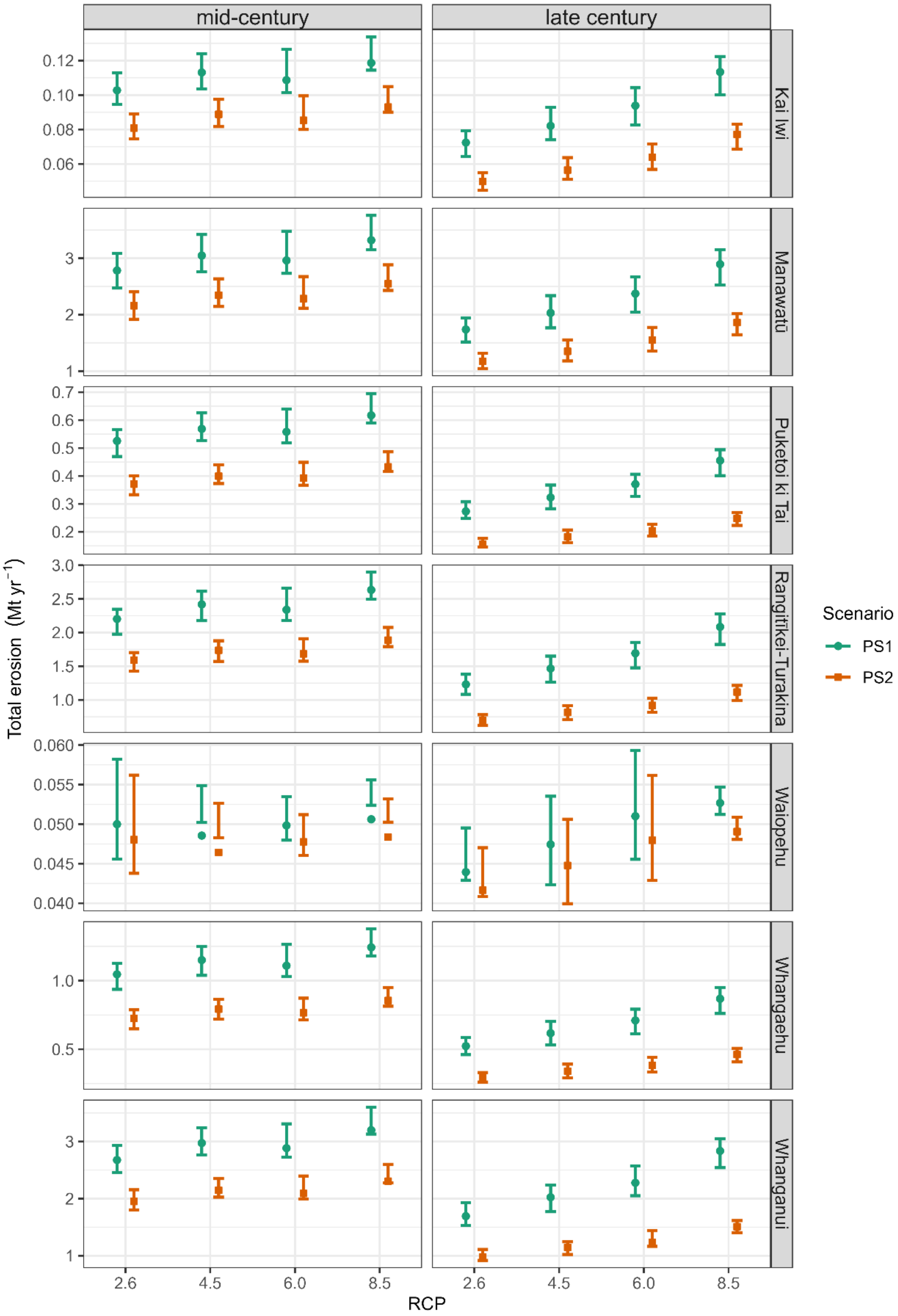

**Figure 19. Total erosion loads for each FMU at mid- and late century, represented by minimum, median, and maximum results for each RCP scenario.**

Note: The selected RCMs do not consistently equate to the equivalent min/median/max values for Waiopehu due to relative differences in total erosion between RCMs at catchment/FMU versus regional scales. For consistency, we present sediment load results for the selected RCMs across all sub-catchments, which allows comparison between sub-catchments for the same RCM.

### 5.3.2 Reductions in suspended sediment load required to meet NPS-FM visual clarity attribute bands under climate change

Suspended sediment load reductions required to achieve NPS-FM attribute bands under projected climate change were modelled in terms of proportional and absolute load reductions for each REC2 segment. These are summarised by the length (in km) and proportion by length of REC2 segments achieving each attribute band in Tables 16 and 17. REC2 segment summaries according to stream order are provided in Appendix G. Proportional reductions for A band, B band, and NBL are shown in Figures 20–22 for each scenario.

Where the baseline visual clarity already achieves A band, B band or NBL, the required reductions for those bands under modelled climate change represent the reductions required to maintain the baseline visual clarity state. This reflects the NPS-FM 2020 policy, which requires attribute targets to be set at or above the baseline state and therefore does not allow for deterioration below baseline visual clarity (Ministry for the Environment 2022a).

For PS1 at mid-century across all RCPs, the proportion of REC2 segments achieving the target ranged from 26% to 38% for A band, 29% to 44% for B band, and 30% to 49% for NBL. At late century these proportions increased to 39% to 69% for A band, 44% to 77% for B band, and 47% to 83% for NBL.

For PS2 at mid-century across all RCPs the proportion of REC2 segments achieving the target ranged from 34% to 58% for A band, 40% to 70% for B band, and 43% to 78% for NBL. At late century these proportions increased to 62% to 77% for A band, 67% to 82% for B band, and 69% to 85% for NBL.

The impact of climate change on sediment loads can be seen spatially in Figures 20–22, where a larger extent of catchments do not meet the target, especially for higher emission scenarios (RCP 8.5) and bands A and B. Pastoral hill country areas are particularly affected by the increase in loads under projected climate change. There is also a pattern of larger proportional load reductions required in lowland coastal REC2 segments, especially for RCP8.5 at late century.

Erosion mitigations implemented in both PS1 and PS2 scenarios increase the proportion of REC2 segments meeting the attribute bands at late century compared to mid-century. However, the proportion decreases when considering the impacts of climate change on sediment loads (Table 18). PS2 generally achieves a higher proportion of REC2 segments meeting the targets compared to PS1 at both mid- and late century.

For comparison, the proportion of REC2 segments achieving bands A, B, and NBL without the effects of climate change were 46%, 67%, and 81% at mid-century (2040) and 68%, 82%, and 88%, respectively, at late century (2090) for PS1. For PS2, the equivalent proportions of segments were 61%, 78%, and 86% at mid-century (2040) and 74%, 85%, and 90% at late century (2090), respectively (Table 18).

**Table 16. Length and proportion of REC2 segments achieving each visual clarity attribute band and NBL (or maintaining baseline visual clarity) by mid- and late century under projected climate change for PS1, represented by minimum, median, and maximum results for each RCP**

| PS1 | | | Length and proportion of REC2 segments achieving visual clarity attribute bands and NBL for each RCP | | | | | | | |
|---|---|---|---|---|---|---|---|---|---|---|
| Period | Attribute band | Statistic | RCP2.6 | | RCP4.5 | | RCP6.0 | | RCP8.5 | |
| | | | km | % | km | % | km | % | km | % |
| Mid-century | A band | min | 13,903 | 38% | 10,796 | 29% | 10,982 | 30% | 10,419 | 28% |
| | | med | 11,634 | 32% | 12,022 | 33% | 11,341 | 31% | 10,913 | 30% |
| | | max | 9,505 | 26% | 10,716 | 29% | 10,847 | 30% | 9,887 | 27% |
| | B band | min | 16,283 | 44% | 12,272 | 33% | 12,579 | 34% | 11,715 | 32% |
| | | med | 13,283 | 36% | 13,696 | 37% | 12,880 | 35% | 12,278 | 33% |
| | | max | 10,576 | 29% | 11,859 | 32% | 12,001 | 33% | 10,838 | 30% |
| | NBL | min | 17,869 | 49% | 13,160 | 36% | 13,459 | 37% | 12,469 | 34% |
| | | med | 14,056 | 38% | 14,405 | 39% | 13,612 | 37% | 12,853 | 35% |
| | | max | 11,050 | 30% | 12,369 | 34% | 12,593 | 34% | 11,307 | 31% |
| Late century | A band | min | 25,255 | 69% | 23,418 | 64% | 19,024 | 52% | 15,408 | 42% |
| | | med | 22,958 | 63% | 19,183 | 52% | 17,870 | 49% | 15,070 | 41% |
| | | max | 20,308 | 55% | 18,381 | 50% | 14,483 | 39% | 14,416 | 39% |
| | B band | min | 28,325 | 77% | 27,030 | 74% | 22,270 | 61% | 17,984 | 49% |
| | | med | 26,348 | 72% | 22,253 | 61% | 20,522 | 56% | 17,247 | 47% |
| | | max | 23,338 | 64% | 21,329 | 58% | 16,662 | 45% | 16,040 | 44% |
| | NBL | min | 30,366 | 83% | 28,880 | 79% | 24,466 | 67% | 20,067 | 55% |
| | | med | 28,244 | 77% | 24,180 | 66% | 22,543 | 61% | 18,739 | 51% |
| | | max | 25,059 | 68% | 23,200 | 63% | 18,253 | 50% | 17,133 | 47% |

**Table 17. Length and proportion of REC2 segments achieving each visual clarity attribute band and NBL (or maintaining baseline visual clarity) by mid- and late century under projected climate change for PS2, represented by minimum, median, and maximum results for each RCP**

| PS2 | | | Length and proportion of REC2 segments achieving visual clarity attribute bands and NBL for each RCP | | | | | | | |
|---|---|---|---|---|---|---|---|---|---|---|
| Period | Attribute band | Statistic | RCP2.6 | | RCP4.5 | | RCP6.0 | | RCP8.5 | |
| | | | km | % | km | % | km | % | km | % |
| Mid-century | A band | min | 21,404 | 58% | 17,676 | 48% | 17,855 | 49% | 15,597 | 42% |
| | | med | 18,468 | 50% | 17,792 | 48% | 17,531 | 48% | 15,486 | 42% |
| | | max | 15,592 | 42% | 15,102 | 41% | 14,871 | 40% | 12,535 | 34% |
| | B band | min | 25,814 | 70% | 21,642 | 59% | 22,041 | 60% | 18,829 | 51% |
| | | med | 22,500 | 61% | 21,491 | 59% | 21,229 | 58% | 18,482 | 50% |
| | | max | 18,953 | 52% | 17,952 | 49% | 17,543 | 48% | 14,510 | 40% |
| | NBL | min | 28,486 | 78% | 24,541 | 67% | 24,862 | 68% | 21,543 | 59% |
| | | med | 25,213 | 69% | 24,185 | 66% | 24,004 | 65% | 20,705 | 56% |
| | | max | 21,528 | 59% | 20,020 | 55% | 19,563 | 53% | 15,614 | 43% |
| Late century | A band | min | 28,053 | 76% | 28,321 | 77% | 25,549 | 70% | 23,729 | 65% |
| | | med | 27,256 | 74% | 25,532 | 70% | 25,524 | 70% | 23,914 | 65% |
| | | max | 26,001 | 71% | 25,581 | 70% | 22,703 | 62% | 23,551 | 64% |
| | B band | min | 29,812 | 81% | 30,225 | 82% | 27,375 | 75% | 25,823 | 70% |
| | | med | 29,018 | 79% | 27,110 | 74% | 27,355 | 74% | 26,060 | 71% |
| | | max | 27,469 | 75% | 27,564 | 75% | 24,424 | 67% | 25,461 | 69% |
| | NBL | min | 30,905 | 84% | 31,277 | 85% | 28,553 | 78% | 27,140 | 74% |
| | | med | 29,937 | 82% | 28,057 | 76% | 28,436 | 77% | 27,378 | 75% |
| | | max | 28,294 | 77% | 28,451 | 77% | 25,352 | 69% | 26,754 | 73% |

**Table 18. Summary comparing the ranges of REC2 segments achieving A band, B band, and NBL (or maintaining baseline visual clarity) across mid-(2040) and late (2090) century with and without climate change impacts**

| Scenario | Period | Attribute band | % of REC2 segments by length achieving visual clarity attribute bands and NBL: | |
|---|---|---|---|---|
| | | | Without climate change | With climate change |
| PS1 | Mid-century (2040) | A band | 46% | 26–38% |
| | | B band | 67% | 29–44% |
| | | NBL | 81% | 30–49% |
| | Late century (2090) | A band | 68% | 39–69% |
| | | B band | 82% | 44–77% |
| | | NBL | 88% | 47–83% |
| PS2 | Mid-century (2040) | A band | 61% | 34–58% |
| | | B band | 78% | 40–70% |
| | | NBL | 86% | 43–78% |
| | Late century (2090) | A band | 74% | 62–77% |
| | | B band | 85% | 67–82% |
| | | NBL | 90% | 69–85% |

Note: The range of values for ‘with climate change’ includes the min, med, and max across all RCPs.

A summary of the ranges for each FMU is provided in Appendix I.

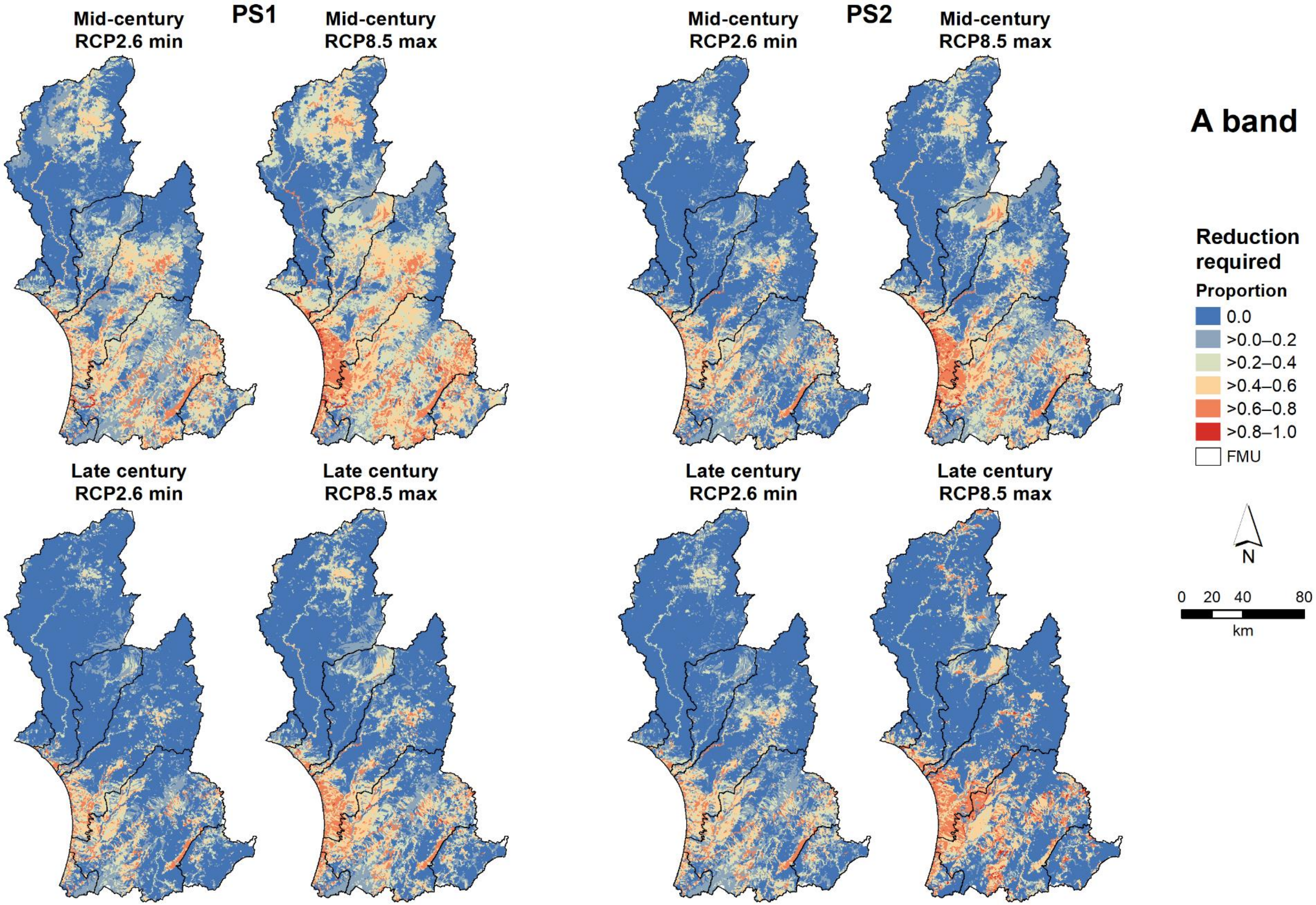

**Figure 20. Proportional reduction required to meet NPS-FM attribute Band A (or maintain baseline visual clarity) for sediment load at mid- and late century, represented by RCP2.6 min and RCP8.5 max for PS1 and PS2.**

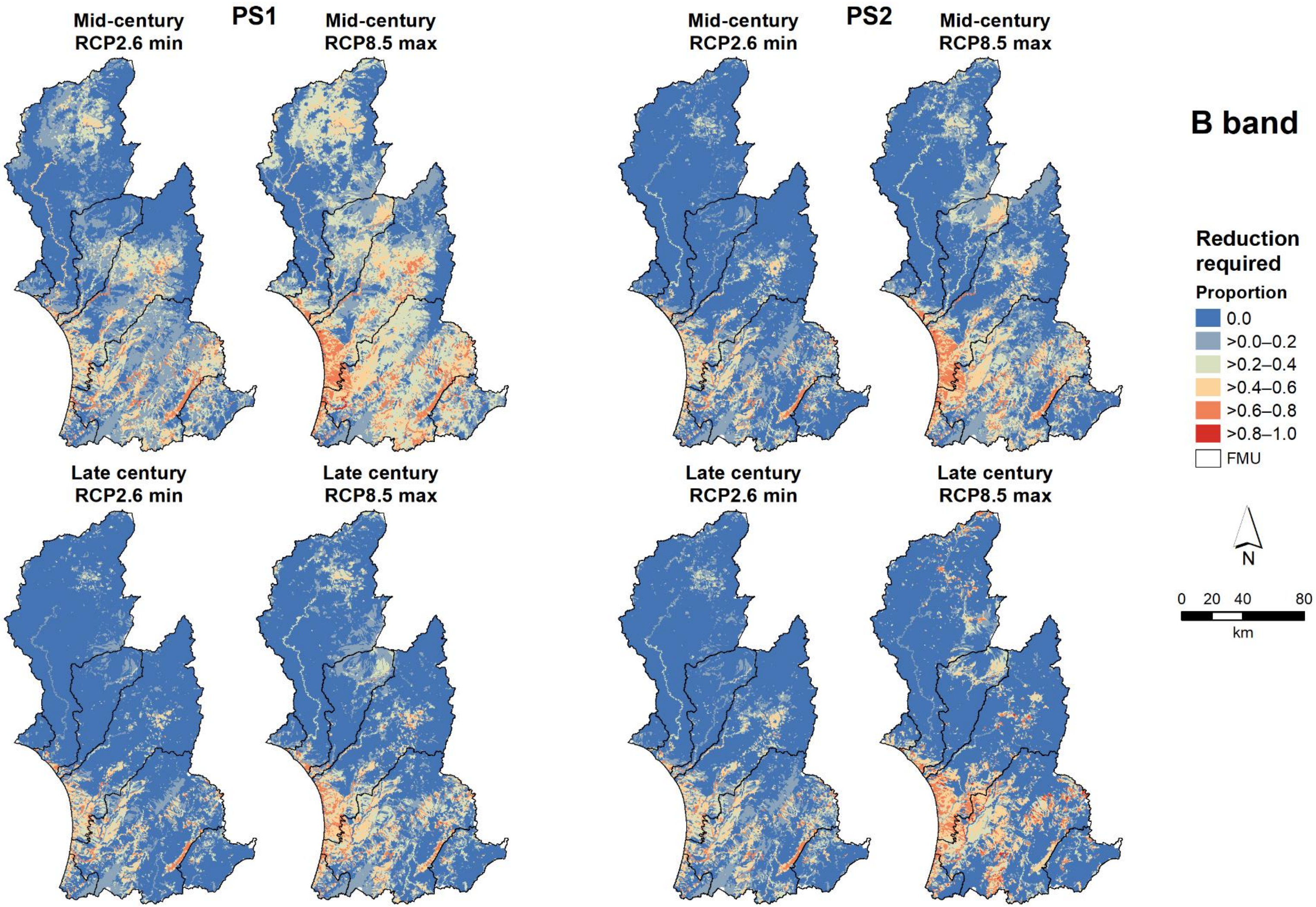

**Figure 21. Proportional reduction required to meet NPS-FM attribute Band B (or maintain baseline visual clarity) for sediment load at mid- and late century, represented by RCP2.6 minimum and RCP8.5 maximum for PS1 and PS2.**

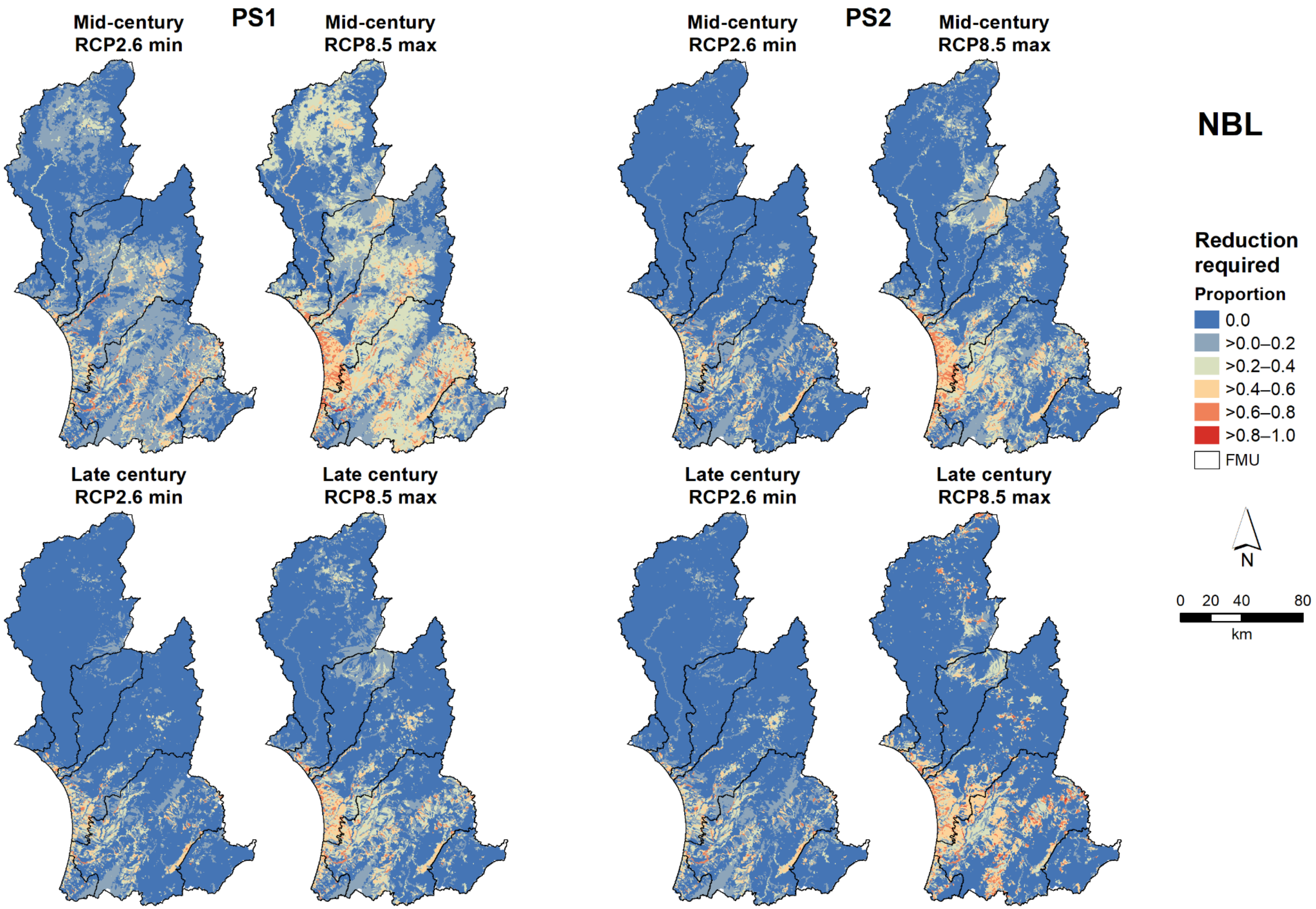

**Figure 22. Proportional reduction required to meet NPS-FM NBL (or maintain baseline visual clarity) for sediment load at mid- and late century, represented by RCP2.6 minimum and RCP8.5 maximum for PS1 and PS2.**

## 5.4 Comparison of PS1 and PS2 with scenarios from Vale et al. 2022

Here we summarise similarities and differences between model results for the two policy scenarios in the present report and the previous scenarios described in Vale et al. 2022.

From the previous modelling, SC1 represented the current state of SLUI/WCS erosion mitigation implementation and maturity to date across the region, with an accompanying future scenario representing the maturation of existing works on farms with existing plans, while no further farm plans or works were completed. SC2 represented a future state comprising SLUI/WCS erosion mitigation implementation and maturity to date, plus the future projected mapping rate of new farm plans, and the projected rate of on-farm erosion mitigation implementation and maturation of works across the region. A full description of the scenarios from Vale et al. 2022 is provided in Appendix D.

The total erosion modelled for the 2021 baseline decreased from 8.99 to 8.80 million tonnes per year (Mt yr$^{-1}$) when comparing the SC1/SC2 scenarios in the previous report to the PS1/PS2 scenarios in the present report. This reduction is related to the inclusion of spatial information on lowland riparian fencing based on data from HRC's Freshwater Team and the SRDM. Like SC2, both PS1 and PS2 show a significant reduction in total erosion by 2100 compared to the scenario with no additional measures (represented by SC1). By 2100, PS1 achieves a slightly larger reduction in total erosion compared to SC2 (48% vs. 47%). However, PS2 is more effective, with a 60% reduction in erosion by 2100, which is mostly achieved (56%) by 2060 (Table 19).

**Table 19. Summary of total erosion load and difference from 2021 baseline compared to scenarios from Vale et al. 2022**

| Scenario | | Total erosion (Mt yr$^{-1}$) | | | | | Difference from 2021 baseline[a] | | | |
|---|---|---|---|---|---|---|---|---|---|---|
| | | 2021 | 2040 | 2060 | 2080 | 2100 | 2040 | 2060 | 2080 | 2100 |
| Vale & Smith 2023 – present report | PS1 | 8.80 | 7.84 | 6.87 | 5.74 | 4.60 | -11% | -22% | -35% | -48% |
| | PS2 | 8.80 | 6.06 | 3.87 | 3.57 | 3.55 | -31% | -56% | -59% | -60% |
| Vale et al. 2022 – previous report | SC1 | 8.99 | 8.79 | 8.79 | 8.79 | 8.79 | -1% | -2% | -2% | -2% |
| | SC2 | 8.99 | 8.19 | 7.18 | 6.02 | 4.85 | -9% | -21% | -34% | -47% |

[a] Difference from the 2021 baseline is in respect to the 2021 baseline from each report.

For SC1, the projected change in total erosion across all RCPs varied from 8% to 60% for mid-century (2040) and from 2% to 119% for late century (2090) when compared to erosion modelled without the impacts of climate change. In the case of SC2, the range was from 7% to 58% for mid-century and from –5% to +93% for late century (Table 20). In contrast, both PS1 and PS2 showed smaller increases in total erosion for mid- and late century when compared to erosion modelled without climate change. PS1 resulted in a change in total erosion ranging from 7% to 46% for mid-century and from –4% to +79% for late century (Table 20). PS2 showed a change in total erosion ranging from 3% to 41% for mid-century and from –16% to +58% for late century (Table 20).

**Table 20. Summary of total erosion by mid- and late century under projected climate change compared to scenarios from Vale et al. 2022**

| Scenario | | Period | Baseline load ($Mt\ yr^{-1}$) 2040 or 2090 | Total erosion ($Mt\ yr^{-1}$) | Difference from mid- and late century baseline loads without climate change (%) |
|---|---|---|---|---|---|
| Vale & Smith 2023 – present report | PS1 | Mid-century | 7.84 | 8.4–12.5 | 7–46% |
| | | Late century | 5.16 | 4.9–10.1 | -4–79% |
| | PS2 | Mid-century | 6.06 | 6.2–9.2 | 3–41% |
| | | Late century | 3.56 | 3.1–5.8 | -16–58% |
| Vale et al. 2022 – previous report | SC1 | Mid-century | 8.79 | 9.5–14.1 | 8–60% |
| | | Late century | 8.79 | 9.0 19.2 | 2–119% |
| | SC2 | Mid-century | 8.19 | 8.7–13.0 | 7–58% |
| | | Late century | 5.43 | 5.2–10.5 | -5– 93% |

The proportion of segments achieving attribute bands decreased with the impacts of climate change compared to without the impacts of climate change on sediment loads for all scenarios (Table 21). SC2 was estimated to partially offset the impacts of climate change, increasing the proportion of REC2 segments that achieve attribute bands and NBL relative to SC1 (Table 21). The proportion of REC2 segments achieving attribute bands was further increased for PS1 and PS2 relative to SC2 at both mid- and late century. For comparison, the proportion of segments achieving NBL ranged from 30% to 49% and 47% to 83% by mid and late century for PS1, and 43–78% and 69–85% by mid- and late century for PS2, compared to 28–45% and 45–79% by mid- and late century for SC2, respectively (Table 21).

**Table 21. Summary comparing the proportion of REC2 segments achieving A band, B band, and NBL (or maintaining baseline visual clarity) across mid-(2040) and late (2090) century with and without climate change impacts[a] compared to scenarios from Vale et al. 2022**

| Scenario | | Period | Attribute band | % of REC2 segments by length achieving visual clarity attribute bands and NBL: | |
|---|---|---|---|---|---|
| | | | | Without climate change | With climate change[a] |
| Vale & Smith 2023 – present report | PS1 | Mid-century (2040) | A band | 46% | 26–38% |
| | | | B band | 67% | 29–44% |
| | | | NBL | 81% | 30–49% |
| | | Late century (2090) | A band | 68% | 39–69% |
| | | | B band | 82% | 44–77% |
| | | | NBL | 88% | 47–83% |
| | PS2 | Mid-century (2040) | A band | 61% | 34–58% |
| | | | B band | 78% | 40–70% |
| | | | NBL | 86% | 43–78% |
| | | Late century (2090) | A band | 74% | 62–77% |
| | | | B band | 85% | 67–82% |
| | | | NBL | 90% | 69–85% |
| Vale et al. 2022 – previous report | SC1 | Mid-century (2040) | A band | 40% | 23–32% |
| | | | B band | 62% | 24–36% |
| | | | NBL | 76% | 25–38% |
| | | Late century (2090) | A band | 40% | 21–33% |
| | | | B band | 62% | 22–38% |
| | | | NBL | 76% | 22–40% |
| | SC2 | Mid-century (2040) | A band | 45% | 24–36% |
| | | | B band | 66% | 27–42% |
| | | | NBL | 79% | 28–45% |
| | | Late century (2090) | A band | 66% | 38–66% |
| | | | B band | 80% | 42–74% |
| | | | NBL | 87% | 45–79% |

[a] The range of values for 'with climate change' includes the min, med, and max across all RCPs.

## 5.5 Model evaluation and limitations

### 5.5.1 Model evaluation

SedNetNZ is designed to predict spatial patterns in erosion and suspended sediment load on a mean annual basis for periods spanning several decades. It is difficult to quantify model performance over such timescales other than through comparison with measurements of suspended sediment load, which has been the main form of SedNetNZ model evaluation (Basher et al. 2018). Often, longer-term suspended sediment load data are unavailable. However, in the Horizons region various rivers have been monitored and the resulting suspended sediment concentration (SSC) and discharge (Q) data have been used to estimate mean annual suspended sediment loads via SSC-Q rating curve methods (Hicks, Semadeni-Davies et al. 2019). We have used these estimates of mean annual suspended sediment load (obtained from the Appendix D of Hicks, Semadeni-Davies et al. 2019) to inform the model calibration.

Previously, Dymond et al. (2016) conducted a sensitivity analysis of the model parameters and found uncertainty of approximately ±50% at the 95% confidence level. The greatest uncertainty arises from the landslide probability density function, landslide sediment delivery ratio (SDR), and gully density. The bank erosion component of SedNetNZ is calibrated separately, as described in Appendix A.

The relationship between mean annual suspended sediment loads estimated from SSC-Q rating curves and the updated 2021 baseline model loads is shown in Figure 23. In general, there is good agreement between the measured loads and the calibrated model, although the level of agreement varies across different catchments. When comparing the sediment loads predicted by the updated version of SedNetNZ in the present report to previous model versions, the predictions are either similar or better in terms of accuracy when compared to the measured loads in the Horizons region (Table 22). The updated baseline loads in the present report are slightly lower than those reported in Vale et al. 2022. This difference is due to the inclusion of additional erosion mitigation measures, such as riparian fencing and planting.

The updated version of SedNetNZ has led to a decrease in the overall predicted region-wide suspended sediment load compared to previous model applications in the region. In 2014 Dymond et al. estimated the region-wide load to be 13.4 Mt $y^{-1}$, which decreased to 12.6 Mt $y^{-1}$ in 2018 with the implementation of SLUI measures (Basher et al. 2020). These earlier estimates are higher compared to the 8.3 Mt $y^{-1}$ predicted for 2021 in the present study. While some of the difference can be attributed to the implementation of additional erosion mitigation measures between 2018 and 2021, most of the decrease is due to updates made to the SedNetNZ model since the previous applications in the region.

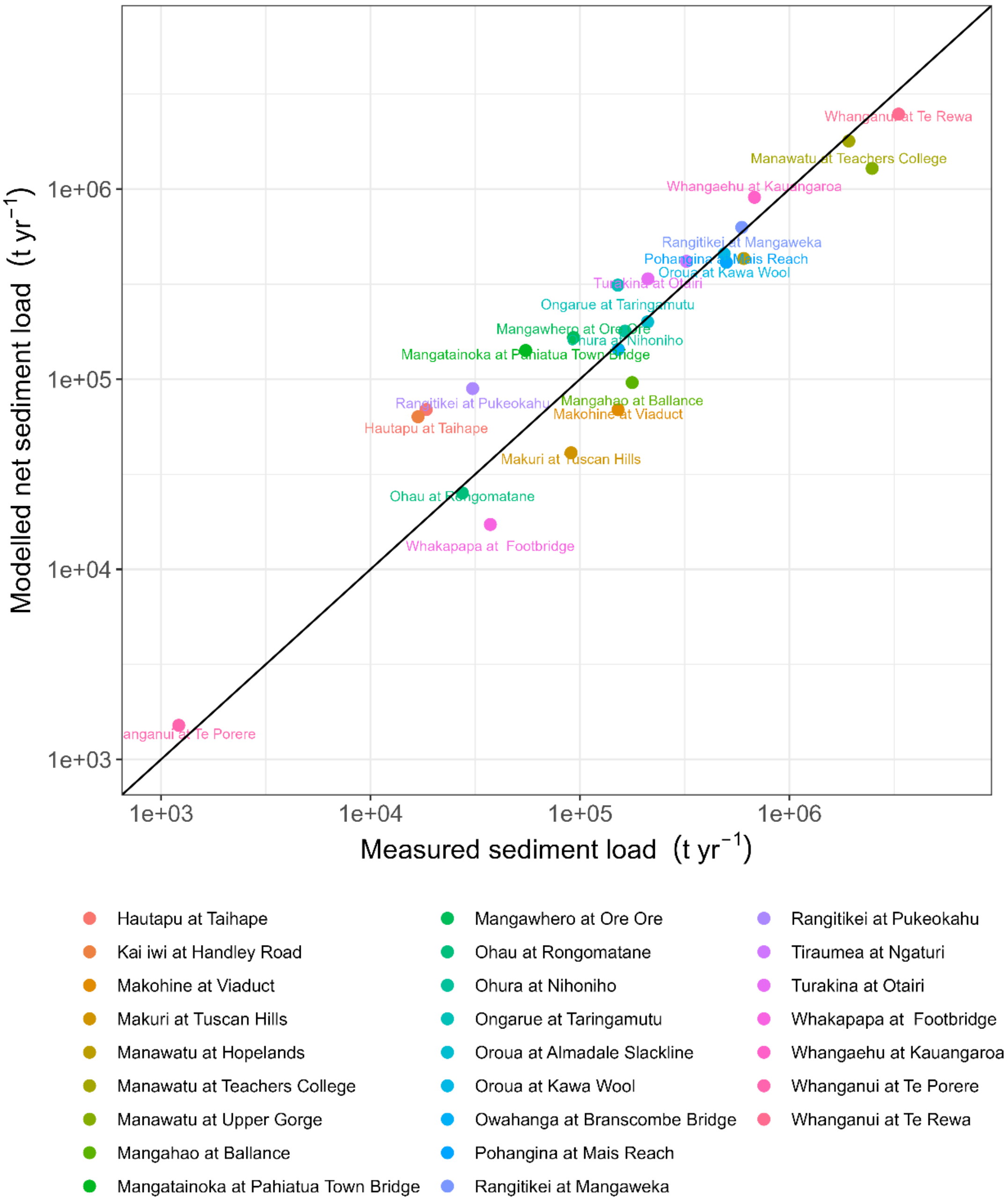

**Figure 23. Mean annual suspended sediment loads estimated using SSC-Q rating curves versus modelled mean annual loads for updated 2021 baseline in this report for river gauging stations in the Horizons region.**

**Table 22. Percentage differences between modelled and measured suspended sediment loads summarised by Basher et al (2018) with reference to previous applications of SedNetNZ in the Horizons region**

| River gauging station | Dymond et al. 2013 % | Dymond et al. 2014 % | Vale et al. 2022 – previous report % | Vale & Smith 2023 – present report % |
|---|---|---|---|---|
| Manawatū at Hopelands | –17 | –21 | –25 | –29 |
| Manawatū at Teachers College | 12 | 3 | –2 | –7 |
| Mangahao at Ballance | –32 | –27 | –39 | –46 |
| Mangatainoka at PTB | 143 | 170 | 179 | 157 |
| Oroua at Almadale | 39 | 72 | –2 | –5 |
| Pohangina at Mais Reach | –1 | –53 | –16 | –18 |
| Tiraumea at Ngāturi | 71 | 28 | 31 | 29 |
| Makuri at Tuscan Hills | | –44 | –54 | –55 |
| Ōhura at Nihoniho | | –14 | 10 | 9 |
| Owahanga at Branscombe Bridge | | 38 | –5 | –6 |
| Rangitīkei at Mangaweka | | 159 | 7 | 6 |
| Rangitīkei at Pukeokahu | | 1,273 | 200 | 190 |
| Whanganui at Te Rewa | | 11 | –25 | –25 |

Note: For comparison, percentage differences between measured and modelled loads are reported for the updated version of SedNetNZ applied in the present report. The predicted sediment loads in this report are expected to be lower than previously measured and modelled sediment loads, given the progress of SLUI and non-SLUI works.

### 5.5.2 Model limitations

The previous report by Vale et al. (2022) highlighted specific limitations in each modelling component, including the representation of erosion processes, climate change projections, the estimation of reductions required to meet visual clarity attribute bands, and reductions in sediment load due to SLUI. These limitations should be considered when interpreting the model outputs. In the present report we summarise the limitations associated with the new scenarios and additional components. For further details, see Appendix E.

#### Lowland mitigation works

The inclusion of riparian fencing as a lowland mitigation measure required modifications to the modelling approach, which introduces uncertainty due to new data inputs.

The riparian fencing and planting data only represent a partial picture of the existing fencing and planting in the region because they capture only new initiatives connected to funding grants. This means they do not account for existing fencing across the region.

To estimate the extent of current fencing in the region, estimates from the SRDM were used. However, this introduces additional uncertainties and biases commonly found in survey data. The SRDM fencing estimates may suffer from non-response and self-selection bias, as some districts had low participation rates. There may also be measurement or recall bias, as the definitions of 'free-flowing streams' and 'minor waterways/drains' are subjective and not clearly defined. Respondents might not accurately recall fencing extents, and there could be a bias towards presenting more favourable information.

Applying SRDM fencing estimates to the REC2 stream network also adds uncertainty because the definitions used in the SRDM do not directly align with available river classifications. A combination of factors such as channel width, stream order, slope, land cover, land use, and district were used to determine the most appropriate application.

The main implication of estimating current riparian fencing is that it limits the length of the remaining stream network available for fencing and, consequently, the potential reduction in sediment load from additional riparian fencing. This limitation also affects the potential improvements in visual clarity and the ability to achieve NPS-FM attribute bands and the NBL.

### PS2: rate of implementation and proportions of land classed as top, high, and low within each farm

PS2 represents a future new policy state, which involves the full implementation of Freshwater Farm Plans (FWFPs) and appropriate works within specified timeframes. The main difference from PS1 is that the implementation of appropriate works on top, high, and low land classifications is scheduled to be completed by 2035, 2045, and 2065, respectively, for each SLUI farm priority class.

To incorporate this into the model, an estimate of the proportion of top, high, and low land within the unmapped farms was required. This introduces some uncertainty because the estimate had to be based on the average proportions of these HEL land types found within mapped WFPs, according to each SLUI priority class, which may not accurately represent the actual distribution of land types in each unmapped farm.

This approach is also subject to the same limitations related to implementation, maturity, and effectiveness of the FWFPs, as well as the definition of 'fully implemented', as described in the previous report by Vale et al. (2022).

## 6 Conclusions and recommendations

- The estimated total erosion for the Horizons region in 2021 is 8.8 Mt $yr^{-1}$, with the majority occurring in the Whanganui, Manawatū, and Rangitīkei-Turakina FMUs. The predicted region-wide net suspended sediment load delivered to the coast in 2021 is 8.3 Mt $yr^{-1}$.
- Under scenarios PS1 and PS2, which represent future policy implementations, there are significant reductions (48% and 60%, respectively) in region-wide suspended sediment loads by late century. PS2 achieves most of the estimated average reduction in load (56%) by 2060.

- In the absence of climate change impacts, it is projected that 90–91% of REC2 segments by length could achieve the NBL by 2100 under these scenarios. Although both scenarios result in similar proportions of REC2 segments meeting NPS-FM attribute bands by late century, PS2 achieves this outcome earlier.
- The sediment load reductions from PS1 and PS2 are greater than those achieved in previous scenario modelling by Vale et al. (2022), which results in a higher proportion of REC2 segments achieving NPS-FM attribute bands. Some lowland REC2 segments still require proportional reductions to achieve the NBL, although the absolute loads are generally low, and lower than in the previous modelling, which did not include non-SLUI lowland riparian fencing and planting data.
- Total erosion for scenario PS1 under projected climate change for the different RCPs ranges from 8.4 to 12.5 Mt $yr^{-1}$ for mid-century, and from 4.9 to 10.1 Mt $yr^{-1}$ for late century. This represents a change of 7–46% and –4% to +79% compared to loads without the effect of climate change.
- The total erosion for scenario PS2 under different RCPs ranges from 6.2 to 9.2 Mt $yr^{-1}$ for mid-century and from 3.1 to 5.8 Mt $yr^{-1}$ for late century. This represents a change of 3–41% for mid-century and –16% to +58% for late century. Only the minimum and median RCP2.6 projections at late century result in a decrease in sediment load.
- The proportion of REC2 segments achieving the NBL under future climate change varies across RCPs, with 30–49% for mid-century and 47–83% for late century under PS1, and 43–78% for mid-century and 69–85% for late century under PS2.
- The projected climate change impact decreased the proportion of REC2 segments meeting the NBL for suspended fine sediment. However, PS1 and PS2 partially offset the climate change effects, resulting in a higher proportion of REC2 segments meeting the NBL compared to the previous scenario (SC1) from Vale et al. 2022, which modelled future climate impacts without further implementation of erosion mitigation works.
- Continued investment in erosion mitigations is necessary to limit the potential impacts of climate change on suspended sediment loads by late century.
- Improvements in model predictions could be made by incorporating region-specific data on erosion control effectiveness, and information on the implementation and maturity of works at the farm scale.
- Further clarification of what constitutes a 'fully implemented' WFP would enhance estimates of the implementation rate for SLUI works on farms.

## 7 Acknowledgements

We thank Horizons Region Council for funding this work. We acknowledge staff from Horizons Regional Council, particularly Maree Patterson, Malcom Todd, Nicolaas Portegys, and Willie McKay, for discussions that defined the scope of work, and Willie McKay for providing spatial data. We thank Andrew Neverman for reviewing the report.

# 8 References

Abernethy B, Rutherfurd ID 2000. The effect of riparian tree roots on the mass-stability of riverbanks. Earth Surface Processes and Landforms 25(9): 921–937.

Alber A, Piégay H 2017. Characterizing and modelling river channel migration rates at a regional scale: case study of south-east France. Journal of Environmental Management 202: 479–493.

Arulanandan K, Gillogley E, Tully R 1980. Development of a quantitative method to predict critical shear stress and rate of erosion of natural undisturbed cohesive soils. USACE, Waterways Experiment Station Technical Report GL-80-5. Vicksburg, MS, USACE.

Basher L, Spiekermann R, Dymond J, Herzig A, Ausseil A-G 2018. SedNetNZ, SLUI and contaminant generation. Part1: Sediment and water clarity. Manaaki Whenua – Landcare Research contract report LC3135, prepared for Horizons Regional Council.

Basher L, Spiekermann R, Dymond J, Herzig A, Hayman E, Ausseil A-G 2020. Modelling the effect of land management interventions and climate change on sediment loads in the Manawatū–Whanganui region. New Zealand Journal of Marine and Freshwater Research 54(3): 490–511.

Basher LR 2013. Erosion processes and their control in New Zealand. Ecosystem services in New Zealand – conditions and trends 2013. Manaaki Whenua Press, pp. 363–374.

Betts H, Basher L, Dymond J, Herzig A, Marden M, Phillips C 2017. Development of a landslide component for a sediment budget model. Environmental Modelling & Software 92: 28–39.

Booker D, Hicks M 2013. Estimating wetted width and fish habitat areas across New Zealand's rivers: wetted widths estimation. NIWA client report: CHC2013-075. Prepared for Department of Conservation.

Brune GM 1953. Trap efficiency of reservoirs. Eos, Transactions American Geophysical Union 34(3): 407–418.

Collins D, Montgomery K, C. Z 2018. Hydrological projections for New Zealand rivers under climate change NIWA Contract Report No. 2018193CH prepared for the Ministry for the Environment.

Crosato A 2009. Physical explanations of variations in river meander migration rates from model comparison. Earth Surface Processes and Landforms 34(15): 2078–2086.

Crozier MJ 2010. Deciphering the effect of climate change on landslide activity: a review. Geomorphology 124(3): 260–267.

Dairy Environment Leadership Group 2013. Sustainable Dairying: Water Accord: a commitment to New Zealand by the dairy sector. http://www.dairynz.co.nz/what-we-do/dairyindustry-strategy/

De Rose RC 2013. Slope control on the frequency distribution of shallow landslides and associated soil properties, North Island, New Zealand. Earth Surface Processes and Landforms 38(4): 356–371.

De Rose RC, Basher LR 2011. Strategy for the development of a New Zealand SedNet. Landcare Research Contract Report LC226 for AgResearch and Ministry of Science and Innovation.

De Rose RC, Prosser IP, Weisse M, Hughes AO 2003. Patterns of erosion and sediment and nutrient transport in the Murray-Darling Basin. CSIRO Land and Water Technical Report 32/03.

Desmet P, Govers G 1996. A GIS procedure for automatically calculating the USLE LS factor on topographically complex landscape units. Journal of Soil and Water Conservation 51(5): 427–433.

Dunn IS 1959. Tractive resistance of cohesive channels. Journal of the Soil Mechanics and Foundations Division 85(3): 1–24.

Dymond J, Herzig A, Ausseil A-G 2014. Using SedNetNZ to assess the impact of the Sustainable Land Use Initiative in the Manawatu-Wanganui region on river sediment loads. Landcare Research Contract Report No. 2014/EXT/1367 prepared for Horizons Regional Council.

Dymond J, Herzig A, Basher L, Betts HD, Marden M, Phillips CJ, Ausseil A-GE, Palmer DJ, Clark M, Roygard J 2016. Development of a New Zealand SedNet model for assessment of catchment-wide soil-conservation works. Geomorphology 257: 85–93.

Dymond J, Herzig A, Betts H, Marden M, Phillips C, Basher L 2013. Application of SedNetNZ for the assessment of critical source areas in the Manawatu catchment. Landcare Research Contract Report LC1697 for AgResearch and MBIE.

Dymond JR, Ausseil A-G, Shepherd JD, Buettner L 2006. Validation of a region-wide model of landslide susceptibility in the Manawatu–Wanganui region of New Zealand. Geomorphology 74(1–4): 70–79.

Dymond JR, Betts HD, Schierlitz CS 2010. An erosion model for evaluating regional land-use scenarios. Journal of Environmental Modelling Software 25(3): 289–298.

Dymond JR, Davies-Colley RJ, Hughes AO and Matthaei CD 2017. Predicting improved optical water quality in rivers resulting from soil conservation actions on land. Science of the Total Environment, 603, pp.584-592.

Dymond JR, Jessen MR, Lovell LR 1999. Computer simulation of shallow landsliding in New Zealand hill country. International Journal of Applied Earth Observation and Geoinformation 1(2): 122–131.

Dymond JR, Shepherd JD 2004. The spatial distribution of indigenous forest and its composition in the Wellington region, New Zealand, from ETM+ satellite imagery. Remote Sensing of Environment 90: 116–125.

Elliott AH, Semadeni-Davies AF, Shankar U, Zeldis JR, Wheeler DM, Plew DR, Rys GJ, Harris SR 2016. A national-scale GIS-based system for modelling impacts of land use on water quality. Environmental Modelling & Software 86: 131–144.

Eyles GO 1983. The distribution and severity of present soil erosion in New Zealand. New Zealand Geographer 39(1): 12–28.

Foster GR, Meyer LD, Onstad CA 1977. A runoff erosivity factor and variable slope length exponents for soil loss estimates. Transactions of the ASAE 20(4): 683–687.

Fryirs KA, Wheaton JM, Brierley GJ 2016. An approach for measuring confinement and assessing the influence of valley setting on river forms and processes. Earth Surface Processes and Landforms 41(5): 701–710.

Fuller IC 2008. Geomorphic impacts of a 100-year flood: Kiwitea Stream, Manawatu catchment, New Zealand. Geomorphology 98(1–2): 84–95.

Fuller IC, Heerdegen RG 2005. The February 2004 floods in the Manawatu, New Zealand: hydrological significance and impact on channel morphology. Journal of Hydrology New Zealand 44(2): 75–90.

Fuller IC, Riedler RA, Glade T, Bell R, Marden M 2016. Landslide-driven erosion and slope-channel coupling in steep, forested terrain, Ruahine Ranges, New Zealand, 1946–2011. Catena 142: 252–268.

Gill MA 1979. Sedimentation and useful life of reservoirs. Journal of Hydrology 44(1): 89–95.

Guy GG 1977. Landslide investigations, Main North Line Railway, South Island, New Zealand. Unpublished thesis, University of Canterbury. http://ir.canterbury.ac.nz/handle/10092/8095.

Hall JE, Holzer DM, Beechie TJ 2007. Predicting river floodplain and lateral channel migration for salmon habitat conservation 1.  Journal of the American Water Resources Association 43(3): 786–797.

Hancox GT 2004. Immediate report on landsliding caused by the 15-20 February 2004 floods in the lower North Island, New Zealand. GNS Immediate Report LD3 & 5 / 942.

Hancox GT, Wright K 2005. Analysis of landsliding caused by the 15–17 February 2004 rainstorm in the Wanganui-Manawatu hill country, southern North Island, New Zealand. Institute of Geological & Nuclear Sciences.

Hanson GJ, Simon A 2001. Erodibility of cohesive streambeds in the loess area of the midwestern USA. Hydrological Processes 15(1): 23–38.

Hawley JG, Dymond JR 1988. How much do trees reduce landsliding? Journal of Soil and Water Conservation 43(6): 495.

Henderson, R, Diettrich, J. 2007. Statistical analysis of river flow data in the Horizons Region. Prepared for Horizons Manawatu Regional Council. NIWA Client Report: CHC2006-154.

Hickin EJ, Nanson GC 1984. Lateral migration rates of river bends. Journal of Hydraulic Engineering 110(11): 1557–1567.

Hicks DM, Haddadchi A, Whitehead A, Shankar U 2019. Sediment load reductions to meet suspended and deposited sediment thresholds. NIWA Client Report 2019100CH prepared for Ministry for the Environment.

Hicks DM, Semadeni-Davies A, Haddadchi A, Shankar U, Plew D 2019. Updated sediment load estimator for New Zealand. NIWA Client Report No: 2018341CH.

Hicks DM, Shankar U 2020. Sediment load reduction to meet visual clarity bottom lines. Memo prepared for Ministry for the Environment.

Hooke JM 1979. An analysis of the processes of river bank erosion. Journal of Hydrology 42(1): 39–62.

Horizons Regional Council 2019a. Hill country erosion and sediment management in the Manawatu Whanganui region. Report No. 19-94.

Horizons Regional Council 2019b. Sustainable Land Use Initiative: Catchment Operations Committee report No. 19-92.

Horizons Regional Council. Implementation of lowland mitigation works for review, Unpublished document.

Hubble TCT, Docker BB, Rutherfurd ID 2010. The role of riparian trees in maintaining riverbank stability: a review of Australian experience and practice. Ecological Engineering 36(3): 292–304.

IPCC 2013. Climate change 2013: the physical science basis. Contribution of Working Group I to the Fifth Assessment Report of the Intergovernmental Panel on Climate Change. Cambridge, UK and New York, NY Cambridge University Press. 1535, doi:10.1017/CBO9781107415324. p.

Julian JP, Torres R 2006. Hydraulic erosion of cohesive riverbanks. Geomorphology 76(1): 193–206.

Konsoer KM, Rhoads BL, Langendoen EJ, Best JL, Ursic ME, Abad JD, Garcia MH 2016. Spatial variability in bank resistance to erosion on a large meandering, mixed bedrock-alluvial river. Geomorphology 252: 80–97.

Landcare Research NZ Ltd 2020. LCDB v5.0 – Land Cover Database version 5.0, Mainland New Zealand. Available from LRIS portal: https://lris.scinfo.org.nz/layer/104400-lcdb-v50-land-cover-database-version-50-mainland-new-zealand/.

Leathwick JR, Morgan F, Wilson G, Rutledge D, McLeod M, Johnston K 2003. Land environments of New Zealand: technical guide. Auckland, David Bateman Ltd.

Manderson A, Douglas G, Mackay A, Dymond JR 2011. SLUI Outcomes project: review of the SLUI database and development of a SLUI outcomes reporting framework. Report prepared for Horizons Regional Council by AgResearch.

Manderson A, Dymond JR, Ausseil A-G 2015. Climate change impacts on water quality outcomes from the Sustainable Land Use Initiative (SLUI). Horizons Report No. 2015/EXT/1451.

Marden M, Herzig A, Basher L 2014. Erosion process contribution to sediment yield before and after the establishment of exotic forest: Waipaoa catchment, New Zealand. Geomorphology 226: 162–174.

Marden M, Phillips CJ, Rowan D 2008. Recurrent displacement of a forested earthflow and implications for forest management, East Coast Region, New Zealand. IAHS publication 325: 491–501.

McCool DK, Foster GR, Mutchler CK, Meyer LD 1989. Revised slope length factor for the universal soil loss equation. Transactions of the ASAE 32(5): 1571–1576.

McIvor I, Douglas G, Dymond JR, Eyles G, Marden M 2011. Pastoral hillslope erosion in New Zealand and the role of poplar and willow trees in its reduction. In: Soil erosion issues in agriculture. Pp. 257–278.

http://www.intechopen.com/articles/show/title/pastoral-hill-slope-erosion-in-new-zealand-and-the-role-of-poplar-and-willow-trees-in-its-reduction.

Ministry for the Environment 2018. Climate change projections for New Zealand: atmospheric projections based on simulations undertaken for the IPCC 5th Assessment. 2nd edn. Wellington, Ministry for the Environment.

Ministry for the Environment 2020. National Policy Statement for Freshwater Management 2020. Wellington, Ministry for the Environment.

Ministry for the Environment 2022a. Guidance for implementing the NPS-FM sediment requirements. Wellington, Ministry for the Environment.

Ministry for the Environment 2022b. Stock exclusion low slope land 2022. Retrieved from https://data.mfe.govt.nz/layer/111150-stock-exclusion-low-slope-land-2022/

Miri SA 1999. Erosion and land use in the Pohangina region: a study using GIS and remote sensing. Unpublished master's thesis, Massey University.

Nanson GC, Hickin EJ 1983. Channel migration and incision on the Beatton River. Journal of Hydraulic Engineering 109(3): 327–337.

Nanson GC, Hickin EJ 1986. A statistical analysis of bank erosion and channel migration in western Canada. Geological Society of America Bulletin 97(4): 497–504.

Neverman A, Djanibekov U, Soliman T, Walsh P, Spiekermann R, Basher L 2019. Impact testing of a proposed suspended sediment attribute: identifying erosion and sediment control mitigations to meet proposed sediment attribute bottom lines and the costs and benefits of those mitigations. Manaaki Whenua – Landcare Research Contract Report LC3574.

Neverman A, Smith HG 2022. SedNetNZ modelling for freshwater planning in Otago. Landcare Research Contract Report LC5016, prepared for Otago Regional Council.

Neverman A, Smith HG, Herzig A, Basher LR 2021a. Modelling baseline suspended sediment loads and load reductions required to achieve Draft Freshwater Objectives for Southland. Manaaki Whenua – Landcare Research Contract Report LC3749, prepared for Environment Southland.

Neverman A, Smith HG, Herzig A, Basher L 2021b. Planning soil conservation for sediment load reduction in Taranaki. Manaaki Whenua – Landcare Research Contract Report LC3942 prepared for Taranaki Regional Council.

Neverman A, Vale SS, Smith HG 2020. Real-time monitoring to detect erosion sources affecting sediment-related water quality. Soil Horizons Issue 29.

Neverman AJ, Donovan M, Smith HG, Ausseil AG, Zammit C 2023. Climate change impacts on erosion and suspended sediment loads in New Zealand. Geomorphology 427: 108607.

Newsome PFJ, Wilde RH, Willoughby EJ 2008. Land Resource Information System spatial data layers: data dictionary. Palmerston North, NZ, Landcare Research. http://digitallibrary.landcareresearch.co.nz/cdm/ref/collection/p20022coll14/id/67.

NIWA 2021. CliFlo: NIWA's National Climate Database on the Web. Available from https://cliflo.niwa.co.nz/

Page MJ, Trustrum NA, Dymond JR 1994. Sediment budget to assess the geomorphic effect of a cyclonic storm, New Zealand. Geomorphology 9(3): 169–188.

Polvi LE, Wohl E, Merritt DM 2014. Modeling the functional influence of vegetation type on streambank cohesion. Earth Surface Processes and Landforms 39(9): 1245–1258.

Reid LM, Page MJ 2003. Magnitude and frequency of landsliding in a large New Zealand catchment. Geomorphology 49(1–2): 71–88.

Renard KG 1997. Predicting soil erosion by water: a guide to conservation planning with the Revised Universal Soil Loss Equation (RUSLE). Washington, DC, United States Government Printing.

Rosewell CJ, Loch RJ 2002. Estimation of the RUSLE soil erodibility factor. In: McKenzie N, Coughlan K, Cresswell H eds Soil physical measurement and interpretation for land evaluation. Melbourne, Australia: CSIRO Publishing.

Semadeni-Davies A, Elliott S 2016. Modelling the effect of stock exclusion on *E. coli* in rivers and streams: national application. Technical Paper No: 2017/10 prepared for Ministry for Primary Industries by NIWA.

Sibson R 1981. A brief description of natural neighbor interpolation. In: Barnett V ed. Interpolating multivariate data. Chichester, UK, John Wiley. Pp. 21–36.

Simon A, Collison AJC 2002. Quantifying the mechanical and hydrologic effects of riparian vegetation on streambank stability. Earth Surface Processes and Landforms 27(5): 527–546.

Smith HG, Herzig A, Dymond JR, Basher LR 2019. Application of a revised SedNetNZ model to the Oreti and Aparima catchments, Southland. Manaaki Whenua – Landcare Research contract report LC3507 prepared for Our Land & Water National Science Challenge.

Smith HG, Spiekermann R, Betts H, Neverman AJ 2020. Application of a revised bank erosion model to update SedNetNZ results for Hawke's Bay. Manaaki Whenua – Landcare Research contract report LC3740, prepared for Hawke’s Bay Regional Council.

Smith HG, Spiekermann R, Betts H, Neverman AJ 2021. Comparing methods of landslide data acquisition and susceptibility modelling: examples from New Zealand. Geomorphology 381: 107660.

Smith HG, Spiekermann R, Dymond J, Basher L 2019. Predicting spatial patterns in riverbank erosion for catchment sediment budgets. New Zealand Journal of Marine and Freshwater Research 53(3): 338–362.

Sood A 2014. Improved bias corrected and downscaled regional climate model data for climate impact studies: validation and assessment for New Zealand. Retrieved from www.researchgate.net/publication/265510643_Improved_Bias_Corrected_and_Downscaled_Regional_Climate_Model_Data_for_Climate_Impact_Studies_Validation_and_Assessment_for_New_Zealand

Spiekermann R, Betts H, Dymond J, Basher L 2017. Volumetric measurement of river bank erosion from sequential historical aerial photography. Geomorphology 296: 193–208.

Thorne CR 1990. Effects of vegetation on riverbank erosion and stability. In: Thornes JB ed. Vegetation and erosion. Chichester, UK, John Wiley & Sons. Pp. 125–144.

Trimble SW 1994. Erosional effects of cattle on streambanks in Tennessee, U.S.A. Earth Surface Processes and Landforms 19(5): 451–464.

Vale SS 2018. Quantifying sediment sources of floodplain deposits in the lower Oroua River using sediment fingerprinting. Manaaki Whenua – Landcare Research contract report LC3287, prepared for Horizons Regional Council.

Vale SS, Smith HG, Matthews A, Boyte S 2021. Determining sediment source contributions to overbank deposits within stopbanks in the Oroua River, New Zealand, using sediment fingerprinting. Journal of Hydrology (NZ) 59(2): 147–172.

Vale SS, Smith HG, Neverman A, Herzig A 2021. Application of SedNetNZ with land management and climate change scenarios and temporal disaggregation in the Bay of Plenty Region. Manaaki Whenua – Landcare Research contract report LC4002, prepared for Bay of Plenty Regional Council.

Vale SS, Smith HG, Neverman A, Herzig A 2022. Application of SedNetNZ with SLUI erosion mitigation and climate change scenarios in the Horizons region to support NPS-FM 2020 implementation. Manaaki Whenua – Landcare Research contract report LC5033, prepared for Horizons Regional Council.

Walker M, Rutherfurd ID 1999. An approach to predicting rates of bend migration in meandering alluvial streams. In: Rutherfurd ID, Bartley R eds. Proceedings of the Second Australian Stream Management Conference, Melbourne, Australia, Cooperative Research Centre for Catchment Hydrology. Pp. 659–665.

Wang G, Gertner G, Liu X, Anderson A 2001. Uncertainty assessment of soil erodibility factor for revised universal soil loss equation. Catena 46(1): 1–14.

Whitehead AL, Booker DJ 2020. NZ river maps: an interactive online tool for mapping predicted freshwater variables across New Zealand. Christchurch, NIWA. https://shiny.niwa.co.nz/nzrivermaps/

Wischmeier WH, Johnson C, Cross B 1971. Soil erodibility nomograph for farmland and construction sites. Journal of Soil and Water Conservation 26(5): 189–193.

Woods R, Hendrikx J, Henderson R, Tait A 2006. Estimating mean flow of New Zealand rivers. Journal of Hydrology New Zealand 45(2): 95–109.

Wynn T, Mostaghimi S 2006. The effects of vegetation and soil type on streambank erosion, Southwestern Virginia, usa1. Journal of the American Water Resources Association 42(1): 69–82.

Yang X, Gray J, Chapman G, Zhu Q, Tulau M, McInnes-Clarke S 2018. Digital mapping of soil erodibility for water erosion in New South Wales, Australia. Soil Research 56(2): 158–170.

Zhang X, Phillips C, Pearce A 1991. Surface movement in an earthflow complex, Raukumara Peninsula, New Zealand. Geomorphology 4(3): 261–272.

Zhang X, Liu X, Zhang M, Dahlgren RA, Eitzel M 2010. A Review of vegetated buffers and a meta-analysis of their mitigation efficacy in reducing nonpoint source pollution. Journal of Environmental Quality 39(1): 76–84.

# Appendix A – SedNetNZ model description

This section provides a description of methods used in the application of SedNetNZ in the Horizons region, as described in Vale et al. 2022 and provided here for ease of reference.

## Surficial erosion

Surficial erosion processes in SedNetNZ (Dymond et al. 2016) are represented by the NZUSLE[2] (Dymond et al. 2010) model:

$$ES = aP^2KLSC \tag{A1}$$

where $ES$ denotes surficial erosion in t km$^{-2}$ yr$^{-1}$, $a$ is a constant (t km$^{-2}$ yr$^{-1}$ mm$^{-2}$) calibrated against measurements (Dymond et al. 2010) with a value of 1.2 x 10$^{-3}$; $P$ is mean annual rainfall (mm); $K$ is the soil erodibility factor (dimensionless), $L$ is the slope length factor, $S$ is the slope steepness factor, and $C$ represents the impact of vegetation cover (dimensionless) (1.0 for bare ground, 0.01 for pasture, and 0.005 for forest and scrub).

We use a revised representation of surficial erosion processes as part of the SedNetNZ model, following Smith, Herzig et al. (2019), which replaces the slope length and slope steepness factors. The uniform slope length factor ($L$) of the NZUSLE (Dymond et al. 2010) is replaced with a factor that better represents the effect of topography on the size of convergent upslope areas contributing overland flow and surficial erosion, as described by Desmet and Govers (1996):

$$L = \frac{\left(A+D^2\right)^{m+1} - A^{m+1}}{D^{m+2} \times x^m \times 22.13^m} \tag{A2}$$

where $L$ is the slope length factor for a given raster cell (pixel), $A$ is the upstream catchment area (m$^2$) at the cell inlet, $D$ is the raster cell width (m), $m$ is the slope length exponent, $x$ = sin $a$+cos $a$, with α being the slope aspect.

The slope length exponent, $m$, is calculated depending on the rill to inter-rill ratio, $\beta$, and the slope gradient, $\theta$, (Foster et al. 1977; McCool et al. 1989; cited in Renard 1997):

$$\beta = \frac{\sin\theta / 0.896}{3 \times (\sin\theta)^{0.8} + 0.56} \tag{A2}$$

$$m = \frac{\beta}{1 + \beta} \tag{A3}$$

We also apply a revised slope factor, $S$, which is calculated according to a threshold in slope gradient $sp$ (%) (Renard 1997):

$$S = \begin{cases} 10.8 \times \sin\theta + 0.03 & with\ sp\ < 9\% \\ 16.8 \times \sin\theta - 0.5 & with\ sp\ \geq 9\% \end{cases} \tag{A4}$$

---

[2] New Zealand Universal Soil Loss Equation.

Furthermore, we apply a revised, spatially variable K factor in the NZUSLE developed in Neverman et al. (2021b) to better represent the spatial variability of soil erodibility, utilising the Fundamental Soil Layers (FSL) to represent soil parameters. We adapted the K factor equations in Wang et al. (2001) and Yang et al. (2018) to the NZUSLE:

$$K = \frac{2.1(12-OM)M^{1.14}10^{-4}+3.25(SS-2)+2.5(PP-3)}{7.59 \times 10} \quad \text{(A5)}$$

where $OM$ is the soil organic matter content, $M$ is the particle size parameter, $SS$ is the soil structure code, and $PP$ is the soil profile permeability code. We use six $PP$ classes, adapted from Rosewell and Loch (2002). The soil structure code was set at $SS$ = 2 because the FSL has insufficient data on soil structure to relate to the SS classes used for calculating $K$. We found the magnitude of $K$ was not sensitive to the choice of $SS$ class value. $M$ is calculated as a function of the proportion of silt and clay:

$$M = Silt(100 - Clay) \quad \text{(A6)}$$

where $Silt$ and $Clay$ are the percentages of silt and clay in the soil, respectively.

$Silt$ was limited to a range of 15–70%, and $OM$ was capped at 4% to fit the nomograph of Wischmeier et al. (1971) used to derive Equation A5 for organic soils. Where there was no FSL information available to calculate a spatially varying K factor, a uniform value of 0.25 was used (Dymond et al. 2010).

## Shallow landslide erosion

Shallow landslides are considered to be the most common form of erosion in New Zealand hill country (Eyles 1983). Typical landslides are seldom greater than 2 m deep, and individual failures are usually of small areal extent (50–100 m$^2$) (Smith et al. 2021). They usually have a debris tail of deposited sediment below their source, which often reaches a stream (for approximately half of debris tails; see Dymond et al. 1999). Landslide occurrence is highly correlated with slope angle, with most failures occurring on slopes steeper than 26 degrees, but landslides can occur on slopes as low as 15 degrees (De Rose 2013; Smith et al. 2021). The expected mass of soil lost to landslide erosion per square kilometre per year, and the connection with a stream, is given by $EL$:

$$EL = \rho \, SDR \, d_l f(s) \quad \text{(A7)}$$

where $\rho$ is the bulk density of soil (t m$^{-3}$), $SDR$ is the sediment delivery ratio, $d_l$ is the mean depth of landslide failure (m), and $f(s)$ is the expected area of landslide scars per square kilometre per year at slope angle $s$ (m$^2$ km$^{-2}$ yr$^{-1}$).

Landslide erosion is estimated for those Erosion Terrains[3] (see Dymond et al. 2010) identified as being susceptible to landslide erosion. $\rho$ is set to 1.5 t m$^{-3}$ (Dymond et al.

---

[3] An Erosion Terrain is a land type with a unique combination of erosion processes and rates, leading to characteristic sediment generation and yields. Erosion Terrains were derived from the New Zealand Land Resource Inventory data and are based on combinations of rock type/parent material, topography, rainfall, and erosion process type and severity. Erosion Terrain coefficients are listed in Dymond et al. 2010.

2016); $SDR$ values are typically 0.5 (Dymond et al. 2016), but vary from 0.1 to 1.0 depending on the specific Erosion Terrain calibrated for the region; $d_l$ is set to 1 m (Page et al. 1994; Reid & Page 2003); and $f(s)$ is determined from previous calibration of SedNetNZ in the Manawatū (Dymond et al. 2016; Betts et al. 2017). Permanent forest cover is estimated to reduce shallow landslide erosion by 90% compared with pasture (Basher 2013; Dymond et al. 2016).

## Earthflow erosion

Slow-moving earthflows (c. 1 m per year) are common in Erosion Terrains underlain by crushed mudstone and argillite (Dymond et al. 2010). The delivery of sediment to streams is via the undercutting of earthflow toes. The mass of soil delivered to streams by earthflows in t km$^{-2}$ a$^{-1}$ is denoted by $EE$ and is estimated as:

$$EE = \rho \, d_e \, v \, ED \tag{A8}$$

Where $\rho$ is the bulk density of soil (t m$^{-3}$), $d_e$ is the mean depth of earthflows (m), $v$ is the mean speed of earthflows (m yr$^{-1}$), and $ED$ is the mean length of stream intersecting earthflow toes in a square kilometre (m km$^{-2}$).

$\rho$ is set to 1.5 t m$^{3}$ (Dymond et al. 2016), $d_e$ is set to 3 m (based on field observation; Dymond et al. 2016), and $v$ is set to 0.1 m yr$^{-1}$ (average from published data; Guy 1977; Zhang et al. 1991; Marden et al. 2008, 2014). $ED$ is set to 1,024 m km$^{-2}$ (from digitising stream lengths on scanned aerial photographs; Dymond et al. 2016).

## Gully erosion

Gullies commonly initiate at channel heads, usually because of excessive surface or subsurface water flow. Once initiated, a gully can continue to expand over long time periods (decades). The mass of soil delivered to streams by gullies, in t km$^{-2}$ yr$^{-1}$, is denoted by $EG$ and is estimated by:

$$EG = \frac{\rho \, A_g \, GD}{T} \tag{A9}$$

where $\rho$ is the bulk density of soil (t m$^{-3}$), $A_g$ is the mean cross-sectional area of gullies (m$^{2}$), $GD$ is the length of gullies in a square kilometre (km km$^{-2}$), and $T$ is the time since gully initiation (in years).

Following Dymond et al. (2016), $\rho$ is set to 1.5 t m$^{-3}$; $A_g$ is set to 900 m$^{2}$ (from field observations), $GD$ is set to 220 m (from digitising gully lengths on scanned aerial photographs), and $T$ is set to 120 years.

## Bank erosion

SedNetNZ represents bank erosion at the reach-scale, whereby the river network is divided into stream links based on the River Environment Classification v2 (REC2). The total mass of material eroded from riverbanks each year is a function of bank height, reach length, and bank migration rate (Dymond et al. 2016):

$$B_j = \rho M_j H_j L_j \qquad \text{(A10)}$$

where $B_j$ is the total eroded mass for the $j$th stream link (t yr$^{-1}$), $\rho$ is the bulk density of the bank material (t m$^{-3}$), $M_j$ is the bank migration rate (m yr$^{-1}$), $H_j$ is the mean bank height (m), and $L_j$ is the length (m) of the $j$th stream link. Bank height is derived from a relationship with mean annual discharge, and bulk density is estimated at 1.5 t m$^{-3}$ (Dymond et al. 2016).

The predicted mass of material eroded from riverbanks represents the gross contribution of sediment supplied to the river channel per year. This does not account for redeposition and storage of eroded bank material on banks or within the channel bed, or the lateral accretion of material on bars with channel migration. Hence, net bank erosion in SedNetNZ is estimated as one-fifth of gross bank erosion, based on results from the Waipaoa River catchment (De Rose & Basher 2011). Overbank vertical accretion of fine sediment on floodplains beyond the active channel is represented separately (Dymond et al. 2016).

Bank migration rate ($M_j$) is represented as a function of six factors as follows:

$$M_j = SP_j Sn_j T_j V_j \left(1 - PR_j\right)\left(1 - PW_j\right) \qquad \text{(A11)}$$

where $M_j$ is the bank migration rate (m yr$^{-1}$) of the $j$th stream link, $SP_j$ is the stream power of the mean annual flood for the $j$th stream link, $Sn_j$ is the channel sinuosity rate factor of the $j$th link, $T_j$ is the soil texture-based erodibility factor of the $j$th link, $V_j$ is the valley confinement factor of the $j$th link, $PR_j$ is the proportion of riparian woody vegetation of the $j$th link, and $PW_j$ is the fraction of bank protection works for the $j$th link (Smith, Spiekermann et al. 2019).

Stream power ($SP_j$) for the mean annual flood ($MAF_j$, m$^3$ s$^{-1}$) is estimated for each stream link by the product of mean annual flood and channel slope ($S_j$). $MAF$ is estimated from a fitted power relationship ($MAF = aq^b$) with mean annual discharge ($q$, m$^3$ s$^{-1}$) using data from long-term river flow gauging within the catchment or region of interest:

$$SP_j = MAF_j S_j = a{q_j}^b S_j \qquad \text{(A12)}$$

Various studies report increasing bank migration rates with increasing bankfull discharge and stream power (Hooke 1979; Nanson & Hickin 1986; Walker & Rutherfurd 1999; Alber & Piégay 2017). While MAF has been shown to relate to bank erosion rates (Dymond et al. 2016), other factors, such as channel sinuosity (Nanson & Hickin 1983), the cohesiveness of bank materials (Julian & Torres 2006), valley confinement (Hall et al. 2007), and riparian woody vegetation (Abernethy & Rutherfurd 2000), are also important, resulting in high levels of spatial variability in bank erosion.

We use the log-normal probability density function to represent the relationship between channel sinuosity and migration rate, which we term the sinuosity rate factor. This function allows us to represent the positive skew observed in the relationship between channel sinuosity and migration rate (Crosato 2009). The dimensionless channel sinuosity rate factor ($Sn_j$) is calculated as

$$Sn_j = \frac{1}{(Sinu_j - 1)\sigma\sqrt{2\pi}}\, e^{\left(-\frac{\left(\ln\left(Sinu_j - 1\right) - \mu\right)^2}{2\sigma^2}\right)} \tag{A13}$$

where $Sinu_j$ is sinuosity of the $j$th stream link of the REC2 network, and $\mu$ and $\sigma$ are the mean and standard deviation parameters that determine the location and scale of the distribution. The $\mu$ and $\sigma$ parameters are fitted using measurements of reach-scale bank migration rates.

The texture of bank material influences bank migration rates (Hickin & Nanson 1984; Julian & Torres 2006; Wynn & Mostaghimi 2006). Our approach is based on an empirical relationship between percent silt + clay content ($SC$) and soil critical shear stress ($\tau_c$) derived by Julian and Torres (2006) using data from Dunn (1959) as follows:

$$\tau_c = 0.1 + 0.1779SC + 0.0028SC^2 - 0.0000234SC^3 \tag{A14}$$

$SC$ is obtained from spatial data on soil textural classes compiled from the FSL (Newsome et al. 2008), which provide national coverage. The soil texture-based erodibility factor ($T_j$) is represented by a power function to characterise the relationship between $\tau_c$ and bank erodibility for the $j$th stream link:

$$T_j = c\tau_{c,j}{}^{-d} \tag{A15}$$

where the c and d parameters are fitted using available bank migration rate data. The choice of a power function is based on experimental (Arulanandan et al. 1980) and field (Hanson & Simon 2001; Julian & Torres 2006) observations of the relationship between stream bank or bed critical shear stress and erodibility.

Floodplain extent and the level of valley confinement are factors that may limit lateral bank migration (Hall et al. 2007; De Rose & Basher 2011). The presence of steep valley sides and/or exposure of bedrock influence spatial patterns of erosion and deposition (Fryirs et al. 2016). Here, we adapt the Australian SedNet model approach to estimate a valley confinement factor ($V_j$) by using the mean slope ($SB_j$) in degrees of a buffer zone either side of the $j$th stream link:

$$V_j = \left(1 - e^{\left(-15/_{SB_j}\right)}\right)^{11} \tag{A16}$$

Woody riparian vegetation typically increases bank stability via the effects of root reinforcement and root cohesion (Abernethy & Rutherfurd 2000; Hubble et al. 2010; Polvi et al. 2014; Konsoer et al. 2016). Woody vegetation can also increase roughness and flow resistance, thereby reducing the boundary shear stress acting on the bank surface (Thorne 1990). In addition, woody vegetation has hydrological effects on bank stability. For example, woody vegetation was found to be more effective than grass cover at lowering soil water content due to increased canopy interception and evapotranspiration, thus improving bank stability (Simon & Collison 2002).

We represent the effect of riparian woody vegetation ($PR_j$) in reducing bank migration rates at the reach scale. Bank migration rates are reduced proportionally to the extent of woody riparian vegetation along the $j^{\text{th}}$ stream link (equation A11). Stream links with complete riparian woody vegetation cover are assumed to erode at 0.05 of the migration rate with no woody cover (De Rose et al. 2003). Spatial information on woody vegetation is obtained from satellite imagery and intersected with the Land Information New Zealand (LINZ) digital stream network obtained from 1:50,000 topographic mapping. The mapped stream network was used in preference to the DEM-derived channel network because it tends to exhibit better planform accuracy, which should improve spatial correspondence between channel position and riparian woody vegetation.

In some cases the LINZ stream network provides poor representation of channel width for wider reaches with exposed gravel. To address this issue, the spatial union of the LINZ river polygons with LCDB v5 'river' and 'gravel and rock' land-cover classes was used to produce revised river polygons. Mapped gravel and rock areas located beyond the extent of the channel network were removed. The revised stream network layer improved alignment between channel banks and mapped woody vegetation when quantifying the reach-scale extent of riparian woody vegetation cover. The proportion of riparian woody vegetation is computed from the intersection of the revised stream network with a 15 m buffer and a classified map of 2002 woody vegetation cover (called EcoSat Woody) derived from Landsat TM at 15 m resolution (Dymond & Shepherd 2004).

We also include representation of channel protection works ($PW_j$) that are designed to reduce bank erosion (e.g. rock riprap, willow edge protection), as well as stopbanks employed for flood protection, where such data are available. We assume that over the multi-decadal model timescale, erosion mitigation would ultimately be targeted to where migrating riverbanks approach stopbanks, or that such interventions have already been implemented to protect stopbank integrity. The proportional length of bank erosion mitigation measures ($PEC_j$) and stopbanks ($PSB_j$) is summed to give the proportion of channel works ($PW_j$) for the $j$th stream link. $PEC_j$ is computed as the length of erosion mitigation measures within a stream link relative to the total length of that link. This assumes erosion mitigation measures are targeted to the eroding bank side. Stopbanks may be located on either side of the channel irrespective of the direction of bank migration. Therefore, $PSB_j$ is computed as the length of stopbanks in a link relative to 2 × link length.

Inputs to the bank erosion model component of SedNetNZ were obtained from national-scale spatial datasets comprising the REC2 and LINZ stream networks, 15 m DEM, FSL for soil data, and EcoSat Woody for 2002 woody vegetation cover. LCDB v5 (Landcare Research NZ Ltd 2020) was not used, despite being more recent, because it has a minimum mapping unit of 10,000 $\text{m}^2$ versus 225 $\text{m}^2$ for EcoSat. This makes LCDB less suitable for characterising narrow corridors of woody vegetation often found along channel banks.

Mean annual discharge estimated for each link in the REC2 stream network is based on an empirical water balance model (Woods et al. 2006) used in the CLUES water quality model (Elliott et al. 2016). Mean annual flood statistics for 47 gauging stations with records >10 years were obtained from an analysis of river flow data for the Horizons region (Henderson & Diettrich 2007). These data were used to fit regional relationships between mean annual discharge and mean annual flood for use in calculating stream power for each REC2 link in the stream network. MAF was best predicted by partitioning the gauging site data into three spatially discrete areas comprising: a) Manawatū and adjacent coastal catchments ($MAF = 40q^{0.81}, R^2 = 0.97, n = 21$); b) Rangitīkei ($MAF = 34q^{0.66}, R^2 = 0.95, n = 9$); and c) Whanganui, Kai Iwi, Whangaehu, and Turakina catchments ($MAF = 26q^{0.79}, R^2 = 0.97, n = 17$). These discrete q/MAF relationships produced a small improvement over a single, region-wide relationship ($R^2 = 0.94$). HRC also provided spatial data on stopbanks and channel protection works, which have been included in the model simulations.

We used a dataset comprising available measured bank migration rates from the Manawatū and Kaipara catchments to calibrate the bank erosion model (Spiekermann et al. 2017; Smith, Spiekermann et al. 2019). Calibration of the bank migration model was performed by minimising the mean square error (MSE) between predicted and observed data by optimising parameter values for the sinuosity ($\mu$ and $\sigma$) and bank soil texture ($c$ and $d$) factors in equations A13 and A15, respectively. This produced reasonable agreement between measured and observed rates of bank migration (Smith, Spiekermann et al. 2019; Figure A1).

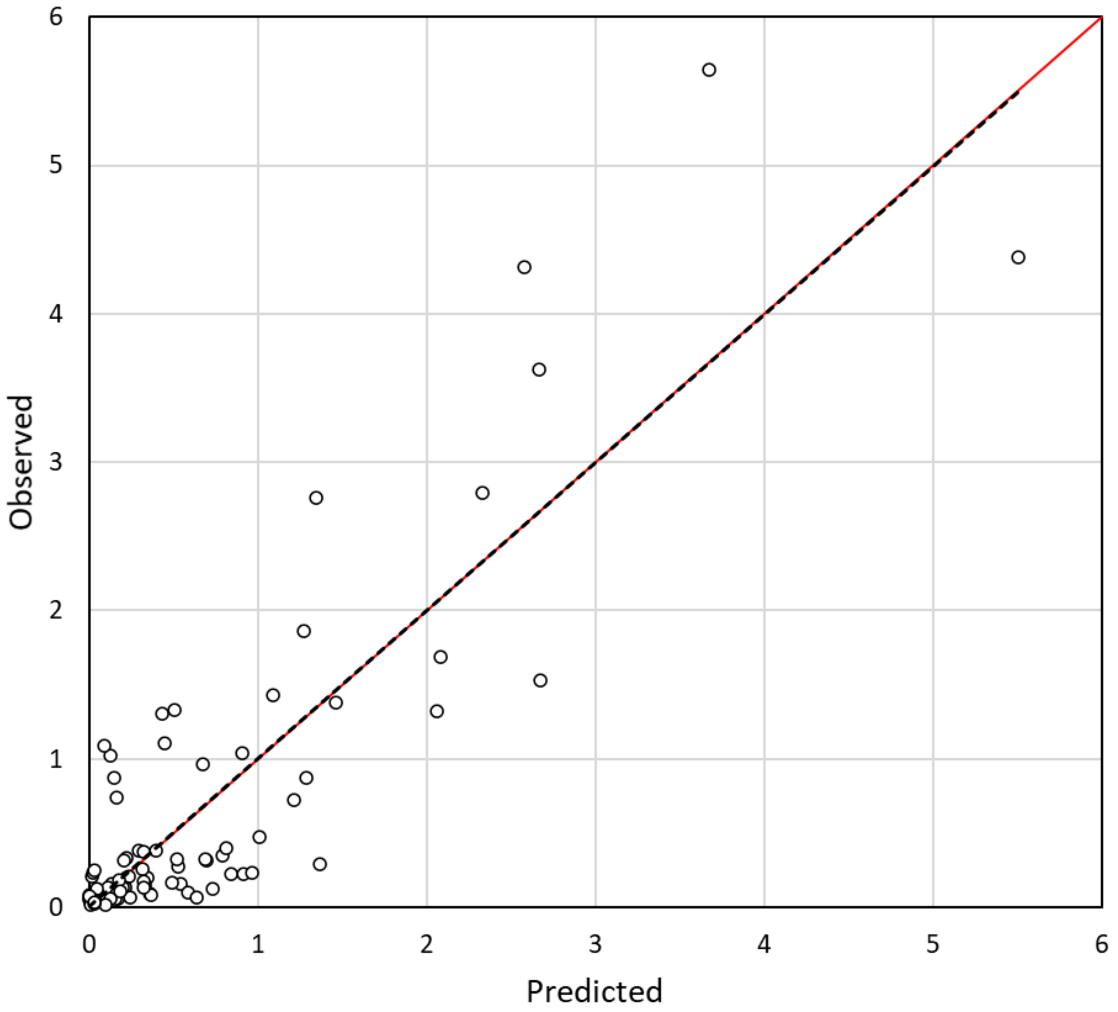

**Figure A1. Plot comparing predicted versus observed bank migration rates (m yr$^{-1}$) based on calibrated parameter values for the sinuosity and erodibility factors. Fitted regression line (black dashed) and the 1:1 line (red) are also shown.**

## Sediment routing

SedNetNZ accounts for the deposition of sediment in lakes and on floodplains as the sediment is transported through the channel network.

To account for sediment trapping through lakes, we apply a revised SedNetNZ sediment routing algorithm. The revised algorithm applies a lake-specific sediment passing factor ($SPF$) to the net routed sediment load at the end of an REC2 sub-catchment draining to a lake. $SPF$ was calculated using an adaptation of Gill's (1979) approximation of Brune's (1953) trap efficiency (the inverse of passing factor) curve for medium sediment:

$$SPF = 1 - \frac{V/_I}{1.02(V/_I) + 0.012} \qquad \text{(A17)}$$

where $V$ is the lake volume and $I$ is the annual inflow to the lake. This is similar to the approach of Hicks, Haddadchi et al. (2019).

The mass of sediment deposited on the floodplain in a given reach is calculated as:

$$F_i = pS_t \frac{L_i accS_i^2}{\sum L_i accS_i^2} \qquad \text{(A18)}$$

where $F_i$is the total floodplain deposition (t yr$^{-1}$) in the $i$th sub-catchment; $p$ is the proportion of the sediment load generated by hillslope erosion per lake or sea-draining catchment that is deposited on floodplains in the catchment, set to 5% based on previous SedNetNZ parameterisation carried out in the Manawatū (Dymond et al. 2016); $S_t$ is the total sediment (t yr$^{-1}$) generated by hillslope erosion per lake or sea-draining catchment; $L_i$ is the reach length (m) on floodplain in the $i$th sub-catchment; and $accS_i$ is the total accumulated (upstream) sediment from hillslope erosion (t yr$^{-1}$) in the $i$th sub-catchment.

# Appendix B – Climate change projections

The effect of future climate change on erosion and suspended sediment loads is modelled following the approach of Basher et al. (2020). Six CMIP5 (Coupled Model Inter-comparison Project) global climate models (GCMs) (BCC-CSM1.1, CESM1-CAM5, GFDL-CM3, GISS-E2-R, HadGEM2-ES, and NorESM1-M) were coupled with the New Zealand Regional Climate Model (Sood 2014) by the Ministry for the Environment (2018) to characterise future temperature and precipitation to 2100 on a 5 km grid.

Four forcing scenarios from the Inter-governmental Panel on Climate Change's fifth assessment report (IPCC AR5; IPCC 2013), known as representative concentration pathways (RCPs), are used to drive the models, and represent different radiative forcing based on greenhouse gas trajectories (Ministry for the Environment 2018). The RCP pathways represent total radiative forcing of 2.6 W $m^{-2}$ (a mitigation pathway), 4.5 W $m^{-2}$ and 6.0 W $m^{-2}$ (stabilisation pathways), and 8.5 W $m^{-2}$ (very high greenhouse gas concentrations), referred to as RCP2.6, RCP4.5, RCP6.0 and RCP8.5, respectively. Variations in the climate change scenarios become more evident after 2035 due to divergence in the radiative forcing pathways (RCPs) (Basher et al. 2020).

The effect of climate change on erosion processes is represented in SedNetNZ using different climatic variables to drive changes in different erosion processes. In the hillslope domain, surficial erosion is modelled for each climate scenario using the estimated change in mean annual rainfall from the RCM models to directly adjust $P$ in Equation A1 (Basher et al. 2020). Mass movement erosion is assumed to change as a function of changing storminess (i.e. a change in storm total rainfall resulting from changes in frequency and magnitude of storm events) across the region. This change in storminess is used to derive a proportional change in the density of shallow landsliding that occurs under each climate scenario, which is used to represent a factor of change, $CF$, in all hillslope mass movement-dominated erosion processes, following Manderson et al. 2015, Basher et al. 2020, and Neverman et al. 2023.

The change in storminess under each climate scenario is calculated by adjusting historical rainfall records (CliFlo; NIWA 2021) by an augmentation factor based on predicted changes in storm rainfall as a result of the change in temperature:

$$R' = R(1 + \Delta T \, AF) \qquad \text{(B1)}$$

where $R'$ is future rainfall, $R$ is historical rainfall, $\Delta T$ is the future absolute change in temperature relative to baseline, and $AF$ is the augmentation factor. $AF$ is derived from the estimated change in rainfall depth per 1°C increase in temperature calculated by the Ministry for the Environment (2018) for a 30 yr ARI 48 h duration rainfall event, which is assumed to represent the dominant landslide triggering event (Basher et al. 2020), giving a value of 0.073. Rain gauges with complete records for the last 50 years across the region were selected from CliFlo (NIWA 2021) and used to represent historical rainfall. At each gauge, Equation B1 was used to calculate $R'$ under temperature changes up to 3°C.

Storm events were then identified in the baseline and future rainfall records as consecutive days where rainfall exceeded 10 mm per day. The storms were considered landslideproducing events if >150 mm of rain fell in a 48 h period during the event. The total rainfall for the storm event was used to estimate the density of shallow landslides produced in each rainfall record for baseline and climate scenarios using the relationship between storm total rainfall and shallow landslide density identified by Reid and Page (2003):

$$LD = mR_s + b \tag{B2}$$

where $LD$ is the density of shallow landslides per km$^2$; $R_S$ is the total rainfall for the storm event; $m$ is the slope of the linear relationship between $LD$ and $R_s$, which was set to 0.72 (Basher et al. 2020); and $b$ is the y-intercept of the relationship, calculated by solving for $b$ under the assumption $LD$ = 0 when $R_s \leq$ 150 mm:

$$0 = 150m + b \tag{B3}$$

$$b = -136.8 \tag{B4}$$

Linear models were developed for the relationship between $LD$ and $\mathit{\Delta T}$ at each rain gauge location, and can be used to estimate the future landslide density given a change in temperature:

$$LD' = a\mathit{\Delta}T + LD \tag{B5}$$

where $LD'$ is the future landslide density; $a$ is the slope of the linear relationship between $\mathit{\Delta}T$ and $LD'$, and therefore the absolute change in landslide density per 1°C of temperature change; and $LD$ is the landslide density for the baseline rainfall record, $R$.

The change factor, $CF$, is then calculated at each rain gauge as the proportional increase in landslide density per 1°C of temperature change, calculated as:

$$CF = \frac{a}{LD} \tag{B6}$$

$CF$ was then interpolated spatially using Sibson's (1981) natural neighbours interpolation. Gauges from across the North Island were included in the interpolation, including five from the Horizons region. This differs from the previous model (Basher et al. 2018, 2020), which used Land Environments of New Zealand (LENZ) level 1 classes to spatialise change factors, using one gauge per LENZ class to derive the change factor and apply it uniformly for the associated class. Two LENZ classes cover most of the Horizons region, each represented by a single rain gauge from the region.

Future rates of mass movement, $MM'$, are then calculated by augmenting the baseline mass movement rate, $MM$, by $CF$ and the change in temperature, $\mathit{\Delta}T$, at the $i^{th}$ pixel of the 5 km temperature change grids for each climate scenario, such that:

$$MM' = MM(1 + CF\mathit{\Delta}T_i) \tag{B7}$$

where $MM$ represents the hillslope mass movement dominated processes, $EL$, $EE$, and $EG$, from Equations A7 to A9.

The effect of climate change on riverbank erosion is represented using indicative change factors to estimate mean annual flood (MAF) for each scenario per REC2 reach used in the bank erosion model (Smith, Herzig et al. 2019). The change factors are based on NIWA's modelling of climate change effects on flow, where proportional changes in MAF were reported for the Manawatū River under RCPs 2.6, 4.5, 6.0, and 8.5 (Collins et al. 2018).

Climate change effects on erosion and suspended sediment loads are reported for the upper (max), lower (min), and median (med) projected changes from the RCM ensemble for mid- and late century.

## Appendix C – Reductions for NPS-FM visual clarity attribute bands

The reductions in suspended sediment loads required to meet NPS-FM (2020) suspended fine sediment objectives were estimated following Neverman et al. (2019), Neverman et al. (2021a, 2021b), and Neverman and Smith (2022) using a national-scale empirical model relating reductions in average annual suspended sediment load to changes in median visual clarity developed by Hicks, Haddadchi et al. (2019), as recommended by the Ministry for the Environment (2022a). The baseline attribute state was based on modelled median visual clarity data for each segment of the REC2 river network supplied by HRC, while the attribute state thresholds were defined using Table C1 (reproduced from the NPS-FM 2020) and the national sediment class map developed for the NPS-FM by Hicks and Shankar (2020). Figure C1 (below) displays the spatial pattern in visual clarity national bottom line (NBL) values across the Horizons region.

The proportional reduction in load required to achieve each attribute band was calculated as a function of the difference between the baseline and minimum numeric attribute state for each band:

$$PR_v = 1 - (V_o/V_b)^{1/a} \qquad \text{(C1)}$$

where $PR_v$ is the minimum proportional reduction in load required to achieve the attribute state, $V_o$ is the minimum visual clarity for each band, $V_b$ is the baseline median visual clarity, and $a$ was assumed to take the national average reported by Hicks, Haddadchi et al. (2019) as –0.76.

Given that the NBL threshold overlaps with the bottom of the range for band C, our analysis examines the reductions required to meet the national bottom line, band B, and band A. Achieving band C requires only a marginal increase in load reduction from that required to achieve the NBL.

To identify which attribute band an REC2 segment would comply with after existing erosion mitigation associated with WFPs is completed, the reduction in mean annual load between the 2021 baseline and future 5 yr interval scenarios was compared to the required load reduction to achieve each attribute band. Where the achieved reduction was higher than the required load reduction, the associated attribute band is considered achievable.

**Table C1. Attribute bands and numeric attribute states for fine suspended sediment**

| Attribute band and description | Numeric attribute state by suspended sediment class (visual clarity (m)) | | | |
|---|---|---|---|---|
| | 1 | 2 | 3 | 4 |
| **A**<br>Minimal impact of suspended sediment on instream biota. Ecological communities are similar to those observed in natural reference conditions. | ≥1.78 | ≥0.93 | ≥2.95 | ≥1.38 |
| **B**<br>Low to moderate impact of suspended sediment on instream biota. Abundance of sensitive fish species may be reduced. | <1.78 and ≥1.55 | <0.93 and ≥0.76 | <2.95 and ≥2.57 | <1.38 and ≥1.17 |
| **C**<br>Moderate to high impact of suspended sediment on instream biota. Sensitive fish species may be lost. | <1.55 and >1.34 | <0.76 and >0.61 | <2.57 and >2.22 | <1.17 and >0.98 |
| National bottom line (NBL) | 1.34 | 0.61 | 2.22 | 0.98 |
| **D**<br>High impact of suspended sediment on instream biota. Ecological communities are significantly altered, and sensitive fish and macroinvertebrate species are lost or at high risk of being lost. | <1.34 | <0.61 | <2.22 | <0.98 |

Source: Reproduced from Table 8 in the NPS-FM 2020.

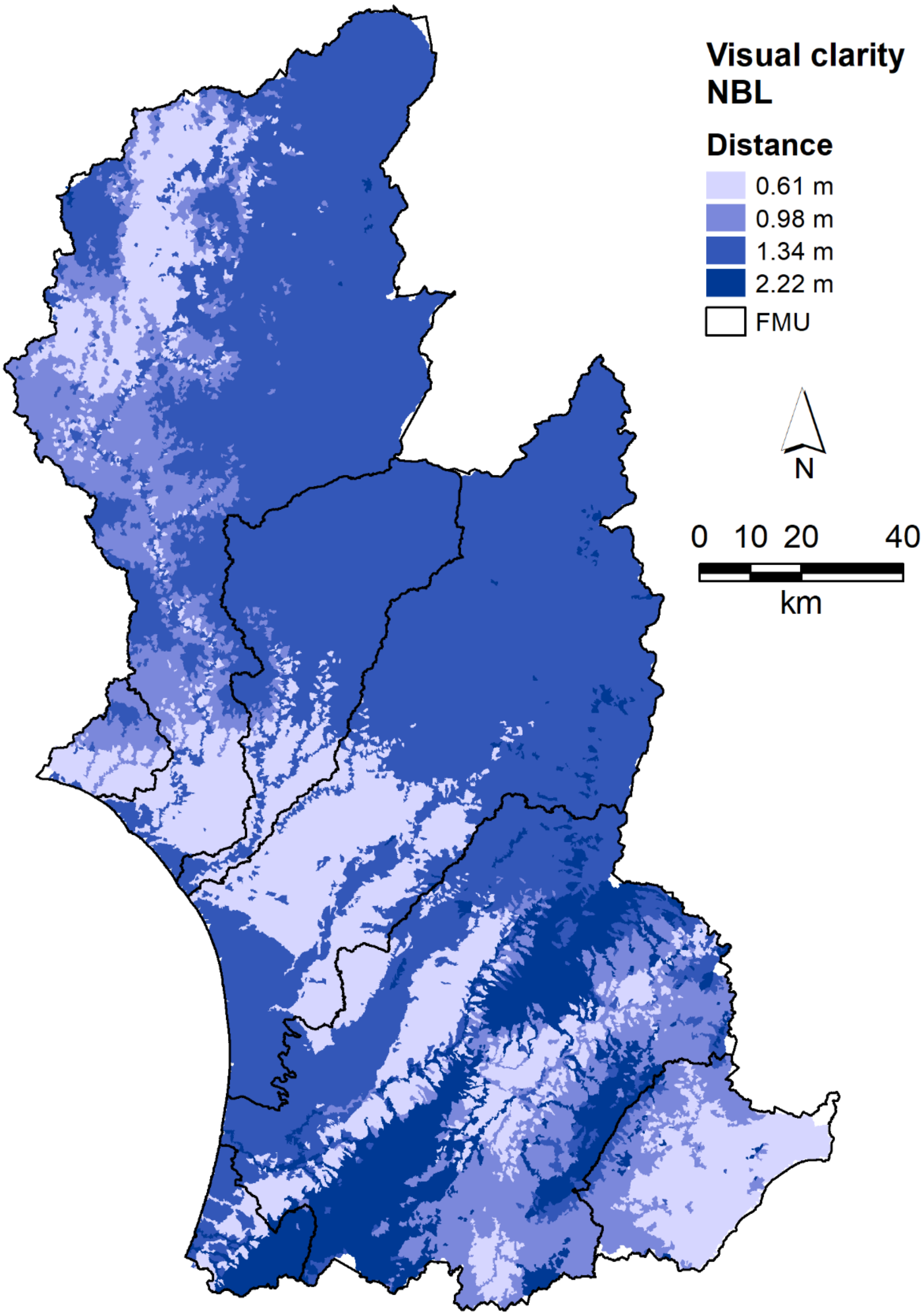

**Figure C1. Required visual clarity for NPS-FM 2020 NBL according to sediment class.**

# Appendix D – Model scenarios used in previous report: Vale et al. 2022

## Model simulations: SLUI scenarios

Region-wide simulations comprise three SLUI/WCS scenarios reflecting the application of WFPs under contemporary climate conditions for 2021 and 5 yr intervals from 2025 to 2100. The scenarios are:

- SC1: current state representing SLUI/WCS erosion mitigation implementation and maturity to date across the region, with an accompanying future scenario representing the maturation of existing works on farms with existing plans, while no further farm plans or works are completed
- SC2: future state representing SLUI/WCS erosion mitigation implementation and maturity to date, plus the future projected mapping rate of new farm plans, and the projected rate of on-farm erosion mitigation implementation and maturation of works across the region
- SC3: future state representing SLUI/WCS erosion mitigation implementation and maturity to date, plus a doubling of the future projected mapping rate of new farm plans, while maintaining the same projected rates of on-farm implementation and maturation of works as SC2.

The impact of projected climate change on suspended sediment loads was modelled for the three scenarios at mid-(2040) and late (2090) century. Six RCMs are used to select the minimum, median, and maximum model projected change across four RCPs for each of the scenarios.

**Table D1 Summary of SedNetNZ SLUI/WCS scenarios from Vale et al. 2022**

| SLUI scenario | Description | Contemporary climate conditions | Projected future climate conditions |
|---|---|---|---|
| SC1: current SLUI/WCS | This scenario represents recent land cover (LCDBv5) and SLUI/WCS works completed to date (2021), including the maturity level of implemented erosion mitigation. The 5 yr intervals represent the maturation of existing works on mapped farms, while no further farm plans or works are completed. | Projections on mean annual suspended sediment loads modelled for 2021, and 5 yr intervals from 2025 to 2100. | Climate change projections on mean annual suspended sediment loads at mid- (2040) and late century (2090). Six RCMs are used to select the minimum, median, and maximum model projected change across 4 RCPs. |
| SC2: future SLUI/WCS | This scenario represents recent land cover (LCDBv5) with both the SLUI/WCS works completed to date, combined with the projected rate of new SLUI/WCS farm plan mapping and the projected rates of implementation and maturation of erosion mitigation. | | |
| SC3: future SLUI/WCS – doubled rate of new farm plans | This scenario represents recent land cover (LCDBv5) with both the SLUI/WCS works completed to date, combined with a doubling of the projected rate of new SLUI/WCS farm plan mapping. The projected rates of implementation and maturation of erosion mitigation remain the same as SC2. | | |

# Appendix E – Model evaluation and limitations

## Model limitations

### *Erosion process representation*

The main limitations in the surficial erosion component of SedNetNZ relate to the calculation of the $C$ and $K$ factors in the NZUSLE, and the availability of suitable input data. The updated model uses a spatially variable K factor instead of the uniform $K$ factor applied in earlier NZUSLE modelling (e.g. Dymond et al. 2014). The further acquisition of higher-resolution soils data for the Horizons region, such as S-map, may improve estimates of surficial erosion.

Shallow landslides are initiated by storm events over a triggering threshold. This means the landslide load in any given year can vary significantly from the mean annual landslide load. This inter-annual variability in landslide occurrence is not represented in SedNetNZ. Instead, the storm-triggered shallow landslide contribution to the sediment load is averaged over a multi-decadal timescale. Calibration data from Manawatū (Dymond et al. 2016) were used to define the slope thresholds for landslide occurrence and density.

Both earthflow and gully erosion are represented in SedNetNZ using a spatial averaging approach based on estimated presence and spatial extent of these erosion features in the Erosion Terrains layer (Dymond et al. 2016). It is therefore possible that earthflow and gully erosion may be represented in sub-catchments that do not contain these features or may not be represented where they are present. Aerial imagery was used to evaluate selected catchments, and Erosion Terrain layers were adjusted if there was no evidence of active gully erosion.

Bank erosion prediction requires high-resolution spatial data on riparian woody vegetation. For this reason, riparian woody vegetation has been derived from 'EcoSat Woody' at 15 m resolution (Dymond & Shepherd 2004), as LCDB is less suitable for representing narrow strips of riparian vegetation due to its minimum mapping unit of 1 ha. Predictions of bank migration rates are therefore based on woody vegetation presence/absence in 2002. A further challenge relates to the spatial correspondence between mapped channel locations and woody vegetation, and changes in channel planform since mapping occurred. Availability of region-wide LiDAR data would enable improved spatial representation of riparian woody vegetation and spatial coherence with channel locations.

### *Climate change projections*

There is a high degree of uncertainty in relation to the climate change projections and their impacts, arising from a) differences between climate models, b) divergent trajectories of future climate change depending on levels of greenhouse gas emissions, and c) how these changes affect erosion processes.

The choice of climate model affects estimates due to the range of models (RCMs), while the divergence in potential climate futures is captured by the four RCPs and produces a large range in potential impacts. This range means there can be considerable difference between the lowest and highest projections, especially at late century, and spatial variation in relative change across the region.

Further uncertainty is introduced concerning the applicability of some assumptions for the whole region. For example, the adjustment for predicting the change in storm rainfall per 1°C temperature increase (+7.3%) assumes that landslides are triggered by an ARI30 48 hr event. A uniform triggering threshold of 150 mm in 48 hr has been used to estimate landslide density, but this threshold may vary for different terrains and different mass movement processes (e.g. Reid & Page 2003; Basher et al. 2020). Projections for bank erosion rely on indicative changes to the modelled MAF from the Manawatū River based on available information (Collins et al. 2018) but this does not capture regional variablity in potential climate impacts on MAF. Nonetheless, this is an improvement on previous modelling of climate change effects using SedNetNZ, which did not include representation of the impact on bank erosion (Basher et al. 2020).

There is also a lack of information on the relationship between climate change and its impact on erosion processes in New Zealand. Basher et al. (2020) identified this knowledge gap, stating there had only been a few studies in New Zealand on the climate change impacts on erosion, and most of these consisted of general statements about likely trends rather than quantifying change. For instance, Crozier (2010) reviewed the basis for assessing the impact of climate change on landslides and found that although there is a strong theoretical basis for increased landslide activity as a result of predicted climate change, there is a high level of uncertainty resulting from the error margins inherent in downscaling GCMs spatially and temporally. Due to this high uncertainty, the results of the climate change projections should be interpreted as indicative of trends rather than absolute values (Basher et al. 2020).

In the present report, we applied a refined method for estimating the effect of projected climate change on erosion compared to previous work (Basher et al. 2018, 2020). The refinements included a) increasing the number of long-term rainfall records used to compute mass movement change factors (section 4.2.4) from two to five in the Horizons region, as well as including gauges bordering the Horizons region; and b) spatially interpolating change factor values across a continuous grid. The interpolation procedure replaces use of LENZ (Leathwick et al. 2003), which previously formed the basis for uniformly applying change factors to LENZ classes within the region.

These changes in how we estimate the effects of climate change on erosion altered the magnitude of projected climate change impacts on suspended sediment loads compared to previous work. For instance, Basher et al. (2020) estimated a region-wide increase in sediment loads of 8.3–24% and 53–224% by 2043 and 2090, respectively, using the previous method. In contrast, we estimate an increase in regional load of 8–60% and 2–119% across all RCPs for SC1 by 2040 and 2090, respectively. This comparison shows a sizeable reduction in the potential increase in sediment loads by end century using the refined method for determining climate change impacts.

However, other factors contribute to these differences, which somewhat limits direct comparison. These include a) use of different baselines for computing relative changes in load (i.e. 2004 in Basher et al. 2020 versus 2021 in the present report), and b) representation of hillslope erosion processes only by Basher et al. (2020) versus hillslope and bank erosion processes in the present study.

### *Reductions required to meet visual clarity attribute bands*

Mean annual suspended sediment load reductions to achieve visual clarity and suspended fine sediment objectives were estimated using equations developed by Hicks, Haddadchi et al. (2019) from simplifications in the relationships reported by Dymond et al. (2017). A key assumption for calculating required load reductions to meet objectives is that for each site, the relationship between suspended sediment load and the flow frequency distribution remain constant. In reality, this relationship may change due to changes in catchment hydrology leading to changes in the relationship between a given flow and suspended sediment load (Hicks, Haddadchi et al. 2019). As data are not presently available to predict these changes, we assume that the associated relationships remain constant. This assumption is particularly important when modelling changes in visual clarity under different scenarios, especially the climate change scenarios. Because these scenarios may significantly change the rainfall regime and land cover, both of which would result in changes in hydrology, the relationship between visual clarity and sediment load may differ at a given REC2 segment compared with the 2021 baseline.

We have estimated the required load reductions using empirical models fitted to a national dataset. This should result in the models being fitted to a wide range of catchment variables and therefore representing the variability across Horizons. Sites from Horizons were used in the national dataset (see Hicks, Haddadchi et al. 2019) but may lead to under- or over estimation of the required reductions at any one location. Also, visual clarity thresholds are based on one of four sediment classes assigned to the REC2 segment, which can lead to abrupt changes in target thresholds for adjacent REC2 segments.

### *SLUI sediment load reduction*

There is significant uncertainty regarding the effectiveness, maturity, and implementation rates of SLUI WFPs, as well as the selection of new farms. The effectiveness of each erosion mitigation used values from previous SedNetNZ modelling, which are based on the literature. Better data on the effectiveness of erosion mitigation at the whole-farm and whole-catchment scale are needed to improve the prediction of sediment load reduction, especially if values can be derived from or calibrated with local data. The maturity rate of each erosion mitigation could also benefit from better data that are locally calibrated to reflect tree species, growing conditions, and success rates of new plantings in the region.

The implementation rate of new works on a farm is one of the more difficult parameters to define. Here we applied it as an average annual proportional rate relative to what would be considered fully implemented as opposed to a set area of works completed per year. The estimated implementation rate was provided by HRC. Since there is no clear definition or measure of what ‘fully implemented’ represents for a given farm, it is difficult to estimate the implementation rate. A standardised measure of the mitigatable area of each farm would help to improve the implementation rate.

Using a farm-based implementation rate also means that the total area of works implemented each year is modelled to increase as new farms are selected and added to the total number of farms having works applied. In practice, the total area of works funded and implemented annually across the region may remain relatively constant. For reasons noted above, estimating the area of works represented by the implementation rate for each farm is challenging. However, if we consider the maximum mitigatable area of a farm to be represented by the area of erodible, high, and top HEL pasture, and the minimum mitigable area to be represented by the area of high and top HEL pasture, then we can approximate a maximum and minimum average annual estimate of the total area of works for the modelling period (2021 to 2100). These maximum and minimum areas were determined for each mapped farm based on the SLUI farm data provided. These areas were then used to derive an average proportion of the pasture area for each SLUI priority class, which could then be applied to unmapped farms at the rate of future selection and associated implementation rate. This results in a minimum and maximum annual average of c. 1780 ha $yr^{-1}$ and c. 4,990 ha $yr^{–1}$, respectively, or a mean c. 3,380 ha $yr^{–1}$ over the simulated period from 2021 to 2100 for SC2 (Table 28).

An approximation of the average annual rate of works according to work type can also be estimated by using the proportion of works applied within the model simulation (Table E1). These proportions were based on the mapped area of past works for each priority class (Table 3), which recognises that works vary based on WFP priority and the terrain they generally represent. The proportions were also weighted by erosion process loads to ensure works were not applied to areas where there were no modelled loads for the erosion process targeted by each works. The resulting approximations should not be overinterpreted since the works proportions they are based on were used to weight the effectiveness (which varies from 70 to 90 %) applied to each farm, and not to determine the actual area of each type of work. A summary of the estimated region-wide proportion of works for the end of the simulated period, and by FMU, is provided in Table E2.

**Table E1. Estimated minimum, maximum, and mean annual average rate of works completed over the simulated period from 2021 to 2100**

| Erosion mitigation works | Estimated area of works per year (ha $yr^{-1}$) | | | | | |
|---|---|---|---|---|---|---|
| | SC2 | | | SC3 | | |
| | min | mean | max | min | mean | max |
| Afforestation | 890 | 1,630 | 2,370 | 1,010 | 1,920 | 2,820 |
| Bush retirement | 450 | 760 | 1,080 | 710 | 1,300 | 1,880 |
| Riparian retirement | 110 | 290 | 470 | 220 | 660 | 1,110 |
| Spaced planting | 320 | 680 | 1,040 | 410 | 940 | 1,470 |
| Gully planting | 10 | 20 | 30 | 10 | 20 | 40 |
| **Total** | **1,780** | **3,380** | **4,990** | **2,360** | **4,840** | **7,320** |

New farms were randomly selected for implementation based on the proportions of each SLUI priority class. We do not know how representative this selection will be of the actual order of new farms selected in the future. We also do not know how sensitive the mean annual local and region-wide loads are to the selection order of new farms. Evaluating the sensitivity of this component would require running multiple iterations of SedNetNZ using different farm selection orders.

**Table E2 Estimated proportion of works for each erosion mitigation type at the end of the simulated period (2100), both region-wide and per FMU**

| Scenario | Erosion mitigation | Proportion of works (%) | | | | | | | |
|---|---|---|---|---|---|---|---|---|---|
| | | Region -wide | FMU | | | | | | |
| | | | Kai Iwi | Manawatū | Puketoi ki Tai | Rangitīkei-Turakina | Waiopehu | Whangaehu | Whanganui |
| SC1 | Afforestation | 44 | 48 | 43 | 69 | 35 | 100 | 24 | 47 |
| | Retirement | 30 | 25 | 16 | 14 | 29 | 0 | 34 | 41 |
| | Riparian retirement | 10 | 6 | 14 | 7 | 18 | 0 | 12 | 5 |
| | Spaced planting | 14 | 15 | 26 | 10 | 17 | 0 | 22 | 6 |
| | Gully planting | 2 | 6 | 1 | 0 | 1 | 0 | 8 | 1 |
| SC2 | Afforestation | 48 | 51 | 42 | 48 | 49 | 32 | 44 | 54 |
| | Retirement | 23 | 17 | 19 | 26 | 23 | 5 | 29 | 22 |
| | Riparian retirement | 9 | 3 | 15 | 4 | 9 | 29 | 9 | 5 |
| | Spaced planting | 20 | 27 | 24 | 22 | 18 | 33 | 18 | 18 |
| | Gully planting | 1 | 1 | 1 | 0 | 1 | 0 | 0 | 0 |
| SC3 | Afforestation | 40 | 42 | 31 | 42 | 42 | 31 | 38 | 47 |
| | Retirement | 26 | 26 | 20 | 34 | 26 | 15 | 28 | 29 |
| | Riparian retirement | 14 | 5 | 25 | 3 | 14 | 22 | 15 | 6 |
| | Spaced planting | 20 | 27 | 23 | 20 | 18 | 32 | 18 | 17 |
| | Gully planting | 1 | 1 | 1 | 0 | 1 | 0 | 0 | 0 |

Note: SC1 represents the past proportions from mapped works (based on HRC data) since no further works are applied in this scenario.

# Appendix F – Length and proportion of River Environment Classification v2 (REC2) segments achieving visual clarity attribute bands and NBL (or maintaining baseline visual clarity), summarised by Freshwater Management Unit (FMU) without the effects of climate change

**Table F1 Length and proportion of REC2 segments achieving visual clarity attribute bands and NBL (or maintaining baseline visual clarity), summarised by FMU and stream order for PS1**

| PS1 | | | | Length of REC2 segments achieving visual clarity attribute bands and NBL | | | | | | | | | |
|---|---|---|---|---|---|---|---|---|---|---|---|---|---|
| **Attribute band** | **FMU** | **Stream order** | **Total length (km)** | **2021** | | **2040** | | **2060** | | **2080** | | **2100** | |
| | | | | **km** | **%** | **km** | **%** | **km** | **%** | **km** | **%** | **km** | **%** |
| A band | Kai Iwi | 1 | 262 | 102 | 39% | 128 | 49% | 145 | 55% | 166 | 63% | 193 | 73% |
| | | 2 | 146 | 58 | 39% | 72 | 49% | 86 | 59% | 108 | 74% | 121 | 83% |
| | | 3 | 68 | 23 | 34% | 26 | 38% | 28 | 41% | 47 | 70% | 56 | 83% |
| | | 4 | 59 | 29 | 49% | 40 | 68% | 45 | 77% | 50 | 85% | 53 | 91% |
| | | 5 | 22 | - | 0% | 3 | 12% | 5 | 24% | 5 | 24% | 11 | 50% |
| | | **Total** | **558** | **212** | **38%** | **269** | **48%** | **309** | **55%** | **376** | **67%** | **435** | **78%** |
| | Manawatū | 1 | 4,825 | 1,203 | 25% | 1,532 | 32% | 1,916 | 40% | 2,380 | 49% | 2,749 | 57% |
| | | 2 | 2,484 | 561 | 23% | 737 | 30% | 911 | 37% | 1,159 | 47% | 1,389 | 56% |
| | | 3 | 1,261 | 257 | 20% | 332 | 26% | 415 | 33% | 566 | 45% | 699 | 55% |
| | | 4 | 651 | 75 | 12% | 118 | 18% | 214 | 33% | 282 | 43% | 351 | 54% |
| | | 5 | 439 | 73 | 17% | 87 | 20% | 117 | 27% | 164 | 37% | 234 | 53% |
| | | 6 | 162 | 5 | 3% | 15 | 9% | 25 | 16% | 101 | 62% | 129 | 80% |
| | | 7 | 119 | - | 0% | - | 0% | 5 | 5% | 42 | 35% | 42 | 35% |
| | | **Total** | **9,941** | **2,173** | **22%** | **2,821** | **28%** | **3,602** | **36%** | **4,695** | **47%** | **5,594** | **56%** |
| | Puketoi ki Tai | 1 | 875 | 202 | 23% | 334 | 38% | 495 | 57% | 639 | 73% | 706 | 81% |
| | | 2 | 435 | 84 | 19% | 138 | 32% | 214 | 49% | 300 | 69% | 354 | 81% |
| | | 3 | 259 | 39 | 15% | 71 | 28% | 110 | 42% | 166 | 64% | 212 | 82% |
| | | 4 | 139 | 13 | 9% | 15 | 11% | 31 | 22% | 61 | 44% | 114 | 82% |

| PS1 | | | | Length of REC2 segments achieving visual clarity attribute bands and NBL | | | | | | | | | |
|---|---|---|---|---|---|---|---|---|---|---|---|---|---|
| **Attribute band** | **FMU** | **Stream order** | **Total length (km)** | **2021** | | **2040** | | **2060** | | **2080** | | **2100** | |
| | | | | **km** | **%** | **km** | **%** | **km** | **%** | **km** | **%** | **km** | **%** |
| A band (cont.) | Puketoi ki Tai (cont.) | 5 | 71 | - | 0% | - | 0% | 1 | 1% | 29 | 41% | 44 | 62% |
| | | 6 | 46 | - | 0% | - | 0% | - | 0% | - | 0% | 22 | 48% |
| | | **Total** | **1,825** | **339** | **19%** | **558** | **31%** | **850** | **47%** | **1,196** | **66%** | **1,452** | **80%** |
| | Rangitīkei-Turakina | 1 | 4,349 | 1,241 | 29% | 1,707 | 39% | 2,241 | 52% | 2,660 | 61% | 2,928 | 67% |
| | | 2 | 2,111 | 592 | 28% | 803 | 38% | 1,046 | 50% | 1,257 | 60% | 1,425 | 68% |
| | | 3 | 1,035 | 289 | 28% | 368 | 36% | 509 | 49% | 663 | 64% | 730 | 71% |
| | | 4 | 480 | 207 | 43% | 243 | 51% | 321 | 67% | 388 | 81% | 410 | 85% |
| | | 5 | 293 | 127 | 43% | 133 | 45% | 135 | 46% | 209 | 71% | 243 | 83% |
| | | 6 | 156 | 19 | 12% | 36 | 23% | 57 | 36% | 91 | 59% | 104 | 66% |
| | | 7 | 139 | - | 0% | - | 0% | - | 0% | 75 | 54% | 122 | 88% |
| | | **Total** | **8,563** | **2,476** | **29%** | **3,289** | **38%** | **4,309** | **50%** | **5,344** | **62%** | **5,962** | **70%** |
| | Waiopehu | 1 | 322 | 69 | 21% | 93 | 29% | 93 | 29% | 93 | 29% | 97 | 30% |
| | | 2 | 161 | 25 | 15% | 33 | 21% | 33 | 21% | 34 | 21% | 39 | 24% |
| | | 3 | 92 | 27 | 29% | 30 | 33% | 30 | 33% | 30 | 33% | 30 | 33% |
| | | 4 | 38 | 19 | 50% | 21 | 55% | 21 | 55% | 21 | 56% | 22 | 57% |
| | | 5 | 34 | 19 | 57% | 23 | 67% | 23 | 68% | 23 | 68% | 23 | 68% |
| | | **Total** | **647** | **159** | **25%** | **199** | **31%** | **200** | **31%** | **201** | **31%** | **210** | **33%** |
| | Whangaehu | 1 | 1,682 | 588 | 35% | 861 | 51% | 1,049 | 62% | 1,191 | 71% | 1,269 | 75% |
| | | 2 | 892 | 326 | 37% | 470 | 53% | 564 | 63% | 640 | 72% | 682 | 76% |
| | | 3 | 409 | 171 | 42% | 225 | 55% | 271 | 66% | 302 | 74% | 324 | 79% |
| | | 4 | 223 | 50 | 22% | 108 | 48% | 128 | 58% | 151 | 68% | 168 | 75% |
| | | 5 | 126 | 42 | 33% | 56 | 44% | 62 | 49% | 107 | 85% | 107 | 85% |
| | | 6 | 145 | - | 0% | - | 0% | - | 0% | 29 | 20% | 136 | 94% |
| | | **Total** | **3,478** | **1,177** | **34%** | **1,720** | **49%** | **2,075** | **60%** | **2,421** | **70%** | **2,686** | **77%** |

| PS1 | | | | Length of REC2 segments achieving visual clarity attribute bands and NBL | | | | | | | | | |
|---|---|---|---|---|---|---|---|---|---|---|---|---|---|
| Attribute band | FMU | Stream order | Total length (km) | 2021 | | 2040 | | 2060 | | 2080 | | 2100 | |
| | | | | km | % | km | % | km | % | km | % | km | % |
| A band (cont.) | Whanganui | 1 | 5,833 | 3,816 | 65% | 4,078 | 70% | 4,375 | 75% | 4,697 | 81% | 4,948 | 85% |
| | | 2 | 2,871 | 1,918 | 67% | 2,046 | 71% | 2,182 | 76% | 2,362 | 82% | 2,516 | 88% |
| | | 3 | 1,397 | 972 | 70% | 1,032 | 74% | 1,093 | 78% | 1,162 | 83% | 1,239 | 89% |
| | | 4 | 790 | 512 | 65% | 557 | 70% | 589 | 75% | 645 | 82% | 728 | 92% |
| | | 5 | 404 | 332 | 82% | 342 | 85% | 350 | 87% | 365 | 90% | 389 | 96% |
| | | 6 | 166 | 28 | 17% | 37 | 22% | 76 | 46% | 96 | 58% | 127 | 77% |
| | | 7 | 247 | - | 0% | - | 0% | - | 0% | - | 0% | 25 | 10% |
| | | **Total** | **11,709** | **7,579** | **65%** | **8,091** | **69%** | **8,664** | **74%** | **9,328** | **80%** | **9,973** | **85%** |
| B band | Kai Iwi | 1 | 262 | 195 | 74% | 207 | 79% | 216 | 82% | 222 | 85% | 233 | 89% |
| | | 2 | 146 | 116 | 79% | 126 | 86% | 129 | 88% | 132 | 90% | 138 | 94% |
| | | 3 | 68 | 50 | 74% | 58 | 85% | 59 | 86% | 62 | 91% | 63 | 92% |
| | | 4 | 59 | 51 | 87% | 51 | 87% | 52 | 89% | 57 | 96% | 59 | 99% |
| | | 5 | 22 | 5 | 24% | 5 | 24% | 11 | 50% | 19 | 85% | 22 | 100% |
| | | **Total** | **558** | **418** | **75%** | **448** | **80%** | **467** | **84%** | **492** | **88%** | **514** | **92%** |
| | Manawatū | 1 | 4,825 | 2,185 | 45% | 2,547 | 53% | 2,902 | 60% | 3,163 | 66% | 3,390 | 70% |
| | | 2 | 2,484 | 1,076 | 43% | 1,266 | 51% | 1,438 | 58% | 1,598 | 64% | 1,734 | 70% |
| | | 3 | 1,261 | 529 | 42% | 615 | 49% | 688 | 55% | 805 | 64% | 896 | 71% |
| | | 4 | 651 | 210 | 32% | 234 | 36% | 314 | 48% | 361 | 55% | 448 | 69% |
| | | 5 | 439 | 159 | 36% | 194 | 44% | 213 | 48% | 268 | 61% | 325 | 74% |
| | | 6 | 162 | 15 | 9% | 62 | 38% | 101 | 62% | 107 | 66% | 161 | 99% |
| | | 7 | 119 | 4 | 4% | 38 | 32% | 42 | 35% | 42 | 35% | 42 | 35% |
| | | **Total** | **9,941** | **4,179** | **42%** | **4,956** | **50%** | **5,697** | **57%** | **6,344** | **64%** | **6,997** | **70%** |
| | Puketoi ki Tai | 1 | 875 | 401 | 46% | 569 | 65% | 677 | 77% | 739 | 84% | 772 | 88% |
| | | 2 | 435 | 156 | 36% | 247 | 57% | 315 | 72% | 363 | 83% | 387 | 89% |

| **PS1** | | | | **Length of REC2 segments achieving visual clarity attribute bands and NBL** | | | | | | | | | |
|---|---|---|---|---|---|---|---|---|---|---|---|---|---|
| **Attribute band** | **FMU** | **Stream order** | **Total length (km)** | **2021** | | **2040** | | **2060** | | **2080** | | **2100** | |
| | | | | **km** | **%** | **km** | **%** | **km** | **%** | **km** | **%** | **km** | **%** |
| B band (cont.) | Puketoi ki Tai (cont.) | 3 | 259 | 89 | 34% | 114 | 44% | 165 | 64% | 208 | 80% | 233 | 90% |
| | | 4 | 139 | 25 | 18% | 46 | 33% | 72 | 52% | 111 | 79% | 130 | 94% |
| | | 5 | 71 | - | 0% | 14 | 19% | 29 | 41% | 42 | 59% | 56 | 79% |
| | | 6 | 46 | - | 0% | - | 0% | - | 0% | 22 | 48% | 22 | 48% |
| | | **Total** | **1,825** | **671** | **37%** | **990** | **54%** | **1,259** | **69%** | **1,484** | **81%** | **1,601** | **88%** |
| | Rangitīkei-Turakina | 1 | 4,349 | 2,455 | 56% | 2,894 | 67% | 3,182 | 73% | 3,415 | 79% | 3,593 | 83% |
| | | 2 | 2,111 | 1,151 | 55% | 1,324 | 63% | 1,482 | 70% | 1,612 | 76% | 1,709 | 81% |
| | | 3 | 1,035 | 571 | 55% | 657 | 63% | 742 | 72% | 808 | 78% | 855 | 83% |
| | | 4 | 480 | 319 | 66% | 353 | 73% | 386 | 80% | 424 | 88% | 441 | 92% |
| | | 5 | 293 | 179 | 61% | 206 | 70% | 246 | 84% | 263 | 90% | 285 | 97% |
| | | 6 | 156 | 36 | 23% | 57 | 36% | 91 | 59% | 104 | 66% | 114 | 73% |
| | | 7 | 139 | - | 0% | 1 | 1% | 74 | 54% | 110 | 79% | 139 | 100% |
| | | **Total** | **8,563** | **4,710** | **55%** | **5,491** | **64%** | **6,203** | **72%** | **6,737** | **79%** | **7,136** | **83%** |
| | Waiopehu | 1 | 322 | 151 | 47% | 173 | 54% | 173 | 54% | 175 | 54% | 177 | 55% |
| | | 2 | 161 | 69 | 43% | 80 | 50% | 80 | 50% | 83 | 51% | 89 | 55% |
| | | 3 | 92 | 48 | 53% | 58 | 63% | 58 | 63% | 58 | 63% | 58 | 63% |
| | | 4 | 38 | 23 | 61% | 24 | 62% | 24 | 62% | 24 | 63% | 24 | 63% |
| | | 5 | 34 | 23 | 68% | 23 | 68% | 23 | 68% | 25 | 74% | 25 | 74% |
| | | **Total** | **647** | **315** | **49%** | **357** | **55%** | **358** | **55%** | **364** | **56%** | **373** | **58%** |
| | Whangaehu | 1 | 1,682 | 1,258 | 75% | 1,351 | 80% | 1,439 | 86% | 1,491 | 89% | 1,520 | 90% |
| | | 2 | 892 | 685 | 77% | 720 | 81% | 765 | 86% | 790 | 89% | 799 | 90% |
| | | 3 | 409 | 320 | 78% | 334 | 81% | 361 | 88% | 365 | 89% | 367 | 90% |
| | | 4 | 223 | 155 | 70% | 166 | 74% | 183 | 82% | 201 | 90% | 204 | 91% |
| | | 5 | 126 | 58 | 46% | 62 | 49% | 107 | 85% | 107 | 85% | 107 | 85% |

| **PS1** | | | | **Length of REC2 segments achieving visual clarity attribute bands and NBL** | | | | | | | | | |
|---|---|---|---|---|---|---|---|---|---|---|---|---|---|
| **Attribute band** | **FMU** | **Stream order** | **Total length (km)** | **2021** | | **2040** | | **2060** | | **2080** | | **2100** | |
| | | | | **km** | **%** | **km** | **%** | **km** | **%** | **km** | **%** | **km** | **%** |
| B band (cont.) | Whangaehu (cont.) | 6 | 145 | - | 0% | - | 0% | 13 | 9% | 138 | 95% | 139 | 96% |
| | | **Total** | **3,478** | **2,476** | **71%** | **2,632** | **76%** | **2,868** | **82%** | **3,092** | **89%** | **3,136** | **90%** |
| | Whanganui | 1 | 5,833 | 4,742 | 81% | 4,913 | 84% | 5,138 | 88% | 5,349 | 92% | 5,494 | 94% |
| | | 2 | 2,871 | 2,366 | 82% | 2,462 | 86% | 2,588 | 90% | 2,683 | 93% | 2,756 | 96% |
| | | 3 | 1,397 | 1,154 | 83% | 1,210 | 87% | 1,261 | 90% | 1,325 | 95% | 1,355 | 97% |
| | | 4 | 790 | 615 | 78% | 658 | 83% | 687 | 87% | 740 | 94% | 773 | 98% |
| | | 5 | 404 | 369 | 91% | 386 | 95% | 392 | 97% | 404 | 100% | 404 | 100% |
| | | 6 | 166 | 79 | 47% | 104 | 63% | 128 | 77% | 137 | 83% | 161 | 97% |
| | | 7 | 247 | - | 0% | - | 0% | 3 | 1% | 26 | 10% | 61 | 25% |
| | | **Total** | **11,709** | **9,325** | **80%** | **9,732** | **83%** | **10,196** | **87%** | **10,665** | **91%** | **11,003** | **94%** |
| NBL | Kai Iwi | 1 | 262 | 240 | 92% | 242 | 92% | 243 | 93% | 249 | 95% | 249 | 95% |
| | | 2 | 146 | 143 | 98% | 143 | 98% | 143 | 98% | 144 | 99% | 144 | 99% |
| | | 3 | 68 | 67 | 98% | 67 | 99% | 67 | 99% | 68 | 100% | 68 | 100% |
| | | 4 | 59 | 56 | 95% | 59 | 99% | 59 | 100% | 59 | 100% | 59 | 100% |
| | | 5 | 22 | 15 | 67% | 19 | 85% | 22 | 100% | 22 | 100% | 22 | 100% |
| | | **Total** | **558** | **521** | **93%** | **530** | **95%** | **535** | **96%** | **542** | **97%** | **542** | **97%** |
| | Manawatū | 1 | 4,825 | 2,969 | 62% | 3,424 | 71% | 3,562 | 74% | 3,713 | 77% | 3,855 | 80% |
| | | 2 | 2,484 | 1,491 | 60% | 1,700 | 68% | 1,787 | 72% | 1,877 | 76% | 1,973 | 79% |
| | | 3 | 1,261 | 708 | 56% | 820 | 65% | 886 | 70% | 944 | 75% | 1,003 | 80% |
| | | 4 | 651 | 329 | 51% | 377 | 58% | 409 | 63% | 476 | 73% | 531 | 82% |
| | | 5 | 439 | 208 | 47% | 246 | 56% | 268 | 61% | 313 | 71% | 375 | 85% |
| | | 6 | 162 | 83 | 51% | 115 | 71% | 121 | 74% | 162 | 100% | 162 | 100% |
| | | 7 | 119 | 42 | 35% | 42 | 35% | 42 | 35% | 42 | 35% | 42 | 35% |
| | | **Total** | **9,941** | **5,829** | **59%** | **6,724** | **68%** | **7,074** | **71%** | **7,528** | **76%** | **7,941** | **80%** |

| PS1 | | | | Length of REC2 segments achieving visual clarity attribute bands and NBL | | | | | | | | | |
|---|---|---|---|---|---|---|---|---|---|---|---|---|---|
| Attribute band | FMU | Stream order | Total length (km) | 2021 | | 2040 | | 2060 | | 2080 | | 2100 | |
| | | | | km | % | km | % | km | % | km | % | km | % |
| NBL (cont.) | Puketoi ki Tai | 1 | 875 | 679 | 78% | 740 | 85% | 784 | 90% | 808 | 92% | 823 | 94% |
| | | 2 | 435 | 298 | 69% | 346 | 80% | 377 | 87% | 395 | 91% | 405 | 93% |
| | | 3 | 259 | 165 | 63% | 188 | 73% | 214 | 83% | 243 | 94% | 251 | 97% |
| | | 4 | 139 | 59 | 43% | 101 | 72% | 109 | 78% | 128 | 92% | 139 | 100% |
| | | 5 | 71 | 29 | 41% | 29 | 41% | 43 | 61% | 59 | 83% | 71 | 100% |
| | | 6 | 46 | - | 0% | 22 | 48% | 22 | 48% | 22 | 48% | 46 | 100% |
| | | **Total** | **1,825** | **1,231** | **67%** | **1,426** | **78%** | **1,550** | **85%** | **1,655** | **91%** | **1,736** | **95%** |
| | Rangitīkei-Turakina | 1 | 4,349 | 3,201 | 74% | 3,431 | 79% | 3,572 | 82% | 3,708 | 85% | 3,818 | 88% |
| | | 2 | 2,111 | 1,456 | 69% | 1,612 | 76% | 1,700 | 81% | 1,781 | 84% | 1,835 | 87% |
| | | 3 | 1,035 | 748 | 72% | 813 | 79% | 852 | 82% | 868 | 84% | 902 | 87% |
| | | 4 | 480 | 393 | 82% | 412 | 86% | 447 | 93% | 450 | 94% | 457 | 95% |
| | | 5 | 293 | 236 | 80% | 246 | 84% | 263 | 90% | 288 | 98% | 289 | 99% |
| | | 6 | 156 | 91 | 59% | 104 | 66% | 104 | 66% | 104 | 66% | 114 | 73% |
| | | 7 | 139 | 16 | 11% | 75 | 54% | 110 | 79% | 139 | 100% | 139 | 100% |
| | | **Total** | **8,563** | **6,140** | **72%** | **6,693** | **78%** | **7,048** | **82%** | **7,337** | **86%** | **7,553** | **88%** |
| | Waiopehu | 1 | 322 | 164 | 51% | 200 | 62% | 201 | 62% | 203 | 63% | 203 | 63% |
| | | 2 | 161 | 77 | 48% | 94 | 59% | 94 | 59% | 98 | 61% | 101 | 62% |
| | | 3 | 92 | 59 | 64% | 64 | 69% | 64 | 69% | 64 | 70% | 64 | 70% |
| | | 4 | 38 | 24 | 62% | 31 | 82% | 31 | 82% | 31 | 82% | 32 | 84% |
| | | 5 | 34 | 23 | 68% | 25 | 74% | 25 | 74% | 25 | 74% | 25 | 74% |
| | | **Total** | **647** | **347** | **54%** | **414** | **64%** | **415** | **64%** | **421** | **65%** | **425** | **66%** |
| | Whangaehu | 1 | 1,682 | 1,494 | 89% | 1,539 | 92% | 1,572 | 93% | 1,593 | 95% | 1,603 | 95% |
| | | 2 | 892 | 797 | 89% | 825 | 92% | 837 | 94% | 842 | 94% | 842 | 94% |
| | | 3 | 409 | 372 | 91% | 390 | 95% | 393 | 96% | 395 | 96% | 395 | 96% |

| PS1 | | | | Length of REC2 segments achieving visual clarity attribute bands and NBL | | | | | | | | | |
|---|---|---|---|---|---|---|---|---|---|---|---|---|---|
| Attribute band | FMU | Stream order | Total length (km) | 2021 | | 2040 | | 2060 | | 2080 | | 2100 | |
| | | | | km | % | km | % | km | % | km | % | km | % |
| NBL (cont.) | Whangaehu (cont.) | 4 | 223 | 175 | 79% | 189 | 85% | 201 | 90% | 205 | 92% | 205 | 92% |
| | | 5 | 126 | 77 | 61% | 107 | 85% | 108 | 85% | 108 | 85% | 111 | 88% |
| | | 6 | 145 | - | 0% | 20 | 14% | 95 | 65% | 140 | 96% | 145 | 100% |
| | | **Total** | **3,478** | **2,915** | **84%** | **3,071** | **88%** | **3,207** | **92%** | **3,284** | **94%** | **3,301** | **95%** |
| | Whanganui | 1 | 5,833 | 5,368 | 92% | 5,485 | 94% | 5,570 | 95% | 5,640 | 97% | 5,689 | 98% |
| | | 2 | 2,871 | 2,647 | 92% | 2,714 | 95% | 2,763 | 96% | 2,806 | 98% | 2,824 | 98% |
| | | 3 | 1,397 | 1,294 | 93% | 1,328 | 95% | 1,359 | 97% | 1,371 | 98% | 1,380 | 99% |
| | | 4 | 790 | 715 | 90% | 749 | 95% | 765 | 97% | 788 | 100% | 788 | 100% |
| | | 5 | 404 | 391 | 97% | 404 | 100% | 404 | 100% | 404 | 100% | 404 | 100% |
| | | 6 | 166 | 134 | 80% | 137 | 83% | 143 | 86% | 166 | 100% | 166 | 100% |
| | | 7 | 247 | 9 | 4% | 24 | 10% | 37 | 15% | 61 | 25% | 156 | 63% |
| | | **Total** | **11,709** | **10,557** | **90%** | **10,841** | **93%** | **11,042** | **94%** | **11,235** | **96%** | **11,406** | **97%** |

**Table F2. Length and proportion of REC2 segments achieving visual clarity attribute bands and NBL (or maintaining baseline visual clarity), summarised by FMU and stream order for PS2**

| PS2 | | | | Length of REC2 segments achieving visual clarity attribute bands and NBL | | | | | | | | | |
|---|---|---|---|---|---|---|---|---|---|---|---|---|---|
| Attribute band | FMU | Stream order | Total length (km) | 2021 | | 2040 | | 2060 | | 2080 | | 2100 | |
| | | | | km | % | km | % | km | % | km | % | km | % |
| A band | Kai Iwi | 1 | 262 | 102 | 39% | 158 | 60% | 185 | 70% | 188 | 72% | 190 | 72% |
| | | 2 | 146 | 58 | 39% | 110 | 75% | 120 | 82% | 122 | 84% | 122 | 84% |
| | | 3 | 68 | 23 | 34% | 50 | 74% | 57 | 84% | 57 | 84% | 57 | 84% |
| | | 4 | 59 | 29 | 49% | 50 | 86% | 59 | 99% | 59 | 99% | 59 | 99% |
| | | 5 | 22 | - | 0% | 5 | 24% | 22 | 98% | 22 | 100% | 22 | 100% |
| | | **Total** | **558** | **212** | **38%** | **374** | **67%** | **442** | **79%** | **449** | **80%** | **450** | **81%** |
| | Manawatū | 1 | 4,825 | 1,203 | 25% | 2,194 | 45% | 2,766 | 57% | 2,831 | 59% | 2,853 | 59% |
| | | 2 | 2,484 | 561 | 23% | 1,086 | 44% | 1,420 | 57% | 1,460 | 59% | 1,467 | 59% |
| | | 3 | 1,261 | 257 | 20% | 509 | 40% | 734 | 58% | 753 | 60% | 758 | 60% |
| | | 4 | 651 | 75 | 12% | 266 | 41% | 411 | 63% | 415 | 64% | 417 | 64% |
| | | 5 | 439 | 73 | 17% | 156 | 35% | 278 | 63% | 287 | 65% | 291 | 66% |
| | | 6 | 162 | 5 | 3% | 81 | 50% | 146 | 90% | 146 | 90% | 146 | 90% |
| | | 7 | 119 | - | 0% | 42 | 35% | 42 | 35% | 42 | 35% | 42 | 35% |
| | | **Total** | **9,941** | **2,173** | **22%** | **4,333** | **44%** | **5,796** | **58%** | **5,934** | **60%** | **5,973** | **60%** |
| | Puketoi ki Tai | 1 | 875 | 202 | 23% | 595 | 68% | 719 | 82% | 734 | 84% | 739 | 84% |
| | | 2 | 435 | 84 | 19% | 266 | 61% | 362 | 83% | 369 | 85% | 369 | 85% |
| | | 3 | 259 | 39 | 15% | 142 | 55% | 227 | 88% | 231 | 89% | 231 | 89% |
| | | 4 | 139 | 13 | 9% | 53 | 38% | 131 | 94% | 137 | 98% | 137 | 98% |
| | | 5 | 71 | - | 0% | 26 | 37% | 53 | 74% | 53 | 74% | 53 | 74% |
| | | 6 | 46 | - | 0% | - | 0% | 22 | 48% | 22 | 48% | 22 | 48% |
| | | **Total** | **1,825** | **339** | **19%** | **1,082** | **59%** | **1,514** | **83%** | **1,545** | **85%** | **1,550** | **85%** |

| PS2 | | | | Length of REC2 segments achieving visual clarity attribute bands and NBL | | | | | | | | | |
|---|---|---|---|---|---|---|---|---|---|---|---|---|---|
| Attribute band | FMU | Stream order | Total length (km) | 2021 | | 2040 | | 2060 | | 2080 | | 2100 | |
| | | | | km | % | km | % | km | % | km | % | km | % |
| A band (cont.) | Rangitīkei-Turakina | 1 | 4,349 | 1,241 | 29% | 2,520 | 58% | 2,955 | 68% | 2,985 | 69% | 3,003 | 69% |
| | | 2 | 2,111 | 592 | 28% | 1,187 | 56% | 1,421 | 67% | 1,443 | 68% | 1,447 | 69% |
| | | 3 | 1,035 | 289 | 28% | 601 | 58% | 710 | 69% | 733 | 71% | 737 | 71% |
| | | 4 | 480 | 207 | 43% | 345 | 72% | 410 | 85% | 410 | 85% | 410 | 85% |
| | | 5 | 293 | 127 | 43% | 199 | 68% | 255 | 87% | 255 | 87% | 255 | 87% |
| | | 6 | 156 | 19 | 12% | 70 | 45% | 118 | 75% | 156 | 100% | 156 | 100% |
| | | 7 | 139 | - | 0% | 21 | 15% | 139 | 100% | 139 | 100% | 139 | 100% |
| | | **Total** | **8,563** | **2,476** | **29%** | **4,943** | **58%** | **6,008** | **70%** | **6,121** | **71%** | **6,148** | **72%** |
| | Waiopehu | 1 | 322 | 69 | 21% | 94 | 29% | 97 | 30% | 98 | 30% | 98 | 30% |
| | | 2 | 161 | 25 | 15% | 34 | 21% | 39 | 24% | 39 | 24% | 39 | 24% |
| | | 3 | 92 | 27 | 29% | 30 | 33% | 31 | 34% | 31 | 34% | 31 | 34% |
| | | 4 | 38 | 19 | 50% | 21 | 57% | 22 | 57% | 22 | 57% | 22 | 57% |
| | | 5 | 34 | 19 | 57% | 23 | 68% | 25 | 74% | 25 | 74% | 25 | 74% |
| | | **Total** | **647** | **159** | **25%** | **202** | **31%** | **214** | **33%** | **215** | **33%** | **215** | **33%** |
| | Whangaehu | 1 | 1,682 | 588 | 35% | 1,164 | 69% | 1,239 | 74% | 1,255 | 75% | 1,263 | 75% |
| | | 2 | 892 | 326 | 37% | 628 | 70% | 652 | 73% | 657 | 74% | 672 | 75% |
| | | 3 | 409 | 171 | 42% | 302 | 74% | 313 | 76% | 313 | 76% | 313 | 76% |
| | | 4 | 223 | 50 | 22% | 151 | 68% | 168 | 75% | 168 | 75% | 168 | 75% |
| | | 5 | 126 | 42 | 33% | 107 | 85% | 107 | 85% | 107 | 85% | 107 | 85% |
| | | 6 | 145 | - | 0% | - | 0% | 136 | 94% | 136 | 94% | 136 | 94% |
| | | **Total** | **3,478** | **1,177** | **34%** | **2,352** | **68%** | **2,616** | **75%** | **2,636** | **76%** | **2,659** | **76%** |
| | Whanganui | 1 | 5,833 | 3,816 | 65% | 4,658 | 80% | 4,971 | 85% | 4,991 | 86% | 5,003 | 86% |
| | | 2 | 2,871 | 1,918 | 67% | 2,347 | 82% | 2,525 | 88% | 2,536 | 88% | 2,539 | 88% |
| | | 3 | 1,397 | 972 | 70% | 1,165 | 83% | 1,265 | 91% | 1,268 | 91% | 1,269 | 91% |

| PS2 | | | | Length of REC2 segments achieving visual clarity attribute bands and NBL | | | | | | | | | |
|---|---|---|---|---|---|---|---|---|---|---|---|---|---|
| Attribute band | FMU | Stream order | Total length (km) | 2021 | | 2040 | | 2060 | | 2080 | | 2100 | |
| | | | | km | % | km | % | km | % | km | % | km | % |
| A band (cont.) | Whanganui (cont.) | 4 | 790 | 512 | 65% | 654 | 83% | 749 | 95% | 749 | 95% | 749 | 95% |
| | | 5 | 404 | 332 | 82% | 356 | 88% | 389 | 96% | 389 | 96% | 389 | 96% |
| | | 6 | 166 | 28 | 17% | 95 | 57% | 135 | 81% | 158 | 95% | 159 | 96% |
| | | 7 | 247 | - | 0% | - | 0% | 80 | 32% | 105 | 43% | 105 | 43% |
| | | **Total** | **11,709** | **7,579** | **65%** | **9,274** | **79%** | **10,114** | **86%** | **10,197** | **87%** | **10,213** | **87%** |
| B band | Kai Iwi | 1 | 262 | 195 | 74% | 222 | 85% | 229 | 87% | 229 | 87% | 230 | 88% |
| | | 2 | 146 | 116 | 79% | 131 | 90% | 133 | 91% | 133 | 91% | 133 | 91% |
| | | 3 | 68 | 50 | 74% | 63 | 92% | 63 | 92% | 63 | 92% | 63 | 92% |
| | | 4 | 59 | 51 | 87% | 57 | 97% | 59 | 100% | 59 | 100% | 59 | 100% |
| | | 5 | 22 | 5 | 24% | 19 | 85% | 22 | 100% | 22 | 100% | 22 | 100% |
| | | **Total** | **558** | **418** | **75%** | **492** | **88%** | **506** | **91%** | **506** | **91%** | **506** | **91%** |
| | Manawatū | 1 | 4,825 | 2,185 | 45% | 3,105 | 64% | 3,418 | 71% | 3,457 | 72% | 3,477 | 72% |
| | | 2 | 2,484 | 1,076 | 43% | 1,547 | 62% | 1,754 | 71% | 1,791 | 72% | 1,800 | 72% |
| | | 3 | 1,261 | 529 | 42% | 767 | 61% | 925 | 73% | 935 | 74% | 940 | 75% |
| | | 4 | 651 | 210 | 32% | 352 | 54% | 477 | 73% | 483 | 74% | 483 | 74% |
| | | 5 | 439 | 159 | 36% | 245 | 56% | 344 | 78% | 346 | 79% | 346 | 79% |
| | | 6 | 162 | 15 | 9% | 101 | 62% | 162 | 100% | 162 | 100% | 162 | 100% |
| | | 7 | 119 | 4 | 4% | 42 | 35% | 42 | 35% | 42 | 35% | 42 | 35% |
| | | **Total** | **9,941** | **4,179** | **42%** | **6,159** | **62%** | **7,122** | **72%** | **7,216** | **73%** | **7,250** | **73%** |
| | Puketoi ki Tai | 1 | 875 | 401 | 46% | 713 | 81% | 780 | 89% | 783 | 90% | 785 | 90% |
| | | 2 | 435 | 156 | 36% | 343 | 79% | 385 | 88% | 393 | 90% | 394 | 91% |
| | | 3 | 259 | 89 | 34% | 199 | 77% | 235 | 91% | 237 | 92% | 237 | 92% |
| | | 4 | 139 | 25 | 18% | 98 | 70% | 137 | 98% | 137 | 98% | 137 | 98% |
| | | 5 | 71 | - | 0% | 29 | 41% | 61 | 87% | 65 | 92% | 65 | 92% |

| **PS2** | | | | **Length of REC2 segments achieving visual clarity attribute bands and NBL** | | | | | | | | | |
|---|---|---|---|---|---|---|---|---|---|---|---|---|---|
| **Attribute band** | **FMU** | **Stream order** | **Total length (km)** | **2021** | | **2040** | | **2060** | | **2080** | | **2100** | |
| | | | | **km** | **%** | **km** | **%** | **km** | **%** | **km** | **%** | **km** | **%** |
| B band (cont.) | Puketoi ki Tai (cont.) | 6 | 46 | - | 0% | 22 | 48% | 46 | 100% | 46 | 100% | 46 | 100% |
| | | **Total** | **1,825** | **671** | **37%** | **1,405** | **77%** | **1,644** | **90%** | **1,662** | **91%** | **1,664** | **91%** |
| | Rangitīkei-Turakina | 1 | 4,349 | 2,455 | 56% | 3,334 | 77% | 3,589 | 83% | 3,603 | 83% | 3,612 | 83% |
| | | 2 | 2,111 | 1,151 | 55% | 1,587 | 75% | 1,711 | 81% | 1,712 | 81% | 1,717 | 81% |
| | | 3 | 1,035 | 571 | 55% | 793 | 77% | 846 | 82% | 853 | 82% | 857 | 83% |
| | | 4 | 480 | 319 | 66% | 420 | 88% | 432 | 90% | 437 | 91% | 437 | 91% |
| | | 5 | 293 | 179 | 61% | 259 | 89% | 285 | 97% | 285 | 97% | 285 | 97% |
| | | 6 | 156 | 36 | 23% | 104 | 66% | 156 | 100% | 156 | 100% | 156 | 100% |
| | | 7 | 139 | - | 0% | 97 | 70% | 139 | 100% | 139 | 100% | 139 | 100% |
| | | **Total** | **8,563** | **4,710** | **55%** | **6,594** | **77%** | **7,159** | **84%** | **7,185** | **84%** | **7,203** | **84%** |
| | Waiopehu | 1 | 322 | 151 | 47% | 173 | 54% | 178 | 55% | 178 | 55% | 178 | 55% |
| | | 2 | 161 | 69 | 43% | 82 | 51% | 89 | 55% | 89 | 55% | 89 | 55% |
| | | 3 | 92 | 48 | 53% | 58 | 63% | 58 | 63% | 58 | 63% | 58 | 63% |
| | | 4 | 38 | 23 | 61% | 24 | 62% | 25 | 65% | 25 | 65% | 25 | 65% |
| | | 5 | 34 | 23 | 68% | 23 | 68% | 25 | 74% | 25 | 74% | 25 | 74% |
| | | **Total** | **647** | **315** | **49%** | **360** | **56%** | **374** | **58%** | **375** | **58%** | **375** | **58%** |
| | Whangaehu | 1 | 1,682 | 1,258 | 75% | 1,480 | 88% | 1,509 | 90% | 1,512 | 90% | 1,519 | 90% |
| | | 2 | 892 | 685 | 77% | 785 | 88% | 790 | 89% | 795 | 89% | 798 | 90% |
| | | 3 | 409 | 320 | 78% | 365 | 89% | 366 | 89% | 366 | 89% | 366 | 89% |
| | | 4 | 223 | 155 | 70% | 201 | 90% | 201 | 90% | 203 | 91% | 204 | 91% |
| | | 5 | 126 | 58 | 46% | 107 | 85% | 107 | 85% | 107 | 85% | 107 | 85% |
| | | 6 | 145 | - | 0% | 81 | 56% | 139 | 96% | 139 | 96% | 139 | 96% |
| | | **Total** | **3,478** | **2,476** | **71%** | **3,019** | **87%** | **3,113** | **89%** | **3,122** | **90%** | **3,134** | **90%** |

| PS2 | | | | Length of REC2 segments achieving visual clarity attribute bands and NBL | | | | | | | | | |
|---|---|---|---|---|---|---|---|---|---|---|---|---|---|
| **Attribute band** | **FMU** | **Stream order** | **Total length (km)** | **2021** | | **2040** | | **2060** | | **2080** | | **2100** | |
| | | | | **km** | **%** | **km** | **%** | **km** | **%** | **km** | **%** | **km** | **%** |
| B band (cont.) | Whanganui | 1 | 5,833 | 4,742 | 81% | 5,372 | 92% | 5,482 | 94% | 5,488 | 94% | 5,498 | 94% |
| | | 2 | 2,871 | 2,366 | 82% | 2,698 | 94% | 2,752 | 96% | 2,756 | 96% | 2,758 | 96% |
| | | 3 | 1,397 | 1,154 | 83% | 1,332 | 95% | 1,356 | 97% | 1,360 | 97% | 1,360 | 97% |
| | | 4 | 790 | 615 | 78% | 743 | 94% | 782 | 99% | 782 | 99% | 782 | 99% |
| | | 5 | 404 | 369 | 91% | 404 | 100% | 404 | 100% | 404 | 100% | 404 | 100% |
| | | 6 | 166 | 79 | 47% | 137 | 83% | 166 | 100% | 166 | 100% | 166 | 100% |
| | | 7 | 247 | - | 0% | 26 | 11% | 116 | 47% | 246 | 99% | 246 | 100% |
| | | **Total** | **11,709** | **9,325** | **80%** | **10,711** | **91%** | **11,058** | **94%** | **11,202** | **96%** | **11,214** | **96%** |
| NBL | Kai Iwi | 1 | 262 | 240 | 92% | 249 | 95% | 249 | 95% | 249 | 95% | 249 | 95% |
| | | 2 | 146 | 143 | 98% | 144 | 99% | 144 | 99% | 144 | 99% | 144 | 99% |
| | | 3 | 68 | 67 | 98% | 68 | 100% | 68 | 100% | 68 | 100% | 68 | 100% |
| | | 4 | 59 | 56 | 95% | 59 | 100% | 59 | 100% | 59 | 100% | 59 | 100% |
| | | 5 | 22 | 15 | 67% | 22 | 100% | 22 | 100% | 22 | 100% | 22 | 100% |
| | | **Total** | **558** | **521** | **93%** | **542** | **97%** | **542** | **97%** | **543** | **97%** | **543** | **97%** |
| | Manawatū | 1 | 4,825 | 2,969 | 62% | 3,674 | 76% | 3,861 | 80% | 3,894 | 81% | 3,912 | 81% |
| | | 2 | 2,484 | 1,491 | 60% | 1,865 | 75% | 1,982 | 80% | 2,013 | 81% | 2,019 | 81% |
| | | 3 | 1,261 | 708 | 56% | 937 | 74% | 1,014 | 80% | 1,025 | 81% | 1,027 | 81% |
| | | 4 | 651 | 329 | 51% | 437 | 67% | 544 | 84% | 552 | 85% | 552 | 85% |
| | | 5 | 439 | 208 | 47% | 278 | 63% | 377 | 86% | 380 | 87% | 380 | 87% |
| | | 6 | 162 | 83 | 51% | 144 | 89% | 162 | 100% | 162 | 100% | 162 | 100% |
| | | 7 | 119 | 42 | 35% | 42 | 35% | 44 | 37% | 57 | 48% | 57 | 48% |
| | | **Total** | **9,941** | **5,829** | **59%** | **7,377** | **74%** | **7,985** | **80%** | **8,083** | **81%** | **8,109** | **82%** |
| | Puketoi ki Tai | 1 | 875 | 679 | 78% | 799 | 91% | 825 | 94% | 827 | 94% | 828 | 95% |
| | | 2 | 435 | 298 | 69% | 388 | 89% | 406 | 93% | 407 | 94% | 411 | 94% |

| PS2 | | | | Length of REC2 segments achieving visual clarity attribute bands and NBL | | | | | | | | | |
|---|---|---|---|---|---|---|---|---|---|---|---|---|---|
| Attribute band | FMU | Stream order | Total length (km) | 2021 | | 2040 | | 2060 | | 2080 | | 2100 | |
| | | | | km | % | km | % | km | % | km | % | km | % |
| NBL (cont.) | Puketoi ki Tai (cont.) | 3 | 259 | 165 | 63% | 229 | 89% | 249 | 96% | 250 | 96% | 250 | 96% |
| | | 4 | 139 | 59 | 43% | 117 | 84% | 137 | 98% | 137 | 98% | 137 | 98% |
| | | 5 | 71 | 29 | 41% | 47 | 67% | 71 | 100% | 71 | 100% | 71 | 100% |
| | | 6 | 46 | - | 0% | 22 | 48% | 46 | 100% | 46 | 100% | 46 | 100% |
| | | **Total** | **1,825** | **1,231** | **67%** | **1,603** | **88%** | **1,735** | **95%** | **1,738** | **95%** | **1,742** | **95%** |
| | Rangitīkei-Turakina | 1 | 4,349 | 3,201 | 74% | 3,668 | 84% | 3,823 | 88% | 3,836 | 88% | 3,850 | 89% |
| | | 2 | 2,111 | 1,456 | 69% | 1,757 | 83% | 1,827 | 87% | 1,828 | 87% | 1,830 | 87% |
| | | 3 | 1,035 | 748 | 72% | 864 | 84% | 904 | 87% | 904 | 87% | 904 | 87% |
| | | 4 | 480 | 393 | 82% | 449 | 94% | 461 | 96% | 461 | 96% | 461 | 96% |
| | | 5 | 293 | 236 | 80% | 286 | 98% | 289 | 99% | 289 | 99% | 289 | 99% |
| | | 6 | 156 | 91 | 59% | 104 | 66% | 156 | 100% | 156 | 100% | 156 | 100% |
| | | 7 | 139 | 16 | 11% | 135 | 97% | 139 | 100% | 139 | 100% | 139 | 100% |
| | | **Total** | **8,563** | **6,140** | **72%** | **7,263** | **85%** | **7,600** | **89%** | **7,614** | **89%** | **7,630** | **89%** |
| | Waiopehu | 1 | 322 | 164 | 51% | 201 | 62% | 205 | 64% | 205 | 64% | 205 | 64% |
| | | 2 | 161 | 77 | 48% | 94 | 59% | 100 | 62% | 101 | 63% | 101 | 63% |
| | | 3 | 92 | 59 | 64% | 64 | 69% | 65 | 71% | 65 | 71% | 65 | 71% |
| | | 4 | 38 | 24 | 62% | 31 | 82% | 32 | 84% | 32 | 84% | 32 | 84% |
| | | 5 | 34 | 23 | 68% | 25 | 74% | 25 | 74% | 25 | 74% | 25 | 74% |
| | | **Total** | **647** | **347** | **54%** | **415** | **64%** | **428** | **66%** | **428** | **66%** | **428** | **66%** |
| | Whangaehu | 1 | 1,682 | 1,494 | 89% | 1,594 | 95% | 1,605 | 95% | 1,606 | 96% | 1,607 | 96% |
| | | 2 | 892 | 797 | 89% | 842 | 94% | 845 | 95% | 847 | 95% | 847 | 95% |
| | | 3 | 409 | 372 | 91% | 395 | 96% | 395 | 96% | 395 | 96% | 395 | 96% |
| | | 4 | 223 | 175 | 79% | 205 | 92% | 205 | 92% | 205 | 92% | 205 | 92% |
| | | 5 | 126 | 77 | 61% | 107 | 85% | 108 | 85% | 108 | 85% | 108 | 85% |

| **PS2** | | | | **Length of REC2 segments achieving visual clarity attribute bands and NBL** | | | | | | | | | |
|---|---|---|---|---|---|---|---|---|---|---|---|---|---|
| **Attribute band** | **FMU** | **Stream order** | **Total length (km)** | **2021** | | **2040** | | **2060** | | **2080** | | **2100** | |
| | | | | **km** | **%** | **km** | **%** | **km** | **%** | **km** | **%** | **km** | **%** |
| NBL (cont.) | Whangaehu (cont.) | 6 | 145 | - | 0% | 140 | 96% | 140 | 96% | 140 | 96% | 140 | 96% |
| | | **Total** | **3,478** | **2,915** | **84%** | **3,283** | **94%** | **3,299** | **95%** | **3,301** | **95%** | **3,302** | **95%** |
| | Whanganui | 1 | 5,833 | 5,368 | 92% | 5,661 | 97% | 5,680 | 97% | 5,682 | 97% | 5,684 | 97% |
| | | 2 | 2,871 | 2,647 | 92% | 2,811 | 98% | 2,826 | 98% | 2,827 | 98% | 2,828 | 99% |
| | | 3 | 1,397 | 1,294 | 93% | 1,373 | 98% | 1,383 | 99% | 1,383 | 99% | 1,383 | 99% |
| | | 4 | 790 | 715 | 90% | 788 | 100% | 788 | 100% | 788 | 100% | 788 | 100% |
| | | 5 | 404 | 391 | 97% | 404 | 100% | 404 | 100% | 404 | 100% | 404 | 100% |
| | | 6 | 166 | 134 | 80% | 166 | 100% | 166 | 100% | 166 | 100% | 166 | 100% |
| | | 7 | 247 | 9 | 4% | 61 | 25% | 247 | 100% | 247 | 100% | 247 | 100% |
| | | **Total** | **11,709** | **10,557** | **90%** | **11,264** | **96%** | **11,494** | **98%** | **11,498** | **98%** | **11,501** | **98%** |

# Appendix G – Length and proportion of River Environment Classification v2 (REC2) segments achieving visual clarity attribute bands and NBL (or maintaining baseline visual clarity), summarised by mid- and late century under projected climate change for each representative concentration pathway (RCP)

**Table G1 Length and proportion of REC2 segments achieving visual clarity attribute bands and NBL (or maintaining baseline visual clarity) by mid-century under projected climate change for PS1, represented by minimum, median, and maximum results for each RCP**

| PS1 | | | | | Length and proportion of REC2 segments achieving visual clarity attribute bands and NBL for each RCP | | | | | | | |
|---|---|---|---|---|---|---|---|---|---|---|---|---|
| **Period** | **Attribute Band** | **Stat** | **Stream order** | **Total length km** | **RCP2.6** | | **RCP4.5** | | **RCP6.0** | | **RCP8.5** | |
| | | | | | **km** | **%** | **km** | **%** | **km** | **%** | **km** | **%** |
| Mid-century | A band | min | 1 | 18,148 | 7,046 | 39% | 5,635 | 31% | 5,712 | 31% | 5,558 | 31% |
| | | | 2 | 9,101 | 3,563 | 39% | 2,783 | 31% | 2,831 | 31% | 2,723 | 30% |
| | | | 3 | 4,521 | 1,760 | 39% | 1,310 | 29% | 1,323 | 29% | 1,242 | 27% |
| | | | 4 | 2,381 | 913 | 38% | 672 | 28% | 714 | 30% | 613 | 26% |
| | | | 5 | 1,388 | 547 | 39% | 351 | 25% | 361 | 26% | 283 | 20% |
| | | | 6 | 676 | 74 | 11% | 44 | 7% | 41 | 6% | - | 0% |
| | | | 7 | 505 | - | 0% | - | 0% | - | 0% | - | 0% |
| | | | **Total** | **36,720** | **13,903** | **38%** | **10,796** | **29%** | **10,982** | **30%** | **10,419** | **28%** |
| | | med | 1 | 18,148 | 6,132 | 34% | 6,408 | 35% | 6,042 | 33% | 5,922 | 33% |
| | | | 2 | 9,101 | 2,962 | 33% | 3,095 | 34% | 2,916 | 32% | 2,791 | 31% |
| | | | 3 | 4,521 | 1,356 | 30% | 1,469 | 32% | 1,367 | 30% | 1,293 | 29% |
| | | | 4 | 2,381 | 746 | 31% | 699 | 29% | 668 | 28% | 630 | 26% |
| | | | 5 | 1,388 | 394 | 28% | 320 | 23% | 315 | 23% | 277 | 20% |
| | | | 6 | 676 | 44 | 7% | 30 | 4% | 33 | 5% | - | 0% |
| | | | 7 | 505 | - | 0% | - | 0% | - | 0% | - | 0% |
| | | | **Total** | **36,720** | **11,634** | **32%** | **12,022** | **33%** | **11,341** | **31%** | **10,913** | **30%** |

| PS1 | | | | | Length and proportion of REC2 segments achieving visual clarity attribute bands and NBL for each RCP | | | | | | | |
|---|---|---|---|---|---|---|---|---|---|---|---|---|
| Period | Attribute Band | Stat | Stream order | Total length km | RCP2.6 | | RCP4.5 | | RCP6.0 | | RCP8.5 | |
| | | | | | km | % | km | % | km | % | km | % |
| Mid-century (cont.) | A band (cont.) | max | 1 | 18,148 | 5,202 | 29% | 5,856 | 32% | 5,886 | 32% | 5,495 | 30% |
| | | | 2 | 9,101 | 2,460 | 27% | 2,777 | 31% | 2,809 | 31% | 2,538 | 28% |
| | | | 3 | 4,521 | 1,090 | 24% | 1,232 | 27% | 1,291 | 29% | 1,121 | 25% |
| | | | 4 | 2,381 | 520 | 22% | 583 | 24% | 596 | 25% | 526 | 22% |
| | | | 5 | 1,388 | 231 | 17% | 267 | 19% | 265 | 19% | 208 | 15% |
| | | | 6 | 676 | 2 | 0% | - | 0% | - | 0% | - | 0% |
| | | | 7 | 505 | - | 0% | - | 0% | - | 0% | - | 0% |
| | | | **Total** | **36,720** | **9,505** | **26%** | **10,716** | **29%** | **10,847** | **30%** | **9,887** | **27%** |
| | B band | min | 1 | 18,148 | 8,248 | 45% | 6,397 | 35% | 6,494 | 36% | 6,275 | 35% |
| | | | 2 | 9,101 | 4,181 | 46% | 3,142 | 35% | 3,224 | 35% | 3,031 | 33% |
| | | | 3 | 4,521 | 2,064 | 46% | 1,484 | 33% | 1,530 | 34% | 1,383 | 31% |
| | | | 4 | 2,381 | 1,042 | 44% | 764 | 32% | 818 | 34% | 683 | 29% |
| | | | 5 | 1,388 | 636 | 46% | 411 | 30% | 441 | 32% | 323 | 23% |
| | | | 6 | 676 | 112 | 17% | 74 | 11% | 73 | 11% | 19 | 3% |
| | | | 7 | 505 | - | 0% | - | 0% | - | 0% | - | 0% |
| | | | **Total** | **36,720** | **16,283** | **44%** | **12,272** | **33%** | **12,579** | **34%** | **11,715** | **32%** |
| | | med | 1 | 18,148 | 6,981 | 38% | 7,352 | 41% | 6,863 | 38% | 6,683 | 37% |
| | | | 2 | 9,101 | 3,361 | 37% | 3,506 | 39% | 3,307 | 36% | 3,134 | 34% |
| | | | 3 | 4,521 | 1,557 | 34% | 1,628 | 36% | 1,530 | 34% | 1,420 | 31% |
| | | | 4 | 2,381 | 839 | 35% | 764 | 32% | 736 | 31% | 699 | 29% |
| | | | 5 | 1,388 | 473 | 34% | 399 | 29% | 387 | 28% | 337 | 24% |
| | | | 6 | 676 | 72 | 11% | 48 | 7% | 56 | 8% | 6 | 1% |
| | | | 7 | 505 | - | 0% | - | 0% | - | 0% | - | 0% |
| | | | **Total** | **36,720** | **13,283** | **36%** | **13,696** | **37%** | **12,880** | **35%** | **12,278** | **33%** |

| PS1 | | | | | Length and proportion of REC2 segments achieving visual clarity attribute bands and NBL for each RCP | | | | | | | |
|---|---|---|---|---|---|---|---|---|---|---|---|---|
| Period | Attribute Band | Stat | Stream order | Total length km | RCP2.6 | | RCP4.5 | | RCP6.0 | | RCP8.5 | |
| | | | | | km | % | km | % | km | % | km | % |
| Mid-century (cont.) | B band (cont.) | max | 1 | 18,148 | 5,809 | 32% | 6,522 | 36% | 6,558 | 36% | 6,056 | 33% |
| | | | 2 | 9,101 | 2,726 | 30% | 3,055 | 34% | 3,091 | 34% | 2,783 | 31% |
| | | | 3 | 4,521 | 1,203 | 27% | 1,356 | 30% | 1,401 | 31% | 1,213 | 27% |
| | | | 4 | 2,381 | 575 | 24% | 629 | 26% | 638 | 27% | 554 | 23% |
| | | | 5 | 1,388 | 248 | 18% | 291 | 21% | 305 | 22% | 228 | 16% |
| | | | 6 | 676 | 16 | 2% | 6 | 1% | 6 | 1% | 5 | 1% |
| | | | 7 | 505 | - | 0% | - | 0% | - | 0% | - | 0% |
| | | | **Total** | **36,720** | **10,576** | **29%** | **11,859** | **32%** | **12,001** | **33%** | **10,838** | **30%** |
| | NBL | min | 1 | 18,148 | 8,911 | 49% | 6,841 | 38% | 6,910 | 38% | 6,674 | 37% |
| | | | 2 | 9,101 | 4,537 | 50% | 3,376 | 37% | 3,441 | 38% | 3,243 | 36% |
| | | | 3 | 4,521 | 2,320 | 51% | 1,595 | 35% | 1,673 | 37% | 1,472 | 33% |
| | | | 4 | 2,381 | 1,149 | 48% | 818 | 34% | 863 | 36% | 711 | 30% |
| | | | 5 | 1,388 | 732 | 53% | 434 | 31% | 479 | 35% | 350 | 25% |
| | | | 6 | 676 | 174 | 26% | 95 | 14% | 92 | 14% | 19 | 3% |
| | | | 7 | 505 | 46 | 9% | - | 0% | - | 0% | - | 0% |
| | | | **Total** | **36,720** | **17,869** | **49%** | **13,160** | **36%** | **13,459** | **37%** | **12,469** | **34%** |
| | | med | 1 | 18,148 | 7,374 | 41% | 7,722 | 43% | 7,253 | 40% | 7,008 | 39% |
| | | | 2 | 9,101 | 3,528 | 39% | 3,689 | 41% | 3,488 | 38% | 3,273 | 36% |
| | | | 3 | 4,521 | 1,671 | 37% | 1,720 | 38% | 1,629 | 36% | 1,496 | 33% |
| | | | 4 | 2,381 | 877 | 37% | 790 | 33% | 772 | 32% | 711 | 30% |
| | | | 5 | 1,388 | 511 | 37% | 434 | 31% | 408 | 29% | 352 | 25% |
| | | | 6 | 676 | 94 | 14% | 51 | 8% | 63 | 9% | 13 | 2% |
| | | | 7 | 505 | - | 0% | - | 0% | - | 0% | - | 0% |
| | | | **Total** | **36,720** | **14,056** | **38%** | **14,405** | **39%** | **13,612** | **37%** | **12,853** | **35%** |

| PS1 | | | | | Length and proportion of REC2 segments achieving visual clarity attribute bands and NBL for each RCP | | | | | | | |
|---|---|---|---|---|---|---|---|---|---|---|---|---|
| | | | | | RCP2.6 | | RCP4.5 | | RCP6.0 | | RCP8.5 | |
| **Period** | **Attribute Band** | **Stat** | **Stream order** | **Total length km** | **km** | **%** | **km** | **%** | **km** | **%** | **km** | **%** |
| Mid-century (cont.) | NBL (cont.) | max | 1 | 18,148 | 6,067 | 33% | 6,820 | 38% | 6,898 | 38% | 6,336 | 35% |
| | | | 2 | 9,101 | 2,836 | 31% | 3,162 | 35% | 3,224 | 35% | 2,887 | 32% |
| | | | 3 | 4,521 | 1,259 | 28% | 1,422 | 31% | 1,479 | 33% | 1,267 | 28% |
| | | | 4 | 2,381 | 606 | 25% | 645 | 27% | 657 | 28% | 571 | 24% |
| | | | 5 | 1,388 | 264 | 19% | 306 | 22% | 322 | 23% | 242 | 17% |
| | | | 6 | 676 | 18 | 3% | 13 | 2% | 13 | 2% | 5 | 1% |
| | | | 7 | 505 | - | 0% | - | 0% | - | 0% | - | 0% |
| | | | **Total** | **36,720** | **11,050** | **30%** | **12,369** | **34%** | **12,593** | **34%** | **11,307** | **31%** |

**Table G2. Length and proportion of REC2 segments achieving visual clarity attribute bands and NBL (or maintaining baseline visual clarity) by late century under projected climate change for PS1, represented by minimum, median, and maximum results for each RCP**

| PS1 | | | | | Length and proportion of REC2 segments achieving visual clarity attribute bands and NBL for each RCP | | | | | | | |
|---|---|---|---|---|---|---|---|---|---|---|---|---|
| **Period** | **Attribute Band** | **Stat** | **Stream order** | **Total length km** | **RCP2.6** | | **RCP4.5** | | **RCP6.0** | | **RCP8.5** | |
| | | | | | **km** | **%** | **km** | **%** | **km** | **%** | **km** | **%** |
| Late century | A band | min | 1 | 18,148 | 12,470 | 69% | 11,881 | 65% | 9,764 | 54% | 8,267 | 46% |
| | | | 2 | 9,101 | 6,248 | 69% | 5,878 | 65% | 4,783 | 53% | 3,901 | 43% |
| | | | 3 | 4,521 | 3,141 | 69% | 2,874 | 64% | 2,326 | 51% | 1,797 | 40% |
| | | | 4 | 2,381 | 1,760 | 74% | 1,553 | 65% | 1,286 | 54% | 874 | 37% |
| | | | 5 | 1,388 | 1,009 | 73% | 883 | 64% | 717 | 52% | 497 | 36% |
| | | | 6 | 676 | 465 | 69% | 265 | 39% | 149 | 22% | 71 | 11% |
| | | | 7 | 505 | 164 | 32% | 84 | 17% | - | 0% | - | 0% |
| | | | **Total** | **36,720** | **25,255** | **69%** | **23,418** | **64%** | **19,024** | **52%** | **15,408** | **42%** |
| | | med | 1 | 18,148 | 11,567 | 64% | 9,926 | 55% | 9,563 | 53% | 8,191 | 45% |
| | | | 2 | 9,101 | 5,673 | 62% | 4,821 | 53% | 4,500 | 49% | 3,853 | 42% |
| | | | 3 | 4,521 | 2,825 | 62% | 2,301 | 51% | 2,113 | 47% | 1,785 | 39% |
| | | | 4 | 2,381 | 1,593 | 67% | 1,273 | 53% | 1,057 | 44% | 780 | 33% |
| | | | 5 | 1,388 | 912 | 66% | 706 | 51% | 551 | 40% | 413 | 30% |
| | | | 6 | 676 | 279 | 41% | 155 | 23% | 86 | 13% | 48 | 7% |
| | | | 7 | 505 | 109 | 22% | - | 0% | - | 0% | - | 0% |
| | | | **Total** | **36,720** | **22,958** | **63%** | **19,183** | **52%** | **17,870** | **49%** | **15,070** | **41%** |
| | | max | 1 | 18,148 | 10,483 | 58% | 9,763 | 54% | 7,913 | 44% | 7,971 | 44% |
| | | | 2 | 9,101 | 5,043 | 55% | 4,625 | 51% | 3,635 | 40% | 3,650 | 40% |
| | | | 3 | 4,521 | 2,442 | 54% | 2,185 | 48% | 1,662 | 37% | 1,666 | 37% |
| | | | 4 | 2,381 | 1,373 | 58% | 1,098 | 46% | 787 | 33% | 701 | 29% |
| | | | 5 | 1,388 | 755 | 54% | 620 | 45% | 427 | 31% | 388 | 28% |
| | | | 6 | 676 | 192 | 28% | 90 | 13% | 58 | 9% | 38 | 6% |
| | | | 7 | 505 | 21 | 4% | - | 0% | - | 0% | - | 0% |
| | | | **Total** | **36,720** | **20,308** | **55%** | **18,381** | **50%** | **14,483** | **39%** | **14,416** | **39%** |

| PS1 | | | | | Length and proportion of REC2 segments achieving visual clarity attribute bands and NBL for each RCP | | | | | | | |
|---|---|---|---|---|---|---|---|---|---|---|---|---|
| Period | Attribute Band | Stat | Stream order | Total length km | RCP2.6 | | RCP4.5 | | RCP6.0 | | RCP8.5 | |
| | | | | | km | % | km | % | km | % | km | % |
| Late century (cont.) | B band | min | 1 | 18,148 | 13,880 | 76% | 13,403 | 74% | 11,154 | 61% | 9,566 | 53% |
| | | | 2 | 9,101 | 7,051 | 77% | 6,721 | 74% | 5,530 | 61% | 4,561 | 50% |
| | | | 3 | 4,521 | 3,560 | 79% | 3,331 | 74% | 2,729 | 60% | 2,113 | 47% |
| | | | 4 | 2,381 | 1,963 | 82% | 1,851 | 78% | 1,538 | 65% | 1,038 | 44% |
| | | | 5 | 1,388 | 1,114 | 80% | 1,043 | 75% | 853 | 61% | 596 | 43% |
| | | | 6 | 676 | 544 | 80% | 518 | 77% | 349 | 52% | 110 | 16% |
| | | | 7 | 505 | 214 | 42% | 164 | 32% | 118 | 23% | 1 | 0% |
| | | | **Total** | **36,720** | **28,325** | **77%** | **27,030** | **74%** | **22,270** | **61%** | **17,984** | **49%** |
| | | med | 1 | 18,148 | 12,976 | 71% | 11,204 | 62% | 10,770 | 59% | 9,388 | 52% |
| | | | 2 | 9,101 | 6,480 | 71% | 5,508 | 61% | 5,083 | 56% | 4,385 | 48% |
| | | | 3 | 4,521 | 3,245 | 72% | 2,701 | 60% | 2,436 | 54% | 2,035 | 45% |
| | | | 4 | 2,381 | 1,864 | 78% | 1,515 | 64% | 1,307 | 55% | 879 | 37% |
| | | | 5 | 1,388 | 1,088 | 78% | 862 | 62% | 727 | 52% | 502 | 36% |
| | | | 6 | 676 | 517 | 76% | 346 | 51% | 178 | 26% | 57 | 8% |
| | | | 7 | 505 | 179 | 35% | 118 | 23% | 21 | 4% | - | 0% |
| | | | **Total** | **36,720** | **26,348** | **72%** | **22,253** | **61%** | **20,522** | **56%** | **17,247** | **47%** |
| | | max | 1 | 18,148 | 11,705 | 64% | 11,109 | 61% | 9,051 | 50% | 8,907 | 49% |
| | | | 2 | 9,101 | 5,724 | 63% | 5,263 | 58% | 4,170 | 46% | 4,038 | 44% |
| | | | 3 | 4,521 | 2,825 | 62% | 2,543 | 56% | 1,939 | 43% | 1,841 | 41% |
| | | | 4 | 2,381 | 1,601 | 67% | 1,378 | 58% | 924 | 39% | 789 | 33% |
| | | | 5 | 1,388 | 923 | 66% | 814 | 59% | 476 | 34% | 417 | 30% |
| | | | 6 | 676 | 423 | 63% | 201 | 30% | 101 | 15% | 49 | 7% |
| | | | 7 | 505 | 138 | 27% | 21 | 4% | - | 0% | - | 0% |
| | | | **Total** | **36,720** | **23,338** | **64%** | **21,329** | **58%** | **16,662** | **45%** | **16,040** | **44%** |

| PS1 | | | | | Length and proportion of REC2 segments achieving visual clarity attribute bands and NBL for each RCP | | | | | | | |
|---|---|---|---|---|---|---|---|---|---|---|---|---|
| Period | Attribute Band | Stat | Stream order | Total length km | RCP2.6 | | RCP4.5 | | RCP6.0 | | RCP8.5 | |
| | | | | | km | % | km | % | km | % | km | % |
| Late century (cont.) | NBL | min | 1 | 18,148 | 14,706 | 81% | 14,163 | 78% | 11,965 | 66% | 10,446 | 58% |
| | | | 2 | 9,101 | 7,509 | 83% | 7,153 | 79% | 6,036 | 66% | 5,028 | 55% |
| | | | 3 | 4,521 | 3,816 | 84% | 3,635 | 80% | 3,060 | 68% | 2,380 | 53% |
| | | | 4 | 2,381 | 2,098 | 88% | 2,008 | 84% | 1,705 | 72% | 1,239 | 52% |
| | | | 5 | 1,388 | 1,203 | 87% | 1,144 | 82% | 1,000 | 72% | 688 | 50% |
| | | | 6 | 676 | 605 | 90% | 553 | 82% | 523 | 77% | 215 | 32% |
| | | | 7 | 505 | 428 | 85% | 223 | 44% | 177 | 35% | 72 | 14% |
| | | | **Total** | **36,720** | **30,366** | **83%** | **28,880** | **79%** | **24,466** | **67%** | **20,067** | **55%** |
| | | med | 1 | 18,148 | 13,785 | 76% | 11,916 | 66% | 11,535 | 64% | 10,123 | 56% |
| | | | 2 | 9,101 | 6,883 | 76% | 5,941 | 65% | 5,528 | 61% | 4,722 | 52% |
| | | | 3 | 4,521 | 3,470 | 77% | 2,957 | 65% | 2,724 | 60% | 2,212 | 49% |
| | | | 4 | 2,381 | 2,013 | 85% | 1,673 | 70% | 1,429 | 60% | 973 | 41% |
| | | | 5 | 1,388 | 1,185 | 85% | 994 | 72% | 810 | 58% | 567 | 41% |
| | | | 6 | 676 | 565 | 84% | 519 | 77% | 372 | 55% | 127 | 19% |
| | | | 7 | 505 | 343 | 68% | 179 | 35% | 144 | 29% | 16 | 3% |
| | | | **Total** | **36,720** | **28,244** | **77%** | **24,180** | **66%** | **22,543** | **61%** | **18,739** | **51%** |
| | | max | 1 | 18,148 | 12,381 | 68% | 11,792 | 65% | 9,699 | 53% | 9,524 | 52% |
| | | | 2 | 9,101 | 6,107 | 67% | 5,652 | 62% | 4,490 | 49% | 4,299 | 47% |
| | | | 3 | 4,521 | 3,072 | 68% | 2,799 | 62% | 2,138 | 47% | 1,961 | 43% |
| | | | 4 | 2,381 | 1,753 | 74% | 1,498 | 63% | 1,115 | 47% | 848 | 36% |
| | | | 5 | 1,388 | 1,020 | 73% | 918 | 66% | 572 | 41% | 450 | 32% |
| | | | 6 | 676 | 526 | 78% | 396 | 59% | 179 | 26% | 50 | 7% |
| | | | 7 | 505 | 201 | 40% | 145 | 29% | 60 | 12% | - | 0% |
| | | | **Total** | **36,720** | **25,059** | **68%** | **23,200** | **63%** | **18,253** | **50%** | **17,133** | **47%** |

**Table G3. Length and proportion of REC2 segments achieving visual clarity attribute bands and NBL (or maintaining baseline visual clarity) by mid-century under projected climate change for PS2, represented by minimum, median, and maximum results for each RCP**

| PS2 | | | | | Length and proportion of REC2 segments achieving visual clarity attribute bands and NBL for each RCP | | | | | | | |
|---|---|---|---|---|---|---|---|---|---|---|---|---|
| Period | Attribute Band | Stat | Stream order | Total length km | RCP2.6 | | RCP4.5 | | RCP6.0 | | RCP8.5 | |
| | | | | | km | % | km | % | km | % | km | % |
| Mid-century | A band | min | 1 | 18,148 | 10,895 | 60% | 9,100 | 50% | 9,182 | 51% | 8,095 | 45% |
| | | | 2 | 9,101 | 5,412 | 59% | 4,465 | 49% | 4,503 | 49% | 3,968 | 44% |
| | | | 3 | 4,521 | 2,656 | 59% | 2,128 | 47% | 2,152 | 48% | 1,893 | 42% |
| | | | 4 | 2,381 | 1,435 | 60% | 1,176 | 49% | 1,206 | 51% | 984 | 41% |
| | | | 5 | 1,388 | 796 | 57% | 678 | 49% | 666 | 48% | 577 | 42% |
| | | | 6 | 676 | 203 | 30% | 128 | 19% | 146 | 22% | 79 | 12% |
| | | | 7 | 505 | 7 | 1% | - | 0% | - | 0% | - | 0% |
| | | | **Total** | **36,720** | **21,404** | **58%** | **17,676** | **48%** | **17,855** | **49%** | **15,597** | **42%** |
| | | med | 1 | 18,148 | 9,639 | 53% | 9,282 | 51% | 9,115 | 50% | 8,183 | 45% |
| | | | 2 | 9,101 | 4,642 | 51% | 4,518 | 50% | 4,441 | 49% | 3,892 | 43% |
| | | | 3 | 4,521 | 2,155 | 48% | 2,159 | 48% | 2,096 | 46% | 1,868 | 41% |
| | | | 4 | 2,381 | 1,210 | 51% | 1,125 | 47% | 1,132 | 48% | 968 | 41% |
| | | | 5 | 1,388 | 669 | 48% | 608 | 44% | 639 | 46% | 529 | 38% |
| | | | 6 | 676 | 154 | 23% | 99 | 15% | 109 | 16% | 47 | 7% |
| | | | 7 | 505 | - | 0% | - | 0% | - | 0% | - | 0% |
| | | | **Total** | **36,720** | **18,468** | **50%** | **17,792** | **48%** | **17,531** | **48%** | **15,486** | **42%** |
| | | max | 1 | 18,148 | 8,242 | 45% | 8,015 | 44% | 7,833 | 43% | 6,656 | 37% |
| | | | 2 | 9,101 | 3,951 | 43% | 3,858 | 42% | 3,786 | 42% | 3,181 | 35% |
| | | | 3 | 4,521 | 1,827 | 40% | 1,788 | 40% | 1,798 | 40% | 1,475 | 33% |
| | | | 4 | 2,381 | 973 | 41% | 897 | 38% | 900 | 38% | 740 | 31% |
| | | | 5 | 1,388 | 525 | 38% | 504 | 36% | 503 | 36% | 446 | 32% |
| | | | 6 | 676 | 74 | 11% | 40 | 6% | 51 | 8% | 38 | 6% |
| | | | 7 | 505 | - | 0% | - | 0% | - | 0% | - | 0% |
| | | | **Total** | **36,720** | **15,592** | **42%** | **15,102** | **41%** | **14,871** | **40%** | **12,535** | **34%** |

| PS2 | | | | | Length and proportion of REC2 segments achieving visual clarity attribute bands and NBL for each RCP | | | | | | | |
|---|---|---|---|---|---|---|---|---|---|---|---|---|
| Period | Attribute Band | Stat | Stream order | Total length km | RCP2.6 | | RCP4.5 | | RCP6.0 | | RCP8.5 | |
| | | | | | km | % | km | % | km | % | km | % |
| Mid-century (cont.) | B band | min | 1 | 18,148 | 12,883 | 71% | 10,933 | 60% | 11,100 | 61% | 9,720 | 54% |
| | | | 2 | 9,101 | 6,442 | 71% | 5,382 | 59% | 5,484 | 60% | 4,744 | 52% |
| | | | 3 | 4,521 | 3,209 | 71% | 2,603 | 58% | 2,674 | 59% | 2,297 | 51% |
| | | | 4 | 2,381 | 1,762 | 74% | 1,523 | 64% | 1,577 | 66% | 1,223 | 51% |
| | | | 5 | 1,388 | 1,004 | 72% | 884 | 64% | 870 | 63% | 679 | 49% |
| | | | 6 | 676 | 367 | 54% | 266 | 39% | 270 | 40% | 163 | 24% |
| | | | 7 | 505 | 147 | 29% | 53 | 10% | 66 | 13% | 4 | 1% |
| | | | **Total** | **36,720** | **25,814** | **70%** | **21,642** | **59%** | **22,041** | **60%** | **18,829** | **51%** |
| | | med | 1 | 18,148 | 11,524 | 64% | 11,114 | 61% | 10,897 | 60% | 9,694 | 53% |
| | | | 2 | 9,101 | 5,573 | 61% | 5,401 | 59% | 5,310 | 58% | 4,622 | 51% |
| | | | 3 | 4,521 | 2,677 | 59% | 2,636 | 58% | 2,587 | 57% | 2,218 | 49% |
| | | | 4 | 2,381 | 1,556 | 65% | 1,376 | 58% | 1,394 | 59% | 1,168 | 49% |
| | | | 5 | 1,388 | 857 | 62% | 757 | 55% | 809 | 58% | 646 | 47% |
| | | | 6 | 676 | 254 | 38% | 186 | 28% | 205 | 30% | 134 | 20% |
| | | | 7 | 505 | 58 | 11% | 21 | 4% | 26 | 5% | - | 0% |
| | | | **Total** | **36,720** | **22,500** | **61%** | **21,491** | **59%** | **21,229** | **58%** | **18,482** | **50%** |
| | | max | 1 | 18,148 | 9,869 | 54% | 9,450 | 52% | 9,217 | 51% | 7,718 | 43% |
| | | | 2 | 9,101 | 4,748 | 52% | 4,542 | 50% | 4,448 | 49% | 3,675 | 40% |
| | | | 3 | 4,521 | 2,265 | 50% | 2,150 | 48% | 2,125 | 47% | 1,699 | 38% |
| | | | 4 | 2,381 | 1,222 | 51% | 1,090 | 46% | 1,052 | 44% | 853 | 36% |
| | | | 5 | 1,388 | 660 | 48% | 583 | 42% | 585 | 42% | 495 | 36% |
| | | | 6 | 676 | 177 | 26% | 137 | 20% | 117 | 17% | 70 | 10% |
| | | | 7 | 505 | 12 | 2% | - | 0% | - | 0% | - | 0% |
| | | | **Total** | **36,720** | **18,953** | **52%** | **17,952** | **49%** | **17,543** | **48%** | **14,510** | **40%** |

| PS2 | | | | | Length and proportion of REC2 segments achieving visual clarity attribute bands and NBL for each RCP | | | | | | | |
|---|---|---|---|---|---|---|---|---|---|---|---|---|
| Period | Attribute Band | Stat | Stream order | Total length km | RCP2.6 | | RCP4.5 | | RCP6.0 | | RCP8.5 | |
| | | | | | km | % | km | % | km | % | km | % |
| Mid-century (cont.) | NBL | min | 1 | 18,148 | 14,003 | 77% | 12,172 | 67% | 12,290 | 68% | 10,850 | 60% |
| | | | 2 | 9,101 | 7,073 | 78% | 6,050 | 66% | 6,126 | 67% | 5,371 | 59% |
| | | | 3 | 4,521 | 3,587 | 79% | 2,963 | 66% | 3,038 | 67% | 2,628 | 58% |
| | | | 4 | 2,381 | 1,966 | 83% | 1,728 | 73% | 1,786 | 75% | 1,459 | 61% |
| | | | 5 | 1,388 | 1,111 | 80% | 987 | 71% | 979 | 71% | 791 | 57% |
| | | | 6 | 676 | 545 | 81% | 466 | 69% | 467 | 69% | 310 | 46% |
| | | | 7 | 505 | 202 | 40% | 175 | 35% | 175 | 35% | 134 | 27% |
| | | | **Total** | **36,720** | **28,486** | **78%** | **24,541** | **67%** | **24,862** | **68%** | **21,543** | **59%** |
| | | med | 1 | 18,148 | 12,679 | 70% | 12,230 | 67% | 12,050 | 66% | 10,666 | 59% |
| | | | 2 | 9,101 | 6,173 | 68% | 5,996 | 66% | 5,919 | 65% | 5,115 | 56% |
| | | | 3 | 4,521 | 3,030 | 67% | 2,965 | 66% | 2,932 | 65% | 2,522 | 56% |
| | | | 4 | 2,381 | 1,738 | 73% | 1,601 | 67% | 1,619 | 68% | 1,345 | 57% |
| | | | 5 | 1,388 | 970 | 70% | 887 | 64% | 929 | 67% | 748 | 54% |
| | | | 6 | 676 | 447 | 66% | 362 | 54% | 395 | 58% | 243 | 36% |
| | | | 7 | 505 | 175 | 35% | 143 | 28% | 159 | 32% | 65 | 13% |
| | | | **Total** | **36,720** | **25,213** | **69%** | **24,185** | **66%** | **24,004** | **65%** | **20,705** | **56%** |
| | | max | 1 | 18,148 | 10,911 | 60% | 10,385 | 57% | 10,123 | 56% | 8,290 | 46% |
| | | | 2 | 9,101 | 5,297 | 58% | 4,974 | 55% | 4,874 | 54% | 3,909 | 43% |
| | | | 3 | 4,521 | 2,579 | 57% | 2,428 | 54% | 2,411 | 53% | 1,884 | 42% |
| | | | 4 | 2,381 | 1,459 | 61% | 1,246 | 52% | 1,197 | 50% | 923 | 39% |
| | | | 5 | 1,388 | 797 | 57% | 682 | 49% | 688 | 50% | 519 | 37% |
| | | | 6 | 676 | 341 | 50% | 238 | 35% | 204 | 30% | 90 | 13% |
| | | | 7 | 505 | 144 | 28% | 67 | 13% | 66 | 13% | - | 0% |
| | | | **Total** | **36,720** | **21,528** | **59%** | **20,020** | **55%** | **19,563** | **53%** | **15,614** | **43%** |

**Table G4. Length and proportion of REC2 segments achieving visual clarity attribute bands and NBL (or maintaining baseline visual clarity) by late century under projected climate change for PS2, represented by minimum, median, and maximum results for each RCP**

| PS2 | | | | | Length and proportion of REC2 segments achieving visual clarity attribute bands and NBL for each RCP | | | | | | | |
|---|---|---|---|---|---|---|---|---|---|---|---|---|
| Period | Attribute Band | Stat | Stream order | Total length km | RCP2.6 | | RCP4.5 | | RCP6.0 | | RCP8.5 | |
| | | | | | km | % | km | % | km | % | km | % |
| Late century | Band A | min | 1 | 18,148 | 13,500 | 74% | 13,762 | 76% | 12,377 | 68% | 11,776 | 65% |
| | | | 2 | 9,101 | 6,811 | 75% | 6,943 | 76% | 6,220 | 68% | 5,891 | 65% |
| | | | 3 | 4,521 | 3,491 | 77% | 3,472 | 77% | 3,114 | 69% | 2,833 | 63% |
| | | | 4 | 2,381 | 2,019 | 85% | 2,004 | 84% | 1,902 | 80% | 1,654 | 69% |
| | | | 5 | 1,388 | 1,176 | 85% | 1,118 | 81% | 1,025 | 74% | 939 | 68% |
| | | | 6 | 676 | 629 | 93% | 594 | 88% | 538 | 80% | 483 | 71% |
| | | | 7 | 505 | 428 | 85% | 428 | 85% | 374 | 74% | 154 | 30% |
| | | | **Total** | **36,720** | **28,053** | **76%** | **28,321** | **77%** | **25,549** | **70%** | **23,729** | **65%** |
| | | med | 1 | 18,148 | 13,189 | 73% | 12,420 | 68% | 12,724 | 70% | 12,131 | 67% |
| | | | 2 | 9,101 | 6,579 | 72% | 6,220 | 68% | 6,280 | 69% | 5,979 | 66% |
| | | | 3 | 4,521 | 3,340 | 74% | 3,065 | 68% | 3,070 | 68% | 2,906 | 64% |
| | | | 4 | 2,381 | 1,986 | 83% | 1,869 | 79% | 1,799 | 76% | 1,606 | 67% |
| | | | 5 | 1,388 | 1,117 | 80% | 1,013 | 73% | 957 | 69% | 846 | 61% |
| | | | 6 | 676 | 616 | 91% | 546 | 81% | 492 | 73% | 344 | 51% |
| | | | 7 | 505 | 428 | 85% | 400 | 79% | 202 | 40% | 102 | 20% |
| | | | **Total** | **36,720** | **27,256** | **74%** | **25,532** | **70%** | **25,524** | **70%** | **23,914** | **65%** |
| | | max | 1 | 18,148 | 12,659 | 70% | 12,747 | 70% | 11,436 | 63% | 12,186 | 67% |
| | | | 2 | 9,101 | 6,289 | 69% | 6,296 | 69% | 5,622 | 62% | 5,882 | 65% |
| | | | 3 | 4,521 | 3,140 | 69% | 3,098 | 69% | 2,690 | 60% | 2,816 | 62% |
| | | | 4 | 2,381 | 1,886 | 79% | 1,795 | 75% | 1,550 | 65% | 1,515 | 64% |
| | | | 5 | 1,388 | 1,033 | 74% | 968 | 70% | 871 | 63% | 808 | 58% |
| | | | 6 | 676 | 567 | 84% | 475 | 70% | 406 | 60% | 263 | 39% |
| | | | 7 | 505 | 428 | 85% | 202 | 40% | 128 | 25% | 81 | 16% |
| | | | **Total** | **36,720** | **26,001** | **71%** | **25,581** | **70%** | **22,703** | **62%** | **23,551** | **64%** |

| PS2 | | | | | Length and proportion of REC2 segments achieving visual clarity attribute bands and NBL for each RCP | | | | | | | |
|---|---|---|---|---|---|---|---|---|---|---|---|---|
| **Period** | **Attribute Band** | **Stat** | **Stream order** | **Total length km** | **RCP2.6** | | **RCP4.5** | | **RCP6.0** | | **RCP8.5** | |
| | | | | | **km** | **%** | **km** | **%** | **km** | **%** | **km** | **%** |
| Late century (cont.) | B band | min | 1 | 18,148 | 14,360 | 79% | 14,698 | 81% | 13,244 | 73% | 12,657 | 70% |
| | | | 2 | 9,101 | 7,318 | 80% | 7,409 | 81% | 6,666 | 73% | 6,327 | 70% |
| | | | 3 | 4,521 | 3,693 | 82% | 3,715 | 82% | 3,343 | 74% | 3,080 | 68% |
| | | | 4 | 2,381 | 2,119 | 89% | 2,089 | 88% | 1,973 | 83% | 1,829 | 77% |
| | | | 5 | 1,388 | 1,223 | 88% | 1,225 | 88% | 1,116 | 80% | 1,032 | 74% |
| | | | 6 | 676 | 670 | 99% | 660 | 98% | 607 | 90% | 531 | 79% |
| | | | 7 | 505 | 428 | 85% | 428 | 85% | 428 | 85% | 368 | 73% |
| | | | **Total** | **36,720** | **29,812** | **81%** | **30,225** | **82%** | **27,375** | **75%** | **25,823** | **70%** |
| | | med | 1 | 18,148 | 14,026 | 77% | 13,158 | 73% | 13,487 | 74% | 13,027 | 72% |
| | | | 2 | 9,101 | 7,035 | 77% | 6,576 | 72% | 6,619 | 73% | 6,422 | 71% |
| | | | 3 | 4,521 | 3,563 | 79% | 3,263 | 72% | 3,299 | 73% | 3,155 | 70% |
| | | | 4 | 2,381 | 2,067 | 87% | 1,942 | 82% | 1,897 | 80% | 1,791 | 75% |
| | | | 5 | 1,388 | 1,247 | 90% | 1,123 | 81% | 1,054 | 76% | 1,001 | 72% |
| | | | 6 | 676 | 653 | 97% | 619 | 91% | 571 | 84% | 465 | 69% |
| | | | 7 | 505 | 428 | 85% | 428 | 85% | 428 | 85% | 201 | 40% |
| | | | **Total** | **36,720** | **29,018** | **79%** | **27,110** | **74%** | **27,355** | **74%** | **26,060** | **71%** |
| | | max | 1 | 18,148 | 13,349 | 74% | 13,633 | 75% | 12,113 | 67% | 12,921 | 71% |
| | | | 2 | 9,101 | 6,612 | 73% | 6,678 | 73% | 5,950 | 65% | 6,278 | 69% |
| | | | 3 | 4,521 | 3,310 | 73% | 3,322 | 73% | 2,888 | 64% | 3,034 | 67% |
| | | | 4 | 2,381 | 1,959 | 82% | 1,871 | 79% | 1,717 | 72% | 1,696 | 71% |
| | | | 5 | 1,388 | 1,161 | 84% | 1,061 | 76% | 959 | 69% | 931 | 67% |
| | | | 6 | 676 | 651 | 96% | 570 | 84% | 487 | 72% | 451 | 67% |
| | | | 7 | 505 | 428 | 85% | 428 | 85% | 310 | 61% | 151 | 30% |
| | | | **Total** | **36,720** | **27,469** | **75%** | **27,564** | **75%** | **24,424** | **67%** | **25,461** | **69%** |

| PS2 | | | | | Length and proportion of REC2 segments achieving visual clarity attribute bands and NBL for each RCP | | | | | | | |
|---|---|---|---|---|---|---|---|---|---|---|---|---|
| Period | Attribute Band | Stat | Stream order | Total length km | RCP2.6 | | RCP4.5 | | RCP6.0 | | RCP8.5 | |
| | | | | | km | % | km | % | km | % | km | % |
| Late century (cont.) | NBL | min | 1 | 18,148 | 14,855 | 82% | 15,172 | 84% | 13,748 | 76% | 13,195 | 73% |
| | | | 2 | 9,101 | 7,611 | 84% | 7,679 | 84% | 6,975 | 77% | 6,630 | 73% |
| | | | 3 | 4,521 | 3,865 | 85% | 3,895 | 86% | 3,521 | 78% | 3,273 | 72% |
| | | | 4 | 2,381 | 2,191 | 92% | 2,169 | 91% | 2,048 | 86% | 1,895 | 80% |
| | | | 5 | 1,388 | 1,265 | 91% | 1,259 | 91% | 1,163 | 84% | 1,103 | 79% |
| | | | 6 | 676 | 676 | 100% | 676 | 100% | 670 | 99% | 617 | 91% |
| | | | 7 | 505 | 442 | 87% | 428 | 85% | 428 | 85% | 428 | 85% |
| | | | **Total** | **36,720** | **30,905** | **84%** | **31,277** | **85%** | **28,553** | **78%** | **27,140** | **74%** |
| | | med | 1 | 18,148 | 14,488 | 80% | 13,591 | 75% | 13,955 | 77% | 13,501 | 74% |
| | | | 2 | 9,101 | 7,258 | 80% | 6,817 | 75% | 6,870 | 75% | 6,655 | 73% |
| | | | 3 | 4,521 | 3,682 | 81% | 3,385 | 75% | 3,424 | 76% | 3,321 | 73% |
| | | | 4 | 2,381 | 2,141 | 90% | 2,007 | 84% | 1,954 | 82% | 1,854 | 78% |
| | | | 5 | 1,388 | 1,269 | 91% | 1,161 | 84% | 1,152 | 83% | 1,070 | 77% |
| | | | 6 | 676 | 671 | 99% | 668 | 99% | 653 | 97% | 549 | 81% |
| | | | 7 | 505 | 428 | 85% | 428 | 85% | 428 | 85% | 428 | 85% |
| | | | **Total** | **36,720** | **29,937** | **82%** | **28,057** | **76%** | **28,436** | **77%** | **27,378** | **75%** |
| | | max | 1 | 18,148 | 13,744 | 76% | 14,019 | 77% | 12,446 | 69% | 13,344 | 74% |
| | | | 2 | 9,101 | 6,813 | 75% | 6,863 | 75% | 6,102 | 67% | 6,479 | 71% |
| | | | 3 | 4,521 | 3,422 | 76% | 3,420 | 76% | 3,011 | 67% | 3,167 | 70% |
| | | | 4 | 2,381 | 2,026 | 85% | 1,919 | 81% | 1,761 | 74% | 1,804 | 76% |
| | | | 5 | 1,388 | 1,191 | 86% | 1,151 | 83% | 1,017 | 73% | 1,028 | 74% |
| | | | 6 | 676 | 670 | 99% | 651 | 96% | 587 | 87% | 508 | 75% |
| | | | 7 | 505 | 428 | 85% | 428 | 85% | 428 | 85% | 424 | 84% |
| | | | **Total** | **36,720** | **28,294** | **77%** | **28,451** | **77%** | **25,352** | **69%** | **26,754** | **73%** |

# Appendix H – Length and proportion of River Environment Classification v2 (REC2) segments achieving visual clarity attribute bands and NBL (or maintaining baseline visual clarity), summarised by Freshwater Management Unit (FMU) at mid- and late century under projected climate change for each representative concentration pathway (RCP)

**Table H1 Length and proportion of REC2 segments achieving visual clarity attribute bands and NBL (or maintaining baseline visual clarity) summarised by FMU at mid-century under projected climate change for PS1, represented by minimum, median, and maximum results for each RCP**

| | | PS1 | | | Length and proportion of REC2 segments achieving visual clarity attribute bands and NBL for each RCP | | | | | | | |
|---|---|---|---|---|---|---|---|---|---|---|---|---|
| Period | Attribute band | FMU | Total length (km) | stat | RCP2.6 | | RCP4.5 | | RCP6.0 | | RCP8.5 | |
| | | | | | km | % | km | % | km | % | km | % |
| Mid-century | A band | Kai Iwi | 558 | min | 280 | 50% | 239 | 43% | 247 | 44% | 217 | 39% |
| | | | | med | 251 | 45% | 227 | 41% | 231 | 41% | 219 | 39% |
| | | | | max | 220 | 39% | 210 | 38% | 208 | 37% | 195 | 35% |
| | | Manawatū | 9,941 | min | 1,170 | 12% | 708 | 7% | 1,078 | 11% | 844 | 8% |
| | | | | med | 1,093 | 11% | 1,156 | 12% | 1,002 | 10% | 1,164 | 12% |
| | | | | max | 822 | 8% | 949 | 10% | 896 | 9% | 828 | 8% |
| | | Puketoi ki Tai | 1,825 | min | 441 | 24% | 284 | 16% | 309 | 17% | 232 | 13% |
| | | | | med | 352 | 19% | 299 | 16% | 306 | 17% | 275 | 15% |
| | | | | max | 303 | 17% | 272 | 15% | 268 | 15% | 240 | 13% |
| | | Rangitīkei-Turakina | 8,563 | min | 3,102 | 36% | 2,418 | 28% | 2,109 | 25% | 2,432 | 28% |
| | | | | med | 2,664 | 31% | 2,801 | 33% | 2,666 | 31% | 2,614 | 31% |
| | | | | max | 1,906 | 22% | 2,548 | 30% | 2,660 | 31% | 2,486 | 29% |
| | | Waiopehu | 647 | min | 199 | 31% | 157 | 24% | 191 | 29% | 133 | 21% |
| | | | | med | 218 | 34% | 273 | 42% | 203 | 31% | 248 | 38% |
| | | | | max | 138 | 21% | 182 | 28% | 168 | 26% | 150 | 23% |

| | | PS1 | | | Length and proportion of REC2 segments achieving visual clarity attribute bands and NBL for each RCP | | | | | | | |
|---|---|---|---|---|---|---|---|---|---|---|---|---|
| Period | Attribute band | FMU | Total length (km) | stat | RCP2.6 | | RCP4.5 | | RCP6.0 | | RCP8.5 | |
| | | | | | km | % | km | % | km | % | km | % |
| Mid-Century (cont.) | A band (cont.) | Whangaehu | 3,478 | min | 1,409 | 41% | 843 | 24% | 786 | 23% | 773 | 22% |
| | | | | med | 716 | 21% | 851 | 24% | 829 | 24% | 643 | 18% |
| | | | | max | 444 | 13% | 680 | 20% | 741 | 21% | 587 | 17% |
| | | Whanganui | 11,709 | min | 7,303 | 62% | 6,146 | 52% | 6,263 | 53% | 5,788 | 49% |
| | | | | med | 6,340 | 54% | 6,414 | 55% | 6,104 | 52% | 5,751 | 49% |
| | | | | max | 5,673 | 48% | 5,874 | 50% | 5,906 | 50% | 5,401 | 46% |
| | B band | Kai Iwi | 558 | min | 330 | 59% | 271 | 49% | 281 | 50% | 229 | 41% |
| | | | | med | 282 | 51% | 245 | 44% | 261 | 47% | 235 | 42% |
| | | | | max | 238 | 43% | 222 | 40% | 217 | 39% | 212 | 38% |
| | | Manawatū | 9,941 | min | 1,759 | 18% | 969 | 10% | 1,630 | 16% | 1,132 | 11% |
| | | | | med | 1,707 | 17% | 1,813 | 18% | 1,481 | 15% | 1,746 | 18% |
| | | | | max | 1,100 | 11% | 1,401 | 14% | 1,279 | 13% | 1,183 | 12% |
| | | Puketoi ki Tai | 1,825 | min | 639 | 35% | 395 | 22% | 434 | 24% | 308 | 17% |
| | | | | med | 472 | 26% | 391 | 21% | 404 | 22% | 345 | 19% |
| | | | | max | 396 | 22% | 345 | 19% | 328 | 18% | 285 | 16% |
| | | Rangitīkei-Turakina | 8,563 | min | 3,771 | 44% | 2,962 | 35% | 2,554 | 30% | 2,881 | 34% |
| | | | | med | 3,117 | 36% | 3,209 | 37% | 3,139 | 37% | 2,967 | 35% |
| | | | | max | 2,268 | 26% | 2,868 | 33% | 3,030 | 35% | 2,792 | 33% |
| | | Waiopehu | 647 | min | 269 | 42% | 217 | 33% | 256 | 40% | 182 | 28% |
| | | | | med | 274 | 42% | 363 | 56% | 257 | 40% | 337 | 52% |
| | | | | max | 194 | 30% | 223 | 35% | 216 | 33% | 187 | 29% |
| | | Whangaehu | 3,478 | min | 1,802 | 52% | 1,071 | 31% | 923 | 27% | 1,027 | 30% |
| | | | | med | 861 | 25% | 1,055 | 30% | 1,021 | 29% | 763 | 22% |
| | | | | max | 533 | 15% | 789 | 23% | 865 | 25% | 677 | 19% |

| Period | Attribute band | PS1<br>FMU | Total length (km) | stat | Length and proportion of REC2 segments achieving visual clarity attribute bands and NBL for each RCP<br>RCP2.6<br>km | <br>RCP2.6<br>% | <br>RCP4.5<br>km | <br>RCP4.5<br>% | <br>RCP6.0<br>km | <br>RCP6.0<br>% | <br>RCP8.5<br>km | <br>RCP8.5<br>% |
|---|---|---|---|---|---|---|---|---|---|---|---|---|
| Mid-Century (cont.) | B band (cont.) | Whanganui | 11,709 | min | 7,713 | 66% | 6,388 | 55% | 6,499 | 56% | 5,956 | 51% |
| | | | | med | 6,569 | 56% | 6,620 | 57% | 6,316 | 54% | 5,885 | 50% |
| | | | | max | 5,846 | 50% | 6,011 | 51% | 6,066 | 52% | 5,502 | 47% |
| | NBL | Kai Iwi | 558 | min | 358 | 64% | 292 | 52% | 303 | 54% | 247 | 44% |
| | | | | med | 306 | 55% | 268 | 48% | 284 | 51% | 245 | 44% |
| | | | | max | 260 | 47% | 226 | 41% | 225 | 40% | 219 | 39% |
| | | Manawatū | 9,941 | min | 2,273 | 23% | 1,304 | 13% | 2,023 | 20% | 1,458 | 15% |
| | | | | med | 2,020 | 20% | 2,139 | 22% | 1,787 | 18% | 1,996 | 20% |
| | | | | max | 1,262 | 13% | 1,629 | 16% | 1,552 | 16% | 1,384 | 14% |
| | | Puketoi ki Tai | 1,825 | min | 878 | 48% | 470 | 26% | 521 | 29% | 350 | 19% |
| | | | | med | 568 | 31% | 473 | 26% | 488 | 27% | 413 | 23% |
| | | | | max | 477 | 26% | 411 | 23% | 394 | 22% | 335 | 18% |
| | | Rangitīkei-Turakina | 8,563 | min | 4,099 | 48% | 3,123 | 36% | 2,725 | 32% | 3,024 | 35% |
| | | | | med | 3,267 | 38% | 3,338 | 39% | 3,289 | 38% | 3,087 | 36% |
| | | | | max | 2,361 | 28% | 2,966 | 35% | 3,143 | 37% | 2,892 | 34% |
| | | Waiopehu | 647 | min | 307 | 47% | 252 | 39% | 296 | 46% | 220 | 34% |
| | | | | med | 309 | 48% | 397 | 61% | 295 | 46% | 372 | 58% |
| | | | | max | 220 | 34% | 255 | 39% | 251 | 39% | 219 | 34% |
| | | Whangaehu | 3,478 | min | 2,018 | 58% | 1,210 | 35% | 961 | 28% | 1,163 | 33% |
| | | | | med | 895 | 26% | 1,098 | 32% | 1,075 | 31% | 793 | 23% |
| | | | | max | 547 | 16% | 814 | 23% | 903 | 26% | 706 | 20% |
| | | Whanganui | 11,709 | min | 7,936 | 68% | 6,508 | 56% | 6,630 | 57% | 6,008 | 51% |
| | | | | med | 6,691 | 57% | 6,692 | 57% | 6,394 | 55% | 5,946 | 51% |
| | | | | max | 5,923 | 51% | 6,067 | 52% | 6,124 | 52% | 5,553 | 47% |

**Table H2 Length and proportion of REC2 segments achieving visual clarity attribute bands and NBL (or maintaining baseline visual clarity) summarised by FMU at late century under projected climate change for PS1, represented by minimum, median, and maximum results for each RCP**

| | | PS1 | | | Length and proportion of REC2 segments achieving visual clarity attribute bands and NBL for each RCP | | | | | | | |
|---|---|---|---|---|---|---|---|---|---|---|---|---|
| Period | Attribute band | FMU | Total length (km) | stat | RCP2.6 | | RCP4.5 | | RCP6.0 | | RCP8.5 | |
| | | | | | km | % | km | % | km | % | km | % |
| Late century | A band | Kai Iwi | 558 | min | 449 | 80% | 369 | 66% | 321 | 57% | 270 | 48% |
| | | | | med | 372 | 67% | 322 | 58% | 292 | 52% | 240 | 43% |
| | | | | max | 339 | 61% | 295 | 53% | 253 | 45% | 226 | 41% |
| | | Manawatū | 9,941 | min | 4,544 | 46% | 3,758 | 38% | 2,790 | 28% | 1,840 | 19% |
| | | | | med | 3,944 | 40% | 2,904 | 29% | 2,488 | 25% | 1,732 | 17% |
| | | | | max | 3,109 | 31% | 2,426 | 24% | 1,626 | 16% | 1,912 | 19% |
| | | Puketoi ki Tai | 1,825 | min | 1,315 | 72% | 1,150 | 63% | 957 | 52% | 753 | 41% |
| | | | | med | 1,233 | 68% | 1,003 | 55% | 870 | 48% | 658 | 36% |
| | | | | max | 1,060 | 58% | 898 | 49% | 772 | 42% | 584 | 32% |
| | | Rangitīkei-Turakina | 8,563 | min | 6,010 | 70% | 5,616 | 66% | 4,339 | 51% | 3,800 | 44% |
| | | | | med | 5,644 | 66% | 4,537 | 53% | 4,462 | 52% | 3,823 | 45% |
| | | | | max | 5,030 | 59% | 4,455 | 52% | 3,459 | 40% | 3,583 | 42% |
| | | Waiopehu | 647 | min | 229 | 35% | 228 | 35% | 189 | 29% | 138 | 21% |
| | | | | med | 282 | 44% | 185 | 29% | 217 | 34% | 196 | 30% |
| | | | | max | 178 | 28% | 194 | 30% | 111 | 17% | 304 | 47% |
| | | Whangaehu | 3,478 | min | 2,633 | 76% | 2,635 | 76% | 2,034 | 58% | 1,461 | 42% |
| | | | | med | 2,085 | 60% | 1,926 | 55% | 1,635 | 47% | 1,500 | 43% |
| | | | | max | 1,904 | 55% | 1,877 | 54% | 1,310 | 38% | 1,378 | 40% |
| | | Whanganui | 11,709 | min | 10,075 | 86% | 9,661 | 83% | 8,394 | 72% | 7,147 | 61% |
| | | | | med | 9,397 | 80% | 8,306 | 71% | 7,906 | 68% | 6,921 | 59% |
| | | | | max | 8,689 | 74% | 8,236 | 70% | 6,951 | 59% | 6,430 | 55% |

| PS1 | | | | | Length and proportion of REC2 segments achieving visual clarity attribute bands and NBL for each RCP | | | | | | | |
|---|---|---|---|---|---|---|---|---|---|---|---|---|
| Period | Attribute band | FMU | Total length (km) | stat | RCP2.6 | | RCP4.5 | | RCP6.0 | | RCP8.5 | |
| | | | | | km | % | km | % | km | % | km | % |
| Late Century (cont.) | B band | Kai Iwi | 558 | min | 514 | 92% | 450 | 81% | 377 | 67% | 302 | 54% |
| | | | | med | 457 | 82% | 380 | 68% | 337 | 60% | 270 | 48% |
| | | | | max | 401 | 72% | 335 | 60% | 284 | 51% | 240 | 43% |
| | | Manawatū | 9,941 | min | 5,639 | 57% | 5,052 | 51% | 3,962 | 40% | 2,695 | 27% |
| | | | | med | 5,251 | 53% | 4,036 | 41% | 3,346 | 34% | 2,537 | 26% |
| | | | | max | 4,221 | 42% | 3,588 | 36% | 2,295 | 23% | 2,385 | 24% |
| | | Puketoi ki Tai | 1,825 | min | 1,501 | 82% | 1,443 | 79% | 1,252 | 69% | 972 | 53% |
| | | | | med | 1,497 | 82% | 1,305 | 72% | 1,131 | 62% | 861 | 47% |
| | | | | max | 1,366 | 75% | 1,150 | 63% | 995 | 55% | 768 | 42% |
| | | Rangitīkei-Turakina | 8,563 | min | 6,666 | 78% | 6,370 | 74% | 5,173 | 60% | 4,485 | 52% |
| | | | | med | 6,331 | 74% | 5,369 | 63% | 5,134 | 60% | 4,338 | 51% |
| | | | | max | 5,820 | 68% | 5,118 | 60% | 4,142 | 48% | 4,043 | 47% |
| | | Waiopehu | 647 | min | 299 | 46% | 300 | 46% | 250 | 39% | 191 | 30% |
| | | | | med | 400 | 62% | 250 | 39% | 278 | 43% | 253 | 39% |
| | | | | max | 218 | 34% | 295 | 46% | 169 | 26% | 325 | 50% |
| | | Whangaehu | 3,478 | min | 3,061 | 88% | 3,141 | 90% | 2,350 | 68% | 1,854 | 53% |
| | | | | med | 2,401 | 69% | 2,100 | 60% | 1,961 | 56% | 1,799 | 52% |
| | | | | max | 2,121 | 61% | 2,140 | 62% | 1,499 | 43% | 1,640 | 47% |
| | | Whanganui | 11,709 | min | 10,646 | 91% | 10,274 | 88% | 8,906 | 76% | 7,486 | 64% |
| | | | | med | 10,011 | 86% | 8,814 | 75% | 8,334 | 71% | 7,189 | 61% |
| | | | | max | 9,191 | 78% | 8,702 | 74% | 7,279 | 62% | 6,640 | 57% |
| | NBL | Kai Iwi | 558 | min | 529 | 95% | 470 | 84% | 398 | 71% | 326 | 58% |
| | | | | med | 478 | 86% | 402 | 72% | 354 | 63% | 288 | 52% |
| | | | | max | 430 | 77% | 355 | 64% | 302 | 54% | 251 | 45% |

| PS1 | | | | | Length and proportion of REC2 segments achieving visual clarity attribute bands and NBL for each RCP | | | | | | | |
|---|---|---|---|---|---|---|---|---|---|---|---|---|
| Period | Attribute band | FMU | Total length (km) | stat | RCP2.6 | | RCP4.5 | | RCP6.0 | | RCP8.5 | |
| | | | | | km | % | km | % | km | % | km | % |
| Late Century (cont.) | NBL (cont.) | Manawatū | 9,941 | min | 6,461 | 65% | 5,842 | 59% | 4,773 | 48% | 3,469 | 35% |
| | | | | med | 6,035 | 61% | 4,709 | 47% | 4,132 | 42% | 3,110 | 31% |
| | | | | max | 4,844 | 49% | 4,289 | 43% | 2,858 | 29% | 2,784 | 28% |
| | | Puketoi ki Tai | 1,825 | min | 1,635 | 90% | 1,595 | 87% | 1,449 | 79% | 1,224 | 67% |
| | | | | med | 1,646 | 90% | 1,514 | 83% | 1,361 | 75% | 1,054 | 58% |
| | | | | max | 1,541 | 84% | 1,398 | 77% | 1,245 | 68% | 905 | 50% |
| | | Rangitīkei-Turakina | 8,563 | min | 7,086 | 83% | 6,791 | 79% | 5,636 | 66% | 5,020 | 59% |
| | | | | med | 6,711 | 78% | 5,796 | 68% | 5,644 | 66% | 4,685 | 55% |
| | | | | max | 6,204 | 72% | 5,579 | 65% | 4,601 | 54% | 4,296 | 50% |
| | | Waiopehu | 647 | min | 341 | 53% | 345 | 53% | 302 | 47% | 226 | 35% |
| | | | | med | 442 | 68% | 293 | 45% | 318 | 49% | 279 | 43% |
| | | | | max | 261 | 40% | 326 | 50% | 186 | 29% | 349 | 54% |
| | | Whangaehu | 3,478 | min | 3,234 | 93% | 3,227 | 93% | 2,661 | 77% | 2,103 | 60% |
| | | | | med | 2,470 | 71% | 2,314 | 67% | 2,120 | 61% | 1,965 | 56% |
| | | | | max | 2,263 | 65% | 2,274 | 65% | 1,579 | 45% | 1,791 | 52% |
| | | Whanganui | 11,709 | min | 11,081 | 95% | 10,610 | 91% | 9,247 | 79% | 7,700 | 66% |
| | | | | med | 10,461 | 89% | 9,152 | 78% | 8,613 | 74% | 7,359 | 63% |
| | | | | max | 9,517 | 81% | 8,978 | 77% | 7,482 | 64% | 6,757 | 58% |

**Table H3 Length and proportion of REC2 segments achieving visual clarity attribute bands and NBL (or maintaining baseline visual clarity) summarised by FMU at mid-century under projected climate change for PS2, represented by minimum, median, and maximum results for each RCP**

| | PS2 | | | | Length and proportion of REC2 segments achieving visual clarity attribute bands and NBL for each RCP | | | | | | | |
|---|---|---|---|---|---|---|---|---|---|---|---|---|
| Period | Attribute band | FMU | Total length (km) | stat | RCP2.6 | | RCP4.5 | | RCP6.0 | | RCP8.5 | |
| | | | | | km | % | km | % | km | % | km | % |
| Mid-century | A band | Kai Iwi | 558 | min | 381 | 68% | 330 | 59% | 338 | 61% | 292 | 52% |
| | | | | med | 340 | 61% | 303 | 54% | 313 | 56% | 287 | 51% |
| | | | | max | 298 | 53% | 266 | 48% | 262 | 47% | 245 | 44% |
| | | Manawatū | 9,941 | min | 2,921 | 29% | 2,000 | 20% | 2,386 | 24% | 1,510 | 15% |
| | | | | med | 2,391 | 24% | 2,042 | 21% | 2,003 | 20% | 1,744 | 18% |
| | | | | max | 1,680 | 17% | 1,411 | 14% | 1,279 | 13% | 1,017 | 10% |
| | | Puketoi ki Tai | 1,825 | min | 932 | 51% | 768 | 42% | 803 | 44% | 598 | 33% |
| | | | | med | 822 | 45% | 689 | 38% | 714 | 39% | 583 | 32% |
| | | | | max | 705 | 39% | 567 | 31% | 540 | 30% | 455 | 25% |
| | | Rangitīkei-Turakina | 8,563 | min | 4,993 | 58% | 4,093 | 48% | 3,732 | 44% | 3,630 | 42% |
| | | | | med | 4,307 | 50% | 4,114 | 48% | 4,144 | 48% | 3,591 | 42% |
| | | | | max | 3,374 | 39% | 3,549 | 41% | 3,584 | 42% | 3,051 | 36% |
| | | Waiopehu | 647 | min | 215 | 33% | 174 | 27% | 208 | 32% | 141 | 22% |
| | | | | med | 235 | 36% | 280 | 43% | 211 | 33% | 253 | 39% |
| | | | | max | 156 | 24% | 184 | 28% | 175 | 27% | 155 | 24% |
| | | Whangaehu | 3,478 | min | 2,397 | 69% | 1,828 | 53% | 1,785 | 51% | 1,629 | 47% |
| | | | | med | 1,717 | 49% | 1,746 | 50% | 1,743 | 50% | 1,415 | 41% |
| | | | | max | 1,370 | 39% | 1,451 | 42% | 1,468 | 42% | 1,041 | 30% |
| | | Whanganui | 11,709 | min | 9,565 | 82% | 8,483 | 72% | 8,603 | 73% | 7,798 | 67% |
| | | | | med | 8,657 | 74% | 8,618 | 74% | 8,404 | 72% | 7,612 | 65% |
| | | | | max | 8,009 | 68% | 7,674 | 66% | 7,564 | 65% | 6,571 | 56% |

| | | PS2 | | | Length and proportion of REC2 segments achieving visual clarity attribute bands and NBL for each RCP | | | | | | | |
|---|---|---|---|---|---|---|---|---|---|---|---|---|
| **Period** | **Attribute band** | **FMU** | **Total length (km)** | **stat** | **RCP2.6** | | **RCP4.5** | | **RCP6.0** | | **RCP8.5** | |
| | | | | | **km** | **%** | **km** | **%** | **km** | **%** | **km** | **%** |
| Mid-century (cont.) | B band | Kai Iwi | 558 | min | 471 | 84% | 409 | 73% | 419 | 75% | 348 | 62% |
| | | | | med | 420 | 75% | 361 | 65% | 380 | 68% | 344 | 62% |
| | | | | max | 354 | 63% | 313 | 56% | 301 | 54% | 277 | 50% |
| | | Manawatū | 9,941 | min | 4,448 | 45% | 3,202 | 32% | 3,894 | 39% | 2,246 | 23% |
| | | | | med | 3,864 | 39% | 3,228 | 32% | 3,148 | 32% | 2,585 | 26% |
| | | | | max | 2,578 | 26% | 2,162 | 22% | 1,904 | 19% | 1,508 | 15% |
| | | Puketoi ki Tai | 1,825 | min | 1,322 | 72% | 1,141 | 62% | 1,168 | 64% | 939 | 51% |
| | | | | med | 1,200 | 66% | 1,064 | 58% | 1,098 | 60% | 911 | 50% |
| | | | | max | 1,081 | 59% | 901 | 49% | 853 | 47% | 685 | 38% |
| | | Rangitīkei-Turakina | 8,563 | min | 6,040 | 71% | 5,149 | 60% | 4,828 | 56% | 4,572 | 53% |
| | | | | med | 5,268 | 62% | 4,986 | 58% | 5,098 | 60% | 4,383 | 51% |
| | | | | max | 4,377 | 51% | 4,328 | 51% | 4,355 | 51% | 3,623 | 42% |
| | | Waiopehu | 647 | min | 289 | 45% | 234 | 36% | 279 | 43% | 189 | 29% |
| | | | | med | 292 | 45% | 373 | 58% | 270 | 42% | 345 | 53% |
| | | | | max | 214 | 33% | 229 | 35% | 220 | 34% | 194 | 30% |
| | | Whangaehu | 3,478 | min | 2,884 | 83% | 2,276 | 65% | 2,128 | 61% | 2,117 | 61% |
| | | | | med | 2,063 | 59% | 2,192 | 63% | 2,189 | 63% | 1,773 | 51% |
| | | | | max | 1,693 | 49% | 1,828 | 53% | 1,863 | 54% | 1,356 | 39% |
| | | Whanganui | 11,709 | min | 10,361 | 88% | 9,231 | 79% | 9,326 | 80% | 8,418 | 72% |
| | | | | med | 9,393 | 80% | 9,287 | 79% | 9,046 | 77% | 8,141 | 70% |
| | | | | max | 8,656 | 74% | 8,191 | 70% | 8,047 | 69% | 6,868 | 59% |
| | NBL | Kai Iwi | 558 | min | 485 | 87% | 432 | 77% | 438 | 78% | 371 | 66% |
| | | | | med | 441 | 79% | 387 | 69% | 406 | 73% | 371 | 66% |
| | | | | max | 379 | 68% | 342 | 61% | 334 | 60% | 313 | 56% |

| | | PS2 | | | Length and proportion of REC2 segments achieving visual clarity attribute bands and NBL for each RCP | | | | | | | |
|---|---|---|---|---|---|---|---|---|---|---|---|---|
| Period | Attribute band | FMU | Total length (km) | stat | RCP2.6 | | RCP4.5 | | RCP6.0 | | RCP8.5 | |
| | | | | | km | % | km | % | km | % | km | % |
| Mid-century (cont.) | NBL (cont.) | Manawatū | 9,941 | min | 5,478 | 55% | 4,210 | 42% | 4,926 | 50% | 3,141 | 32% |
| | | | | med | 4,839 | 49% | 4,201 | 42% | 4,160 | 42% | 3,222 | 32% |
| | | | | max | 3,438 | 35% | 2,678 | 27% | 2,423 | 24% | 1,809 | 18% |
| | | Puketoi ki Tai | 1,825 | min | 1,524 | 84% | 1,417 | 78% | 1,436 | 79% | 1,268 | 69% |
| | | | | med | 1,497 | 82% | 1,407 | 77% | 1,436 | 79% | 1,253 | 69% |
| | | | | max | 1,422 | 78% | 1,224 | 67% | 1,153 | 63% | 873 | 48% |
| | | Rangitīkei-Turakina | 8,563 | min | 6,633 | 77% | 5,860 | 68% | 5,553 | 65% | 5,231 | 61% |
| | | | | med | 5,963 | 70% | 5,610 | 66% | 5,774 | 67% | 4,943 | 58% |
| | | | | max | 5,058 | 59% | 4,893 | 57% | 4,908 | 57% | 3,872 | 45% |
| | | Waiopehu | 647 | min | 327 | 51% | 272 | 42% | 317 | 49% | 233 | 36% |
| | | | | med | 327 | 51% | 407 | 63% | 301 | 47% | 376 | 58% |
| | | | | max | 239 | 37% | 260 | 40% | 256 | 40% | 229 | 35% |
| | | Whangaehu | 3,478 | min | 3,213 | 92% | 2,565 | 74% | 2,312 | 66% | 2,457 | 71% |
| | | | | med | 2,220 | 64% | 2,402 | 69% | 2,360 | 68% | 2,020 | 58% |
| | | | | max | 1,817 | 52% | 2,078 | 60% | 2,132 | 61% | 1,511 | 43% |
| | | Whanganui | 11,709 | min | 10,826 | 92% | 9,785 | 84% | 9,880 | 84% | 8,843 | 76% |
| | | | | med | 9,926 | 85% | 9,771 | 83% | 9,567 | 82% | 8,520 | 73% |
| | | | | max | 9,175 | 78% | 8,547 | 73% | 8,356 | 71% | 7,006 | 60% |

**Table H4 Length and proportion of REC2 segments achieving visual clarity attribute bands and NBL (or maintaining baseline visual clarity) summarised by FMU at late century under projected climate change for PS2, represented by minimum, median, and maximum results for each RCP**

| PS2 | | | | | Length and proportion of REC2 segments achieving visual clarity attribute bands and NBL for each RCP | | | | | | | |
|---|---|---|---|---|---|---|---|---|---|---|---|---|
| Period | Attribute band | FMU | Total length (km) | stat | RCP2.6 | | RCP4.5 | | RCP6.0 | | RCP8.5 | |
| | | | | | km | % | km | % | km | % | km | % |
| Late century | A band | Kai Iwi | 558 | min | 472 | 85% | 454 | 81% | 425 | 76% | 381 | 68% |
| | | | | med | 463 | 83% | 424 | 76% | 398 | 71% | 352 | 63% |
| | | | | max | 440 | 79% | 396 | 71% | 368 | 66% | 330 | 59% |
| | | Manawatū | 9,941 | min | 5,582 | 56% | 5,470 | 55% | 4,895 | 49% | 4,260 | 43% |
| | | | | med | 5,526 | 56% | 4,973 | 50% | 4,879 | 49% | 4,096 | 41% |
| | | | | max | 5,018 | 50% | 4,688 | 47% | 3,973 | 40% | 4,232 | 43% |
| | | Puketoi ki Tai | 1,825 | min | 1,557 | 85% | 1,572 | 86% | 1,503 | 82% | 1,436 | 79% |
| | | | | med | 1,591 | 87% | 1,540 | 84% | 1,501 | 82% | 1,395 | 76% |
| | | | | max | 1,546 | 85% | 1,501 | 82% | 1,442 | 79% | 1,323 | 72% |
| | | Rangitīkei-Turakina | 8,563 | min | 6,627 | 77% | 6,647 | 78% | 5,882 | 69% | 5,803 | 68% |
| | | | | med | 6,537 | 76% | 6,015 | 70% | 6,292 | 73% | 5,924 | 69% |
| | | | | max | 6,277 | 73% | 6,195 | 72% | 5,461 | 64% | 5,749 | 67% |
| | | Waiopehu | 647 | min | 233 | 36% | 250 | 39% | 213 | 33% | 162 | 25% |
| | | | | med | 290 | 45% | 212 | 33% | 242 | 37% | 209 | 32% |
| | | | | max | 204 | 32% | 223 | 34% | 139 | 21% | 314 | 48% |
| | | Whangaehu | 3,478 | min | 2,746 | 79% | 2,942 | 85% | 2,456 | 71% | 2,213 | 64% |
| | | | | med | 2,379 | 68% | 2,344 | 67% | 2,265 | 65% | 2,368 | 68% |
| | | | | max | 2,294 | 66% | 2,455 | 71% | 2,037 | 59% | 2,316 | 67% |
| | | Whanganui | 11,709 | min | 10,834 | 93% | 10,987 | 94% | 10,176 | 87% | 9,474 | 81% |
| | | | | med | 10,469 | 89% | 10,024 | 86% | 9,947 | 85% | 9,569 | 82% |
| | | | | max | 10,223 | 87% | 10,123 | 86% | 9,284 | 79% | 9,287 | 79% |

| PS2 | | | | | Length and proportion of REC2 segments achieving visual clarity attribute bands and NBL for each RCP | | | | | | | |
|---|---|---|---|---|---|---|---|---|---|---|---|---|
| Period | Attribute band | FMU | Total length (km) | stat | RCP2.6 | | RCP4.5 | | RCP6.0 | | RCP8.5 | |
| | | | | | km | % | km | % | km | % | km | % |
| Late Century (cont.) | B band | Kai Iwi | 558 | min | 503 | 90% | 478 | 86% | 453 | 81% | 409 | 73% |
| | | | | med | 484 | 87% | 456 | 82% | 439 | 79% | 382 | 68% |
| | | | | max | 460 | 83% | 436 | 78% | 392 | 70% | 373 | 67% |
| | | Manawatū | 9,941 | min | 6,303 | 63% | 6,323 | 64% | 5,706 | 57% | 5,050 | 51% |
| | | | | med | 6,434 | 65% | 5,724 | 58% | 5,534 | 56% | 5,076 | 51% |
| | | | | max | 5,724 | 58% | 5,602 | 56% | 4,666 | 47% | 4,996 | 50% |
| | | Puketoi ki Tai | 1,825 | min | 1,653 | 91% | 1,667 | 91% | 1,560 | 85% | 1,543 | 85% |
| | | | | med | 1,693 | 93% | 1,601 | 88% | 1,597 | 88% | 1,521 | 83% |
| | | | | max | 1,635 | 90% | 1,587 | 87% | 1,552 | 85% | 1,493 | 82% |
| | | Rangitīkei-Turakina | 8,563 | min | 7,008 | 82% | 7,032 | 82% | 6,246 | 73% | 6,241 | 73% |
| | | | | med | 6,903 | 81% | 6,391 | 75% | 6,655 | 78% | 6,347 | 74% |
| | | | | max | 6,656 | 78% | 6,477 | 76% | 5,862 | 68% | 6,131 | 72% |
| | | Waiopehu | 647 | min | 301 | 46% | 320 | 49% | 278 | 43% | 217 | 33% |
| | | | | med | 401 | 62% | 271 | 42% | 306 | 47% | 269 | 42% |
| | | | | max | 244 | 38% | 320 | 49% | 195 | 30% | 341 | 53% |
| | | Whangaehu | 3,478 | min | 3,044 | 88% | 3,226 | 93% | 2,672 | 77% | 2,405 | 69% |
| | | | | med | 2,457 | 71% | 2,419 | 70% | 2,425 | 70% | 2,547 | 73% |
| | | | | max | 2,351 | 68% | 2,570 | 74% | 2,073 | 60% | 2,510 | 72% |
| | | Whanganui | 11,709 | min | 11,000 | 94% | 11,177 | 95% | 10,460 | 89% | 9,957 | 85% |
| | | | | med | 10,646 | 91% | 10,248 | 88% | 10,399 | 89% | 9,920 | 85% |
| | | | | max | 10,399 | 89% | 10,572 | 90% | 9,685 | 83% | 9,618 | 82% |
| | NBL | Kai Iwi | 558 | min | 515 | 92% | 483 | 86% | 461 | 83% | 416 | 74% |
| | | | | med | 492 | 88% | 462 | 83% | 441 | 79% | 392 | 70% |
| | | | | max | 469 | 84% | 441 | 79% | 400 | 72% | 380 | 68% |

| PS2 | | | | | Length and proportion of REC2 segments achieving visual clarity attribute bands and NBL for each RCP | | | | | | | |
|---|---|---|---|---|---|---|---|---|---|---|---|---|
| Period | Attribute band | FMU | Total length (km) | stat | RCP2.6 | | RCP4.5 | | RCP6.0 | | RCP8.5 | |
| | | | | | km | % | km | % | km | % | km | % |
| Late Century (cont.) | NBL (cont.) | Manawatū | 9,941 | min | 6,853 | 69% | 6,916 | 70% | 6,272 | 63% | 5,670 | 57% |
| | | | | med | 6,961 | 70% | 6,199 | 62% | 6,126 | 62% | 5,627 | 57% |
| | | | | max | 6,171 | 62% | 6,064 | 61% | 5,070 | 51% | 5,475 | 55% |
| | | Puketoi ki Tai | 1,825 | min | 1,689 | 93% | 1,734 | 95% | 1,657 | 91% | 1,641 | 90% |
| | | | | med | 1,751 | 96% | 1,708 | 94% | 1,696 | 93% | 1,597 | 87% |
| | | | | max | 1,703 | 93% | 1,695 | 93% | 1,654 | 91% | 1,575 | 86% |
| | | Rangitīkei-Turakina | 8,563 | min | 7,220 | 84% | 7,265 | 85% | 6,488 | 76% | 6,434 | 75% |
| | | | | med | 7,084 | 83% | 6,594 | 77% | 6,857 | 80% | 6,581 | 77% |
| | | | | max | 6,835 | 80% | 6,634 | 77% | 6,010 | 70% | 6,390 | 75% |
| | | Waiopehu | 647 | min | 344 | 53% | 362 | 56% | 314 | 49% | 255 | 39% |
| | | | | med | 449 | 69% | 309 | 48% | 346 | 53% | 300 | 46% |
| | | | | max | 280 | 43% | 345 | 53% | 215 | 33% | 370 | 57% |
| | | Whangaehu | 3,478 | min | 3,216 | 92% | 3,274 | 94% | 2,824 | 81% | 2,580 | 74% |
| | | | | med | 2,490 | 72% | 2,457 | 71% | 2,471 | 71% | 2,590 | 74% |
| | | | | max | 2,365 | 68% | 2,602 | 75% | 2,085 | 60% | 2,540 | 73% |
| | | Whanganui | 11,709 | min | 11,068 | 95% | 11,243 | 96% | 10,537 | 90% | 10,145 | 87% |
| | | | | med | 10,710 | 91% | 10,329 | 88% | 10,498 | 90% | 10,291 | 88% |
| | | | | max | 10,471 | 89% | 10,669 | 91% | 9,919 | 85% | 10,023 | 86% |

# Appendix I – Summary comparing the ranges of River Environment Classification v2 (REC2) segments achieving A band, B band, and NBL with and without climate change impacts summarised by FMU for PS1 and PS2

**Table I1 Summary comparing the ranges of REC2 segments achieving A band, B band, and NBL (or maintaining baseline visual clarity) across mid-(2040) and late (2090) century with and without climate change impacts summarised by FMU for PS1**

| | PS1 | | % of REC2 segments by length achieving visual clarity attribute bands and NBL: | |
|---|---|---|---|---|
| Period | FMU | Attribute band | Without climate change | With climate change |
| Mid-century (2040) | Kai Iwi | A band | 48% | 35–50% |
| | | B band | 80% | 38–59% |
| | | NBL | 95% | 39–64% |
| | Manawatū | A band | 28% | 7–12% |
| | | B band | 50% | 10–18% |
| | | NBL | 68% | 13–23% |
| | Puketoi ki Tai | A band | 31% | 13–24% |
| | | B band | 54% | 16–35% |
| | | NBL | 78% | 18–48% |
| | Rangitīkei-Turakina | A band | 38% | 22–36% |
| | | B band | 64% | 26–44% |
| | | NBL | 78% | 28–48% |
| | Waiopehu | A band | 31% | 21–42% |
| | | B band | 55% | 28–56% |
| | | NBL | 64% | 34–61% |
| | Whangaehu | A band | 49% | 13–41% |
| | | B band | 76% | 15–52% |
| | | NBL | 88% | 16–58% |
| | Whanganui | A band | 69% | 46–62% |
| | | B band | 83% | 47–66% |
| | | NBL | 93% | 47–68% |
| Late century (2090) | Kai Iwi | A band | 73% | 41–80% |
| | | B band | 90% | 43–92% |
| | | NBL | 97% | 45–95% |
| | Manawatū | A band | 52% | 16–46% |
| | | B band | 67% | 23–57% |
| | | NBL | 78% | 28–65% |
| | Puketoi ki Tai | A band | 73% | 32–72% |
| | | B band | 85% | 42–82% |
| | | NBL | 94% | 50–90% |
| | Rangitīkei-Turakina | A band | 66% | 40–70% |
| | | B band | 81% | 47–78% |
| | | NBL | 87% | 50–83% |
| | Waiopehu | A band | 32% | 17–47% |
| | | B band | 57% | 26–62% |
| | | NBL | 65% | 29–68% |
| | Whangaehu | A band | 74% | 38–76% |
| | | B band | 90% | 43–90% |
| | | NBL | 95% | 45–93% |
| | Whanganui | A band | 83% | 55–86% |
| | | B band | 93% | 57–91% |
| | | NBL | 97% | 58–95% |

Note: The range of values for 'with climate change' includes the min, med, and max across all RCPs.

**Table I2 Summary comparing the ranges of REC2 segments achieving A band, B band, and NBL (or maintaining baseline visual clarity) across mid-(2040) and late (2090) century with and without climate change impacts summarised by FMU for PS2**

| Period | PS2 FMU | Attribute band | % of REC2 segments by length achieving visual clarity attribute bands and NBL: Without climate change | With climate change |
|---|---|---|---|---|
| Mid-century (2040) | Kai Iwi | A band | 67% | 44–68% |
| | | B band | 88% | 50–84% |
| | | NBL | 97% | 56–87% |
| | Manawatū | A band | 44% | 10–29% |
| | | B band | 62% | 15–45% |
| | | NBL | 74% | 18–55% |
| | Puketoi ki Tai | A band | 59% | 25–51% |
| | | B band | 77% | 38–72% |
| | | NBL | 88% | 48–84% |
| | Rangitīkei-Turakina | A band | 58% | 36–58% |
| | | B band | 77% | 42–71% |
| | | NBL | 85% | 45–77% |
| | Waiopehu | A band | 31% | 22–43% |
| | | B band | 56% | 29–58% |
| | | NBL | 64% | 35–63% |
| | Whangaehu | A band | 68% | 30–69% |
| | | B band | 87% | 39–83% |
| | | NBL | 94% | 43–92% |
| | Whanganui | A band | 79% | 56–82% |
| | | B band | 91% | 59–88% |
| | | NBL | 96% | 60–92% |
| Late century (2090) | Kai Iwi | A band | 80% | 59–85% |
| | | B band | 91% | 67–90% |
| | | NBL | 97% | 68–92% |
| | Manawatū | A band | 60% | 40–56% |
| | | B band | 73% | 47–65% |
| | | NBL | 81% | 51–70% |
| | Puketoi ki Tai | A band | 85% | 72–87% |
| | | B band | 91% | 82–93% |
| | | NBL | 95% | 86–96% |
| | Rangitīkei-Turakina | A band | 72% | 64–78% |
| | | B band | 84% | 68–82% |
| | | NBL | 89% | 70–85% |
| | Waiopehu | A band | 33% | 21–48% |
| | | B band | 58% | 30–62% |
| | | NBL | 66% | 33–69% |
| | Whangaehu | A band | 76% | 59–85% |
| | | B band | 90% | 60–93% |
| | | NBL | 95% | 60–94% |
| | Whanganui | A band | 87% | 79–94% |
| | | B band | 96% | 82–95% |
| | | NBL | 98% | 85–96% |

Note: The range of values for ‘with climate change’ includes the min, med, and max across all RCPs.

horizons

REGIONAL COUNCIL

horizons.govt.nz

**24 hour freephone** 0508 800 800
**fax** 06 952 2929 | **email** help@horizons.govt.nz
Private Bag 11025, Manawatu Mail Centre, Palmerston North 4442